UNCLASSIFIED

AD. 295 555

Reproduced
by the

ARMED SERVICES TECHNICAL INFORMATION AGENCY
ARLINGTON HALL STATION
ARLINGTON 12, VIRGINIA

UNCLASSIFIED

63-2-3

29 555

ASTIA

295 555

THE RESPONSE OF AN AUTOMATIC PHASE CONTROL

SYSTEM TO FM SIGNALS AND NOISE

by

Donald L. Schilling

Research Report No. PIBMRI-1040-62

for

MRI

POLYTECHNIC INSTITUTE OF BROOKLYN

MICROWAVE RESEARCH INSTITUTE
ELECTRICAL ENGINEERING DEPARTMENT

THE RESPONSE OF AN AUTOMATIC PHASE CONTROL
SYSTEM TO FM SIGNALS AND NOISE

by

Donald L. Schilling

Polytechnic Institute of Brooklyn
Microwave Research Institute
55 Johnson Street
Brooklyn 1, New York
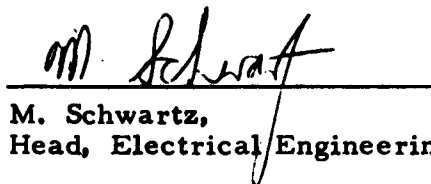
June 1962

Title Page
Acknowledgment
Abstract
Table of Contents (3 pages)
List of Figures (3.pages)
136 Pages of Text
Distribution List

Donald L. Schilling
Assistant Professor, Electrical Engineering

Approved by:

M. Schwartz,
Head, Electrical Engineering

ACKNOWLEDGMENT

TABLE OF CONTENTS

TABLE OF CONTENTS (Cont'd.)

TABLE OF CONTENTS (Cont'd.)

LIST OF FIGURES

LIST OF FIGURES (Cont'd.)

LIST OF FIGURES (Cont'd.)

ABSTRACT

THE RESPONSE OF AN AUTOMATIC PHASE
CONTROL SYSTEM TO FM SIGNALS AND NOISE

by

Donald L. Schilling

Adviser: Mischa Schwartz

Submitted in partial fulfillment of the
requirements for the Degree of Doctor of
Philosophy (Electrical Engineering)

An Automatic Phase Control System is analyzed to determine its response to frequency modulated signals and narrow-band Gaussian noise. Emphasis is placed on the System's response to frequency ramp modulated signals. In constradistinction to previous analyses, the assumptions of a linearized system and of a S/N ratio greater than unity were not made.

The response of the System to an FM signal is obtained using a perturbation technique and perturbing about the solution to the nonlinear pendulum problem. A piecewise-linear solution is also presented and used to extend the class of solutions obtainable when using the perturbation technique. It is shown that the perturbation technique results in an excellent approximation to the actual System response which was determined experimentally. However, the technique is only valid when the System is underdamped. The piecewise-linear technique does not result in as good an approximation, but it can be used when the System is critically-damped, or over-damped. Utilizing these techniques, the response of the APC System to a frequency ramp modulated signal was obtained, the initial conditions required for the System to synchronize to a frequency ramp modulated signal determined, and the use of the System as an FM demodulated discussed in detail.

The response of the Automatic Phase Control System to narrow-band Gaussian noise is next obtained. An iteration technique is used and convergence is proven. It is shown that the APC System responds to noise as an open-loop System rather than as a closed-loop System. The phase jitter present in the output of the System is shown to represent a non-stationary Gaussian distribution.

The last section of the dissertation discusses the response of an Automatic Phase Control System to FM Signals embedded in noise. An iteration technique is used and a first iteration taken. The results obtained from this first approximation yield a qualitative understanding of the effect of the System parameters on the probability of synchronizing to a signal when the input S/N ratio is much less than unity. This discussion is then extended experimentally. It is shown that a critically-damped System can tolerate a lower S/N ratio than an underdamped or overdamped System.

Chapter 1

INTRODUCTION

1.1 Statement of the Problem

The Automatic Phase Control (APC) System is the basic element in many communication[1.1] and radar[1.2] systems. The resultant device is capable of locking to an accelerating target whose return signal is deeply embedded in noise.

The APC System is analyzed in order to determine its response to frequency modulated signals and noise. Emphasis is placed on frequency ramp modulated signals. The system can be described by a second-order nonlinear differential equation. This equation also represents the response of a pendulum to an applied force and a nonlinear friction force.

1.2 Summary of Prior Work

In previous analyses the phase plane technique was used to obtain the response of the APC System to a frequency ramp modulated signal.[1.3] This technique helped to provide a qualitative understanding of the problem. Quantitative results have been derived by linearizing the differential equation and solving the linearized problem.[1.4] The results obtained in this manner were highly restrictive. They were valid only when the frequency and phase of the incoming signal were similar to the initial frequency and phase of the APC System. (This is analogous to the motion of a pendulum whose swing is restricted to small angles.) In addition, the assumption of a linearized system required that the signal-to-noise (S/N) ratio of the incoming signal (and associated noise) be much greater than unity[1.5] and that the noise be limited.

1.3 Summary of Results Obtained

In contradistinction to the analyses performed by previous investigators, the assumptions of linearizing the system, limiting the noise, and requiring that the S/N ratio be greater than unity, will not be made.

Chapter 2 describes the response of an APC System to an FM signal. An exact solution to the nonlinear problem is obtained using a perturbation technique. Perturbations are taken about the solution to the pendulum problem The result obtained is useful in obtaining solutions to the problem when large phase errors exist A piecewise-linear analysis is also presented, to extend the results obtained using the perturbation technique.

Chapter 3 discusses the response of the APC System to noise, when no signal is present Using an iterative procedure it is shown that the APC System acts as an open loop device to noise.

The response of an APC System to an FM signal and noise is discussed in Chapter 4 An iteration technique is used to obtain qualitative results describing the operation of the System when the S/N ratio is much less than unity These results are then extended experimentally in Chapter 5

Chapter 5 presents some experimental results which verify the theory presented in this dissertation

1.4 Mathematical Formulation of the Problem

A typical APC System is shown in Fig. 1 1 If no noise is present, the input signal

$$e_c(t) = S \sin \phi_l(t) \quad S \sin(\omega_l t + \alpha \int_o^t e_m(\cdot)d\cdot) \tag{1.4.1}$$

and the output of the voltage controlled oscillator (VCO)

$e_c(t) = S \sin \phi_1(t)$

PHASE DETECTOR

MULTIPLIER

$BW = \omega_0$

$e_v(t) = \cos \phi_2(t)$

VOLTAGE CONTROLLED OSCILLATOR (VCO)

ω_0

FILTER H(p)

$e_d(t) = G_1 S \sin(\phi_2(t) - \phi_1(t)) = G_1 S \sin \phi(t)$

$e_o(t) = \int_0^t h(t-\lambda) e_d(\lambda) d\lambda$
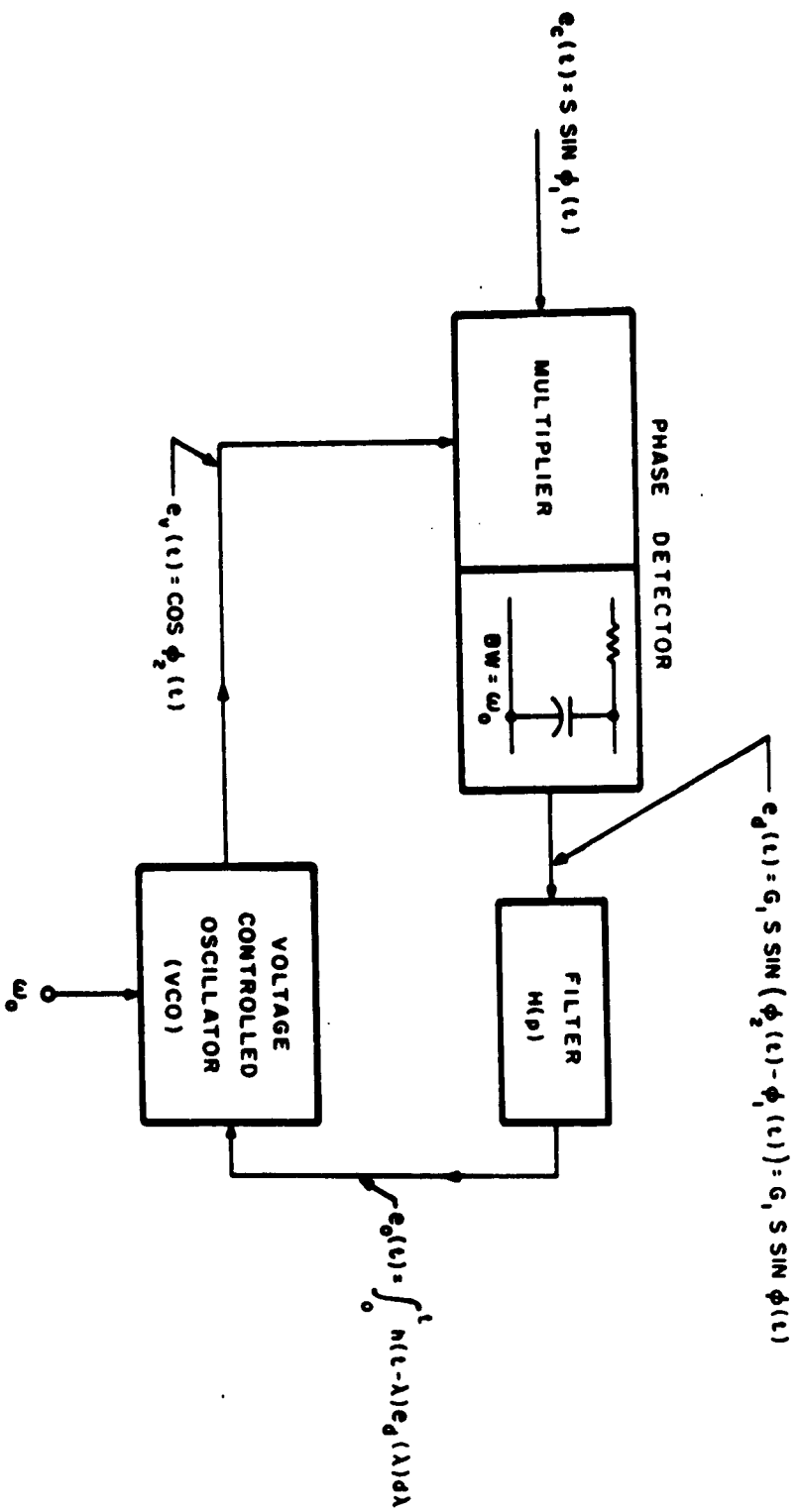
FIG. 1.1   AN AUTOMATIC PHASE CONTROL SYSTEM

A-100-Z-0041

$$e_v(t) = \cos \phi_2(t) = \cos(\omega_2 t + G_2 \int_0^t e_o(\lambda)d\lambda) \qquad (1.4.2)$$

are multiplied in the phase detector. The phase detector consists of a multiplier followed by a low-pass RC filter. It is assumed that the bandwidth, ω_0 , of the RC filter is much larger than the difference frequency, $\dot{\phi}_2 - \dot{\phi}_1$, obtained when multiplying e_c and e_v . The resulting difference frequency signal

$$e_d(t) = G_1 S \sin(\phi_2 - \phi_1)$$

$$= G_1 S \sin(\Omega t + G_2 \int_0^t e_o(\lambda)d\lambda - \alpha \int_0^t e_m(\lambda)d\lambda) \qquad (1.4.3)$$

represents the input to the filter. In the above equations

$$\Omega = \omega_2 - \omega_1$$

G_1 is the gain of the phase detector

G_2 is the sensitivity of the voltage
controlled oscillator (rad/sec/volt),

and $\alpha e_m(t)$ is the frequency modulation of the input signal. The voltage output of the filter,

$$e_o(t) = \int_0^t h(t - \lambda)e_d(\lambda)d\lambda \qquad (1.4.4)$$

corrects the frequency of the VCO, ($h(t)$ is the impulsive response of the filter). Thus the frequency of the VCO attempts to follow the instantaneous frequency of the input signal. When noise is present, the input voltage

$$e_c(t) = N(t) + S \sin \phi_1(t) \quad . \qquad (1.4.5)$$

The frequency of the VCO still attempts to follow the instantaneous frequency of the input signal, $\dot{\phi}_1$, but is hindered by frequency jitter caused by the input noise.

Due to practical limitations, the APC System is usually operated at an IF frequency. To obtain the IF frequency, the incoming signal (and associated noise) is heterodyned using a local oscillator and passed through an IF filter, having a center frequency, ω_2, which is the same as the initial frequency of the VCO. It will be assumed throughout this dissertation that the single tuned IF filter exhibits a completely flat response to all input signals. The frequency of the input signal, $\dot{\phi}_1$, need not be the same as the initial frequency of the VCO, ω_2. It is however, assumed that the bandwidth of the IF filter, α, is always much greater than $|\dot{\phi}_1 - \omega_2|$. The incoming noise is initially white Gaussian noise. After having been passed through the IF filter, the noise appears at the input of the APC System as narrow-band Gaussian noise, with a center frequency, ω_2, and a bandwidth, α.

THE RESPONSE OF AN APC SYSTEM TO AN FM SIGNAL

2.1 Introduction

The type of filter used greatly influences the performance of an APC System. It limits the frequency range of operation of the system and restricts the type of input signals to which it can be synchronized.

If no filter is used, the response of the system shown in Fig. 1.1, to an input signal, $e_c(t)$, is given by

$$\frac{d\phi}{dt} + \omega_n \sin \phi = \Omega - \alpha e_m(t) \tag{2.1.1}$$

where

$$\phi = \phi_2 - \phi_1$$

$$\Omega = \omega_2 - \omega_1$$

and

$$\omega_n = G_1 G_2 S \quad .$$

Equation (2.1.1) can be normalized by letting

$$\tau = \omega_n t$$

$$\Omega_n = \Omega/\omega_n$$

and

$$\alpha_n = \alpha/\omega_n \quad .$$

Equation (2.1.1), then can be written as

$$\frac{d\phi}{d\tau} + \sin \phi = \Omega_n - \alpha_n e_m(\tau) \quad . \tag{2.1.2}$$

The solution to this equation can be easily obtained if $\alpha_n = 0$; then

$$\phi(\tau) = -2 \tan^{-1} \frac{1}{\Omega_n} \cdot \qquad (2.1.3)$$

$$\left[\frac{-\left(1 - \sqrt{1 - \Omega_n^2}\right) + \left(1 + \sqrt{1 - \Omega_n^2}\right)e^{-\sqrt{1 - \Omega_n^2}\,\tau}}{1 - e^{-\sqrt{1 - \Omega_n^2}\,\tau}} \right] \cdot$$

In order that $\phi(\tau)$ be a real function,

$$|\Omega_n| \leq 1 \quad . \qquad (2.1.4)$$

It should be noted that this result can be obtained directly from Eq. (2.1.1). If $\alpha_n = 0$,

$$\sin \phi_{(\text{steady state})} = \Omega_n \quad . \qquad (2.1.5)$$

Equation (2.1.5) also requires that $|\Omega_n| \leq 1$. Therefore, the initial frequency error, Ω , must be less than the overall system sensitivity, ω_n , if the system is to synchronize to the frequency of the input signal. If

$$\alpha_n e_m(\tau) \ll \Omega_n \qquad (2.1.6)$$

$\phi(\tau)$ can be obtained using a perturbation technique. If ramp modulation is applied,

$$e_m(\tau) = \tau \quad . \qquad (2.1.7)$$

This system is incapable of synchronizing to a frequency ramp modulated signal.

If an RC low-pass filter with the transfer function

$$H(p) = -\frac{1}{1 + \frac{p}{\omega_a}}$$ (2.1.8)

is used, the response of the system of Fig. 1.1 to an output signal, $e_c(t)$, is[2.1]

$$\frac{d^2\phi}{dt^2} + \omega_a \frac{d\phi}{dt} + \omega_a\omega_n \sin \phi = \omega_a\left(\Omega - \alpha e_m(t) - \frac{\alpha}{\omega_a} \frac{de_m(t)}{dt}\right).$$ (2.1.9)

This system represents the equation of a pendulum with an applied force and a linear friction force.

If $\alpha = 0$, the steady state condition is

$$\sin \phi_{(steady\ state)} = -\Omega_n .$$ (2.1 10)

This again represents a system where $|\Omega_n| \leq |$. This system is incapable of synchronizing to the input signal if ramp modulation is applied (i.e., $e_m(t) = t$).

To enable the system to synchronize to a signal whose frequency varies linearly with time, when the signal is embedded in noise, an active phase lag filter as shown in Fig. 2 1 is employed.[2.2] Using this filter in the system shown in Fig. 1.1, the second-order nonlinear differential equation describing the performance of the system becomes

$$\frac{d^2\phi}{dt^2} + \omega_n\zeta\cos \phi \frac{d\phi}{dt} + \omega_n\omega_a \sin \phi = -\alpha \frac{de_m(t)}{dt}$$ (2.1.11)

$$A = -3 \times 10^6$$

$$\zeta = \frac{R_2}{R_1}$$

$$\omega_0 = \frac{1}{R_1 C_2}$$

$$H(p) \approx -|A|\left(\frac{\omega_0}{p} + 1\right) / \left(\frac{\omega_0}{p} + \zeta\right)$$

$$e_0(t) = -\zeta e_\theta(t) - \omega_0 \int_0^t e_\theta(\lambda)\,d\lambda, \qquad \zeta << \frac{A}{\omega_0}$$
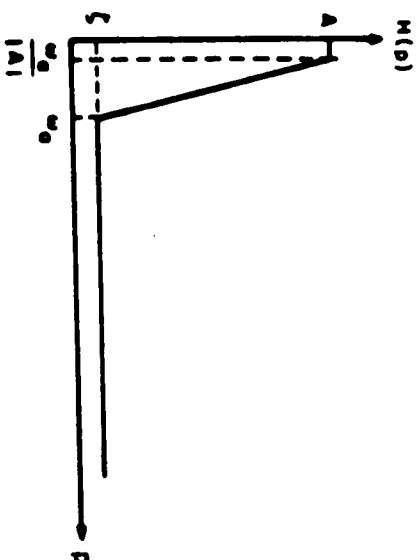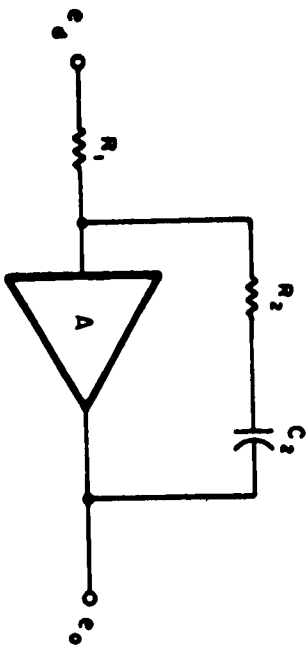
FIG 2.1 THE PHASE LAG FILTER USED TO ENHANCE A FREQUENCY MODULATED SIGNAL, EMBEDDED IN NOISE

A-100-2-0042

where
$$\zeta = R_2/R_1 ,$$
$$\omega_a = 1/R_1 C_2 , \text{ rad/sec},$$
$$\omega_n = G_1 G_2 S \text{ rad/sec},$$
$$\phi = \phi_2 - \phi_1 \text{ rad},$$
$$\Omega = \omega_2 - \omega_1 \text{ rad/sec}$$

and $\alpha e_m(t)$ represents the frequency modulation of the input signal. It should be noted that the loop gain (or sensitivity) of the system, ω_n, can be considered equal to unity, and its actual magnitude considered as part of the magnitude of the parameters of the phase lag filter.

Equation (2.1.11) can be simplified and written in normalized form:

$$\frac{d^2\phi}{d\tau^2} + \epsilon \cos \phi \frac{d\phi}{d\tau} + \sin \phi = -a \frac{de_m}{d\tau} \qquad (2.1.12)$$

where
$$\tau = \sqrt{\omega_a \omega_n} \, t ,$$
$$\epsilon = \sqrt{\omega_n/\omega_a} \, \zeta ,$$
$$a = \alpha/\omega_n \omega_a$$
and
$$\Omega_n = \Omega/\sqrt{\omega_a \omega_n} .$$

If $\epsilon = a = 0$, this equation becomes the well-known pendulum equation. If 'a' is not zero, the equation represents the motion of a pendulum with an applied force. The presence of the term, $\epsilon \cos \phi \frac{d\phi}{d\tau}$ represents a nonlinear friction force, which damps the motion of the pendulum as long as $|\phi| < \frac{\pi}{2}$. When $|\phi| > \frac{\pi}{2}$, the coefficient of friction, $\epsilon \cos \phi$ becomes negative.

Before proceeding to an analytical solution of the problem, it is useful to qualitatively consider the operation of the system using the results of a phase plane analysis.

2.2 Phase Plane Analysis[2,3]

If frequency ramp modulation is present,

$$a \frac{de_m}{d\tau} = \text{constant} .$$

To simplify the notation used, $\frac{de_m}{d\tau}$ is chosen equal to unity. Equation (2.1.12) can be rewritten as

$$\phi'' + \epsilon \cos \phi \, \phi' + \sin \phi = -a , \qquad (2.2.1)$$

where $\qquad \phi' = d\phi/d\tau$

and the equation of constant phase is therefore,

$$\frac{dp}{d\phi} = - \frac{a + \sin \phi + \epsilon p \cos \phi}{p} \qquad (2.2.2)$$

where $\qquad\qquad\qquad p = \frac{d\phi}{d\tau} .$

If the input signal, $e_c(t)$, is unmodulated (a = 0), a phase plane analysis shows that locking will always eventually occur. Depending on the initial conditions, locking will occur with the final phase error $0, 2\pi, 4\pi,..., 2n\pi$. The time required for locking to occur clearly increases as the final phase error increases.

It is seen from Eq. (2.2.1) that when the system is synchronized to an unmodulated input signal, the frequency error is zero. It has been shown[2,4] that the maximum permissable initial frequency error, Ω_n, (when the initial phase error (ϕ) is zero) for locking to occur (with a final phase error, ϕ = 0), increases as the damping coefficient, ϵ , increases. This is illustrated in Fig. 2.2. It would seem from Fig. 2.2
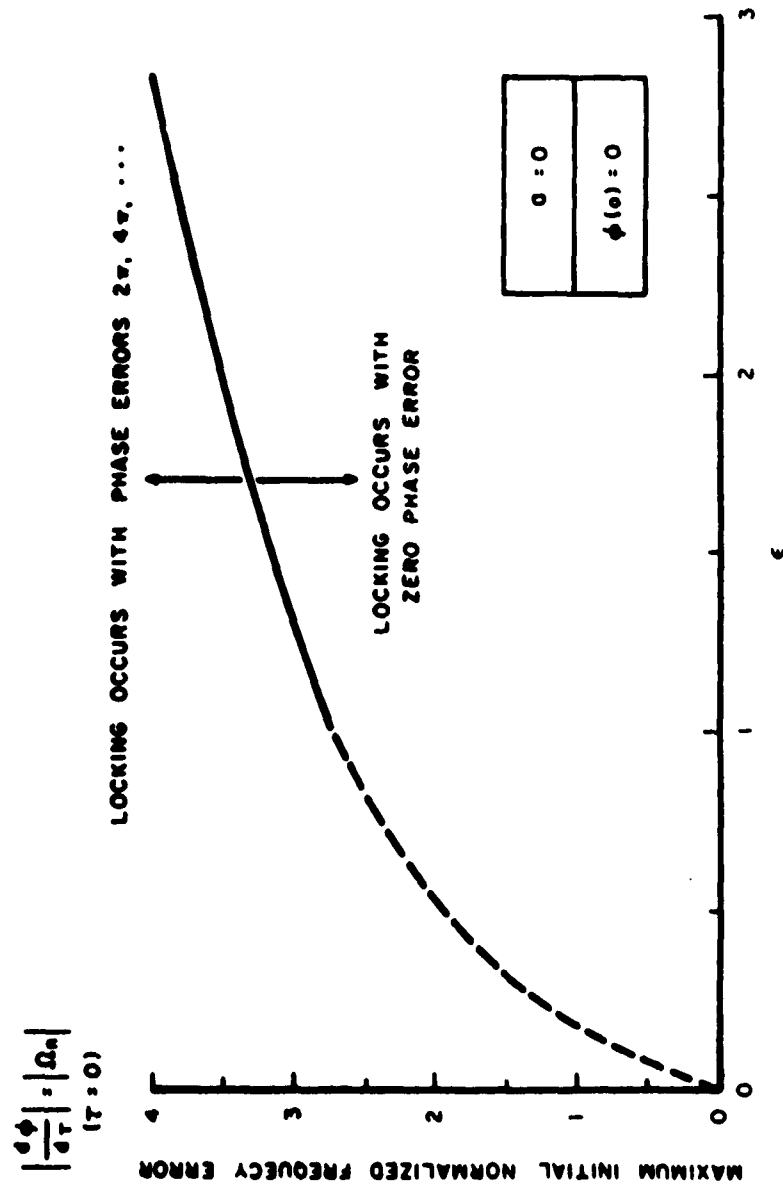
FIG. 2.2 MAGNITUDE OF MAXIMUM NEGATIVE FREQUENCY ERROR (WITH AN INITIAL PHASE OF ZERO) FOR THE APC SYSTEM TO SYNCHRONIZE TO AN UNMODULATED SIGNAL, WITH A FINAL PHASE ERROR OF ZERO

A-100-2-0043

that to insure locking about $\phi = 0$, ϵ should be made as large as possible. The APC System, however, was designed to operate under conditions involving a signal embedded in noise. As ϵ is increased, the noise emanating from the filter also increases. Thus, a compromise must be made.

As 'a' increases, the set of initial conditions for which locking will occur, decreases. From Eq. (2.2.1), it is seen that at steady state, $\sin \phi = -a$. Therefore, if $a > 1$, ϕ does not exist. To insure locking, 'a' must be less than unity. Even when 'a' is less than unity, locking cannot always be achieved.

The frequency error $\dot{\phi}(t)$ is given by,

$$\dot{\phi}(t) = \dot{\phi}_2(t) - \dot{\phi}_1(t) \quad . \tag{2.2.3}$$

For the case of a frequency ramp,

$$\dot{\phi}_1(t) = \omega_1 + at \quad . \tag{2.2.4}$$

It is seen that

$$\dot{\phi}(t) = \dot{\phi}_2(t) - \omega_1 - at \quad . \tag{2.2.5}$$

When $t = 0$, $\dot{\phi}(t) = \Omega$. Then, if $\Omega > 0$, even if $\dot{\phi}_2(t)$ does not change rapidly, $\dot{\phi}(t)$ will eventually go through zero. If, however, $\Omega < 0$, $\dot{\phi}_2(t)$ must follow rapidly and overtake $\dot{\phi}_1(t)$ to cause $\dot{\phi}(t)$ to go through zero. It is apparent that $\dot{\phi}(t)$ going through zero need not be a sufficient condition for locking to occur. It is, however, a necessary condition.

Figure 2.3 is a sketch of a phase portrait when $\epsilon = \sqrt{2}$, and $a = 1/4$. It is seen from this figure that a limit cycle of the second kind exists. If the initial frequency error, Ω_n , is more negative than the frequency of the limit cycle,

-16-

BELOW THIS PHASE PATH
LOCKING OCCURS WITHIN $|\phi| \leq \pi$

$\tau = \sqrt{\omega_g \, \omega_n} \; t$

ϕ

2π

$\frac{3\pi}{2}$

π

$\frac{\pi}{2}$

$\frac{d\phi}{d\tau}$

Ω_o

A DIVERGING PATH

$a = \frac{1}{4}$

$\epsilon = \frac{\sqrt{2}}{2}$

$-\frac{\pi}{2}$

$-\pi$

$-\frac{3\pi}{2}$

-2π

NO LOCKING CAN OCCUR
BELOW THIS LIMIT CYCLE

A LIMIT CYCLE OF THE SECOND KIND
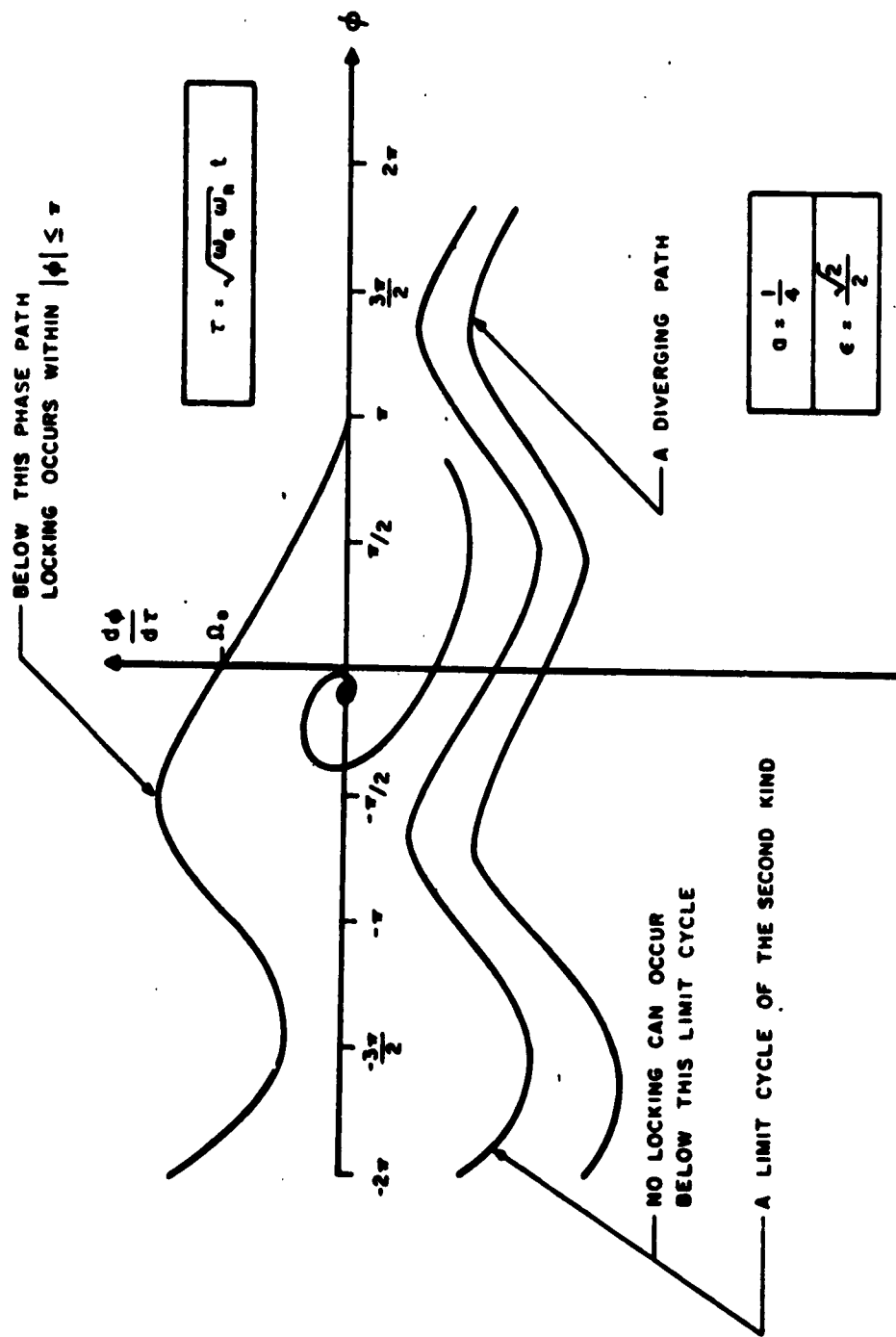
FIG. 2.3   PHASE SKETCH, SHOWING SECOND ORDER LIMIT CYCLE WHEN $a = \frac{1}{4}$

A-100-Z-0044

locking will never occur. If, however, the initial frequency error, Ω_n , lies above the limit cycle, locking will always occur. In particular, if the initial frequency error is greater than Ω_B locking will not occur when the phase error, ϕ , is less than π , but the system will eventually lock

As 'a' increases the limit cycle becomes less negative. If, a $>$ 1/2 , the limit cycle no longer exists. The effect of this on the system performance is illustrated in Fig. 2.4 for a $=$ $\sqrt{3}/2$. The maximum negative value of Ω_n that will allow locking has decreased. In addition, if $\Omega_n > 0$, locking still may not occur. A typical divergent path is shown for the case $\Omega_n = \Omega_0$. However, if Ω_n is even larger than Ω_0 , such as $\Omega_n = \Omega_1$, it is possible that locking may occur about $\phi = \frac{5\pi}{3}$. Thus, the frequency axis of the phase plane (corresponding to zero phase error) can be broken into alternating "bands." If the frequency error is more negative than Ω_A , no locking will occur. If the frequency error is bounded by

$$\Omega_A < \Omega_n < \Omega_B ,$$

(2.2.6)

the system will synchronize to the input signal and the resulting phase error will be

$$\phi_{\text{(steady state)}} : -\sin^{-1} \frac{\sqrt{3}}{2} := -\frac{\pi}{3}$$

(2.2.7)

If the frequency error is bounded by Ω_B and an upper-bound Ω_C , so that,

$$\Omega_B \leq \Omega_n \leq \Omega_C$$

(2.2.8)

the system will not synchronize to the incoming signal. If the frequency is bounded by Ω_C and some upper-bound Ω_D
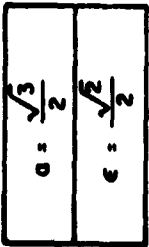
FIG. 2.4 PHASE SKETCH SHOWING REGION OF LOCK WHEN $a = \frac{\sqrt{3}}{2}$

A-100-Z-0045

the system will lock and a resultant phase error

$$\phi_{(\text{steady state})} = -\sin^{-1}\frac{\sqrt{3}}{2} + 2\pi = \frac{5\pi}{3} \qquad (2.2.9)$$

will occur.

When noise is present, it can easily push the frequency error from a stable band to an unstable band. Thus, when operating with noise, 'a' is adjusted to be less than $\frac{1}{2}$. This requires that the slope of the frequency ramp, α, satisfy the inequality

$$\alpha < \frac{1}{2}(\omega_a \omega_n) . \qquad (2.2.10)$$

This result is significant in as much as it sets a lower bound on $\omega_a \omega_n$. In Chapter 4, it will be shown that $\omega_a \omega_n$ should be reduced in order to reduce phase jitter in the output, e_v. Equation (2.2.10) therefore limits the amount by which the phase jitter can be decreased.

It is also of interest to determine the time required for the system to lock, given a set of initial conditions. To determine the time required to move between two points on a path in the phase plane, the equation of the path is required. In any given problem, an approximate path can be found,[2.5] and the time, τ, can be found:[2.6]

$$\tau_{ab} = \int_a^b \frac{d\phi}{\phi'} . \qquad (2.2.11)$$

As previously noted, if $a = \epsilon = 0$, Eq. (2.2.1) reduces to the pendulum equation. In this case, the equation of constant phase Eq. (2.2.2) can be integrated. If, when $\phi = 0$, $\phi'(0) = \Omega_n$; ϕ' becomes

$$\phi' = \sqrt{\Omega_n^2 - 4 \sin^2(\frac{\phi}{2})} \qquad (2.2.12)$$

and

$$\tau_{ab} = \int_a^b \frac{d\left(\frac{\phi}{2}\right)}{\sqrt{\left(\frac{\Omega_n}{2}\right)^2 - \sin^2\left(\frac{\phi}{2}\right)}} \quad . \tag{2.2.13}$$

The time, τ , that it takes a pendulum to move $\frac{1}{4}$ of a cycle is[2.7]

$$\tau = K(k^2) \tag{2.2.14}$$

where $K(k^2)$ is the complete elliptic integral of the first kind. When $\Omega_n < 2$,

$$k^2 = \left(\frac{\Omega_n}{2}\right)^2 = \sin^2\left(\frac{\phi_{max}}{2}\right) \quad . \tag{2.2.15}$$

If $\phi_{max} \leq 128°$, then $|\Omega_n| \leq 1.8$. The time, T , (in seconds) required by the pendulum to complete a full period is bounded by

$$2\pi \leq (\omega_a\omega_n)^{\frac{1}{2}} T \leq 9 \quad . \tag{2.2.16}$$

When $\Omega_n > 2$, the motion of the pendulum is no longer bounded. The pendulum now continually rotates in one direction. If some damping were present, the path of the pendulum would be perturbed, and the pendulum would rotate until, when $\phi = 2n\pi$, the velocity of the pendulum, Ω_n, became less than two.

The concept of perturbing the motion of the pendulum by a friction force and an applied force will be discussed in detail in the following section.

2.3 A Perturbation Solution[2.8]

The equation describing the APC System can be rewritten in the form:

$$\phi'' + \sin \phi = -\epsilon \cos \phi \, \phi' - ae_m' \tag{2.3.1}$$

If ϵ and 'a' are each less than unity, a solution using the perturbation technique can be found. For locking to occur, it was previously shown that 'a' should be less than $\frac{1}{2}$. No such fundamental restriction on ϵ exists. As previously discussed, ϵ should not be too large as it increases the noise in the system. Although choosing ϵ less than unity restricts the range of usefulness of the solution, the solution obtained using the perturbation technique is valid even when the phase error, $\phi(\tau)$, and the frequency error $\phi'(\tau)$ are large. This should be contrasted to the results that can be obtained using a linear analysis,[2,9] where, although ϵ can take on any value, the solution is restricted to small values of $\phi(\tau)$.[*]

A solution to Eq. (2.3.1) can be written in the form:

$$\phi(\tau) = \Phi_o(\tau) + \epsilon \, \Phi_1(\tau) + a \, \Phi_2(\tau) + 0 \, (\epsilon^2, a^2, \epsilon a) . \quad (2.3.2)$$

Substituting Eq. (2.3.2) into Eq. (2.3.1) and neglecting second order terms, we get:

$$\Phi_o'' + \sin \Phi_o = 0 \qquad\qquad (2.3.3)$$

$$\Phi_1' + \frac{\sin \Phi_o}{\Phi_o'} \, \Phi_1 = - \frac{1}{\Phi_o'} \int_o^\tau \Phi_o'^2 \cos \Phi_o \, d\tau \qquad (2.3.4)$$

and

$$\Phi_2' + \frac{\sin \Phi_o}{\Phi_o'} \, \Phi_2 = - \frac{1}{\Phi_o'} \int_o^\tau e_m'(\tau) \Phi_o'(\tau) d\tau . \qquad (2.3.5)$$

---

[*] See Appendix A.

Without any loss of generality, the solution to Eq. (2.3.1) can be simplified if the initial conditions are:

$$\phi(o) = 0 = \Phi_o(o) \qquad (2.3.6)$$

and

$$\phi'(o) = \Omega_n = \sqrt{4k^2} = \Phi_o'(o) \qquad (2.3.7)$$

and

$$\Phi_1(o) = \Phi_2(o) = \Phi_1'(o) = \Phi_2'(o) = 0 \qquad (2.3.8)$$

where

$$k^2 = \sin^2\left(\frac{\phi_{max}}{2}\right) . \qquad (2.3.9)$$

Equation (2.3.3) is the equation of a pendulum having an initial velocity, Ω_n, but no initial displacement. As seen previously, to keep the motion of the pendulum bounded, i.e.,

$$-\pi \le \Phi_o \le \pi \qquad (2.3.10)$$

the initial velocity of the pendulum, Φ_o', is

$$|\Phi_o'(o)| = |\Omega_n| < 2 . \qquad (2.3.11)$$

The solution to Eq. (2.3.3) is given by

$$\Phi_o(\tau) = 2 \sin^{-1}\left(\sqrt{k^2}\ \mathrm{sn}\tau\right) . \qquad (2.3.12)$$

Equation (2.3.4), Eq. (2.3.5) and the differential equations resulting from second-order terms, are all first-order linear

differential equations, with time varying coefficients. The solution to this type of equation is well known.

The phase error, $\phi(\tau)$, is then

$$\phi(\tau) = 2 \sin^{-1}\left(\sqrt{k^2}\,sn\tau\right) \qquad (2.3.13)$$

$$-\epsilon\left(\frac{2cn\tau}{3\sqrt{k^2}}\right)\int_0^\tau d\tau \left[\frac{(1 - k^2)\tau + (2k^2 - 1)E(am\tau,k^2) + 2k^2 sn\tau cn\tau dn\tau}{cn^2\tau}\right]$$

$$+a\left(\frac{cn\tau}{\sqrt{k^2}}\right)\int_0^\tau dx \left[\frac{\int_0^x \sin^{-1}\left(\sqrt{k^2}\,snu\right)\dfrac{de_m(u)}{du}\,du}{cn^2 x}\right] + 0(\epsilon^2, a^2, \epsilon a)$$

where $E(am\tau, k^2)$ is the elliptic integral of the second kind.[2.10]

The elliptic functions $sn\tau$ and $cn\tau$ are periodic and can be represented by a Fourier series.[2.11]

$$sn\tau = \frac{2\sqrt{q}\cdot\pi}{\sqrt{k^2}\,K(k^2)}\left[\frac{\sin x}{1 - q} + \frac{q\sin 3x}{1 - q^3} + \frac{q^2\sin 5x}{1 - q^5} + \ldots\right] \quad (2.3.14)$$

and

$$cn\tau = \frac{2\sqrt{q}\,\pi}{\sqrt{k^2}\cdot K(k^2)}\left[\frac{\cos x}{1 + q} + \frac{q\cos 3x}{1 + q^3} + \frac{q^2\cos 5x}{1 + q^5} + \ldots\right] \quad (2.3.15)$$

where
$$x = \frac{\pi\tau}{2K(k^2)}$$

and
$$q = e^{-\pi\left[\frac{K(1 - k^2)}{K(k^2)}\right]} .$$

If $cn\tau$ is approximated by the first term in the series, $\phi(\tau)$ can be easily determined.

2.3 1 The Response to a Frequency Ramp Modulated Signal

If $e'_m(\tau) = 1$ (the case of a frequency ramp), the complete solution is

$$\phi(\tau) \simeq \pm 2 \sin^{-1}\left(\sqrt{k^2} \, sn\tau\right) \tag{2.3.16}$$

$$\mp\epsilon\left(\frac{2\sqrt{k^2}}{3}\right)cn\tau\left[\frac{(1 - k^2)K^4(1 + q)^2}{q\pi^4}\left(\frac{\pi\tau}{2K} \tan \frac{\pi\tau}{2K} + \ell n \mid \cos \frac{\pi\tau}{2K} \mid\right)\right.$$

$$+(2k^2 - 1)\frac{K^2(1 + q)^2}{4q\pi^2}\left(\frac{\pi\tau}{2K} \tan \frac{\pi\tau}{2K} + \ell n \mid \cos \frac{\pi\tau}{2K} \mid\right)$$

$$-(2k^2 - 1)\frac{2K^2(1 + q)}{\pi^2} \ell n \mid \cos \frac{\pi\tau}{2K} \mid$$

$$\left.-2 \, \ell n\left(\frac{4\sqrt{q}}{\frac{2K}{\pi} \sqrt{k^2}(1 + q)}\right) - 2 \, \ell n \mid \cos \frac{\pi\tau}{2K} \mid\right]$$

$$-a\left(\frac{\sqrt{k^2}K^3(1+q)^2}{2\pi^3 q}\right)$$

$$cn\tau\left[\tan \frac{\pi\tau}{2K} \sin^{-1}\left(\frac{2\pi\sqrt{q}}{K(1 - q)} \sin \frac{\pi\tau}{2K}\right)\right.$$

$$\left.+ \ell n \left| \frac{\frac{2\pi\sqrt{q}}{K(1 - q)} \cos \frac{\pi\tau}{2K} + \sqrt{1 - \frac{4\pi^2 q}{K^2(1 - q)^2} \sin^2\frac{\pi\tau}{2K}}}{1 + \frac{2\pi\sqrt{q}}{K(1 - q)}} \right| \right]$$

where $0 \leq \tau \leq K(k^2)$.

It is seen that k^2 is a parameter of Eq. (2.3.16). As the system locks, this parameter decreases, as does the maximum value of the phase error, ϕ_{max} , and the maximum frequency error. Therefore, when using Eq. (2.3.16), a new set of initial conditions must be chosen whenever the phase error becomes equal to zero. For example, consider that at time,

τ_i , the phase error became zero. Then the frequency error at time, τ_i , is Ω_n^i . This frequency error can be determined either by differentiating Eq. (2.3.16), or graphically. It was found that an estimate of Ω_n^i obtained graphically by approximating Ω_n^i by:

$$\Omega_n^i = \frac{d\phi}{d\tau}\bigg|_{\tau = \tau_i} \simeq \frac{\Delta\phi}{\Delta\tau}\bigg|_{\tau = \tau_i} \qquad (2.3.17)$$

yielded satisfactory results. Knowing Ω_n^i , k_i^2 can be determined from the relation:

$$k_i^2 = \frac{\left(\Omega_n^i\right)^2}{4} \qquad (2.3.18)$$

when $\Omega_n^i > 0$, $\Phi_o^i(\tau)$ is positive. $\Phi_1^i(\tau)$, representing the friction term, always opposes the motion of $\Phi_o^i(\tau)$ (the pendulum term) and is therefore negative. When $\Omega_n^i < 0$, $\Phi_o^i(\tau)$ is negative, $\Phi_1^i(\tau)$ is now positive. Thus, the signs preceding Φ_o and Φ_1 alternate as shown in Eq. (2.3.16). $\Phi_2^i(\tau)$ maintains the same sign since it represents the slope of the frequency ramp.

Equation (2.3.16) reduces to the expression obtained using the simple linearization procedure as the maximum phase error becomes small. At steady state $\phi(\infty)$ approaches '-a'.

The solution for the case of a frequency ramp modulated signal is shown in Fig. 2.5 In this example the parameters chosen were:

$$a = 0.157 \ , \ \epsilon = 0.25 \ , \qquad (2.3.19)$$

and $\quad \frac{d\phi}{d\tau}\bigg|_{\tau = 0} = \Omega_{n_o} = 1.6 \ , \ $ when $\phi(o) = 0$. $\qquad (2.3.20)$
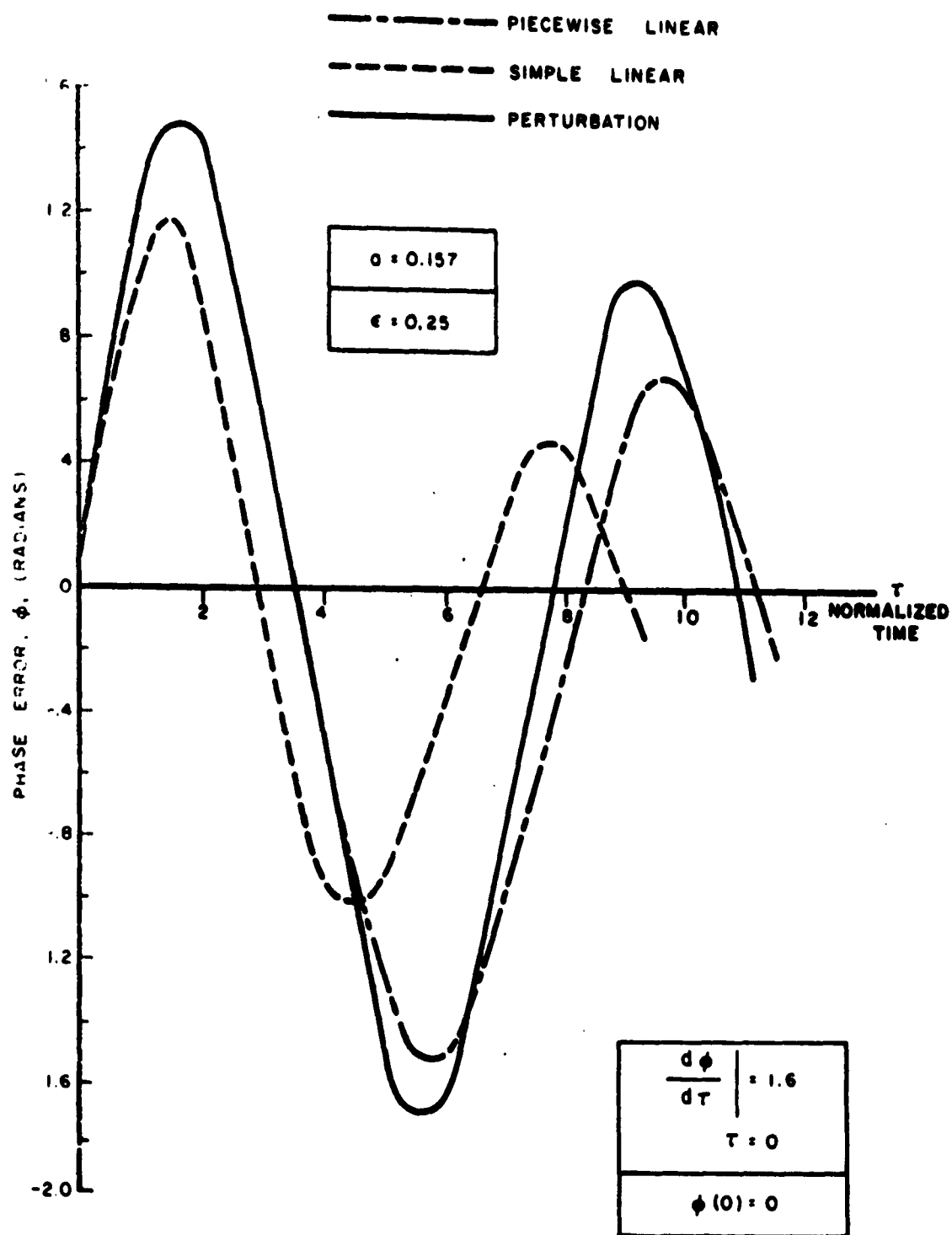
FIG. 2.5   A COMPARISON OF THE APPROXIMATE SOLUTIONS USED TO OBTAIN THE RESPONSE OF THE APC SYSTEM TO A FREQUENCY RAMP MODULATED SIGNAL

An interesting characteristic of the perturbation solution, as
seen in Fig. 2.5 is that not only does the period decrease with
time, τ , but the negative half cycle takes longer to complete
than does the preceding positive half cycle. The reason for
this is that on the positive half cycle $\phi_{max} < \frac{\pi}{2}$. The co-
efficient of friction, $\epsilon \cos \phi$, although small, is still
positive. During the negative half cycle, due to the offset
caused by the frequency ramp, the friction term has less ef-
fect on the result. In this example, $|\phi_{max}| > \frac{\pi}{2}$, and the
friction term is actually negative over part of the negative
half cycle. Thus, the time-to-complete the negative portion
of the cycle is increased.

As the magnitude of the phase error decreases the per-
turbation technique yields results similar to those obtained
using the simple linear analysis.

Although the perturbation technique yields more accurate
results than the linear analysis it is somewhat more difficult
to use. A simple technique, which takes into account the pos-
sibility of negative damping, has also been investigated. This
is a piecewise-linear analysis and is here described.

2.4 A Piecewise-Linear Solution

A piecewise-linear solution was obtained using the ap-
proximation shown in Fig. 2.6. Using this solution the ef-
fects of various types of frequency modulation were investi-
gated. In addition, the maximum initial frequency error, to
achieve locking, was determined. This result is most impor-
tant when a $\neq$ 0 , since when a $=$ 0 the APC System will
eventually synchronize to the input signal.

Rewriting Eq. (2.2.1) for convenience,

$$\frac{d^2\phi}{d\tau^2} + \epsilon \cos \phi \frac{d\phi}{d\tau} + \sin \phi - -a \frac{de_m}{d\tau} \qquad (2.2.1)$$
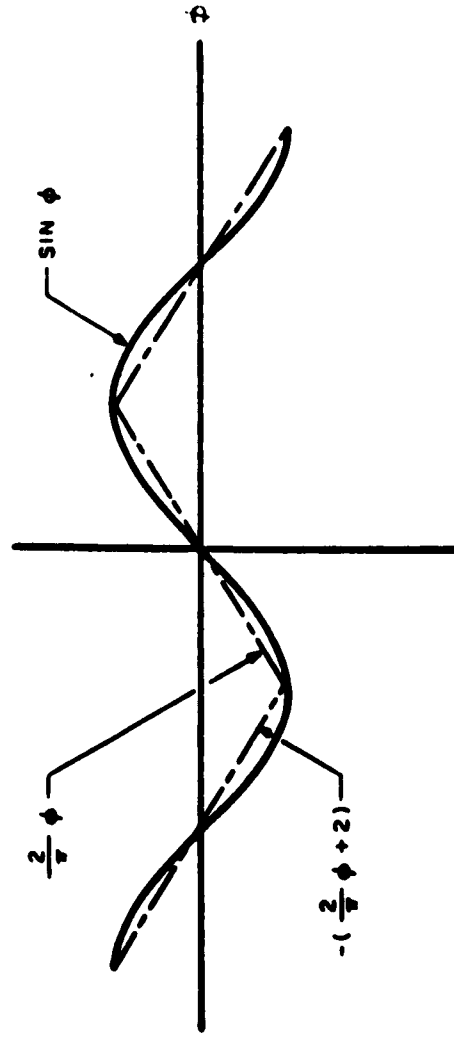
PIECEWISE – LINEAR
APPROXIMATION OF A
SINE WAVE
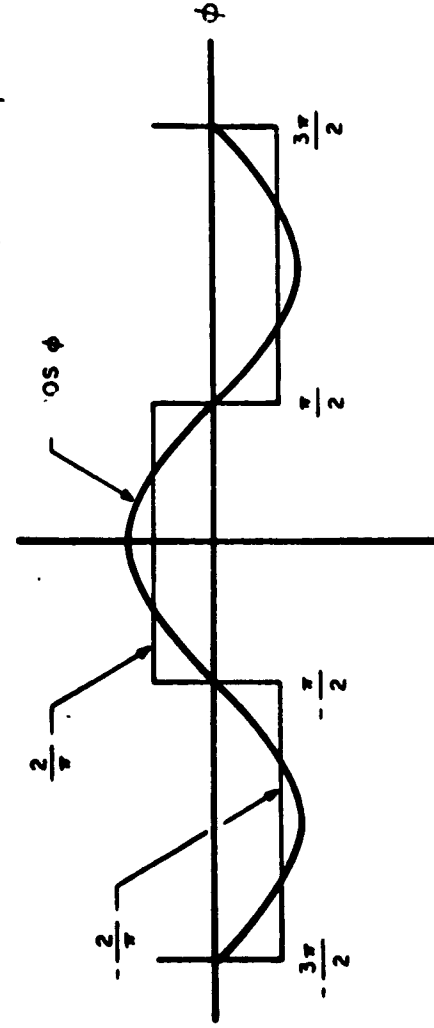
PIECEWISE – LINEAR
APPROXIMATION OF A
COSINE WAVE

SIN φ

$\frac{2}{\pi} \phi$

$-(\frac{2}{\pi} \phi + 2)$

COS φ

$\frac{2}{\pi}$

$-\frac{2}{\pi}$

$\frac{3\pi}{2}$

$\frac{\pi}{2}$

$-\frac{\pi}{2}$

$-\frac{3\pi}{2}$

A-100-2-0047

FIG. 2.6   A PIECEWISE LINEAR APPROXIMATION

and using Fig. 2.6, the piecewise-linear equations become:

$$\frac{d^2\phi}{dv^2} + \sqrt{\frac{2}{\pi}}\, \epsilon\, \frac{d\phi}{dv} + \phi = -\sqrt{\frac{\pi}{2}}\, a\, \frac{de_m}{dv} \quad, \quad -\frac{\pi}{2} \leq \phi \leq \frac{\pi}{2} \qquad (2.4.1)$$

and

$$\frac{d^2\phi}{dv^2} - \sqrt{\frac{2}{\pi}}\, \epsilon\, \frac{d\phi}{dv} - \phi = \pi - \sqrt{\frac{\pi}{2}}\, a\, \frac{de_m}{dv} \quad, \quad -\frac{3\pi}{2} \leq \phi \leq -\frac{\pi}{2}$$
$$(2.4.2)$$

where

$$v = \sqrt{\frac{2}{\pi}}\, \tau = \sqrt{\frac{2}{\pi}\, \omega_a \omega_n}\; t \quad .$$

Equation (2.4.1) and Eq. (2.4.2) can be normalized. The normalized equations are:

$$\frac{d^2\phi}{dv^2} + \epsilon_1\, \frac{d\phi}{dv} + \phi = -a_1 \frac{de_m}{dv} \quad, \quad -\frac{\pi}{2} \leq \phi \leq \frac{\pi}{2} \qquad (2.4.3)$$

and

$$\frac{d^2\phi}{dv^2} - \epsilon_1\, \frac{d\phi}{dv} - \phi = \pi - a_1\, \frac{de_m}{dv} \quad, \quad -\frac{3\pi}{2} \leq \phi \leq -\frac{\pi}{2} \qquad (2.4.4)$$

where

$$\epsilon_1 = \sqrt{\frac{2}{\pi}}\, \epsilon = \sqrt{\frac{2}{\pi}\left(\frac{\omega_n}{\omega_a}\right)}\, \zeta$$

and

$$a_1 = \sqrt{\frac{\pi}{2}}\, a = \sqrt{\frac{\pi}{2}}\, \frac{\alpha}{(\omega_a \omega_n)} \quad .$$

2.4.1 The Response to a Frequency Ramp

Using the case of ramp modulation, a comparison was made between the results obtained using the perturbation piecewise-linear, and simple-linear techniques. In this example, the parameters chosen were:

$$a = 0.157, \quad \epsilon = 0.25$$

and

$$\left. \frac{d\phi}{d\tau} \right|_{\tau \, = \, 0} = \Omega_{n_o} = 1.6 \, , \quad \text{when} \quad \phi(o) = 0 \, .$$

The piecewise-linear solution for this case is:

$$\phi(\tau) = e^{-0.0\upsilon \cdot} \left(\alpha_1 \cos \sqrt{\frac{2}{\pi}} \, \tau + \alpha_2 \sin \sqrt{\frac{2}{\pi}} \, \tau \right) - \frac{\pi}{2}(0.157) \tag{2.4.5}$$

and

$$\phi(\tau) = \beta_1 e^{0.88\tau} + \beta_2 e^{-0.72\tau} - \pi \left(1 - \frac{0.157}{2} \right) \, . \tag{2.4.6}$$

The constants, α_1, α_2, β_1 and β_2 can be evaluated using the initial conditions and the boundary conditions. The simple-linear solution for this case is

$$\phi(\tau) = e^{-\frac{\tau}{8}}(\gamma_1 \cos \tau + \gamma_2 \sin \tau) - 0.157 \, . \tag{2.4.7}$$

A comparison of Eq. (2.4.5) and Eq. (2.4.7) reveals that the frequency of the piecewise-linear solution is $\sqrt{\frac{2}{\pi}}$ times the frequency of the simple-linear solution. In addition the solution obtained using the simple-linear technique has greater damping

than the result given by Eq. (2.4.5) for the piecewise-linear approximation.

These differences are illustrated in Fig. 2.5 which compares the results obtained using the perturbation, piece-wise-linear, and the simple-linear solutions. It is clear, from this figure that the piecewise-linear solution is a better approximation of the perturbation solution than the simple linear solution.

2.4.2 Initial Conditions Required to Insure Locking

Using Eq. (2.4.4), the necessary and sufficient conditions for an APC System to synchronize (lock) to a frequency ramp modulated signal can be shown to be:

$$\left|\frac{d\phi}{d\tau}\right| = |\Omega_n| < \begin{cases} \sqrt{\frac{\pi}{2}}\left(1 - \frac{\epsilon_1}{2}\right)(1 - a) \ , \ \epsilon_1 << 2 \ \text{(underdamped)} \\[3mm] \sqrt{\frac{\pi}{2}}(\sqrt{2} - 1)(1 - a) \ , \ \epsilon_1 = 2 \ \text{(critically damped)} \\[3mm] \sqrt{\frac{\pi}{2}}\frac{(1 - a)}{\epsilon_1} \qquad , \ \epsilon_1 >> 2 \ \text{(overdamped)} \end{cases}$$

$$(2.4.8)$$

when

$$\phi = -\frac{\pi}{2} \ \text{radians}$$

and where

$$a \leq 1 \ . \qquad\qquad (2.4.9)$$

The result obtained using the piecewise-linear solution Eq. (2.4.8) is compared with the result obtained graphically from a set of phase portraits[2.12] in Fig. 2.7. It is seen
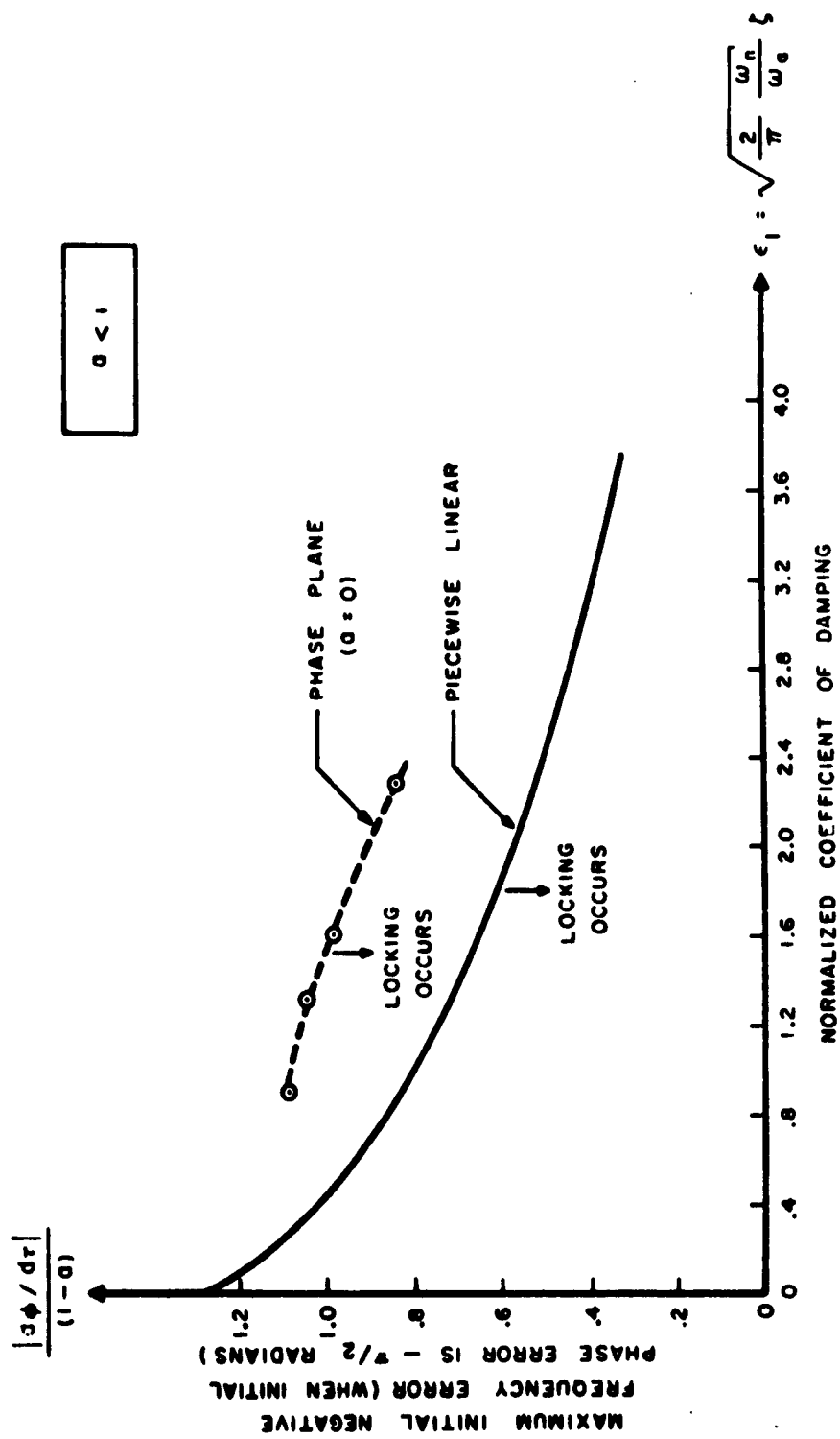
FIG. 2.7 THE CONDITIONS FOR THE APC SYSTEM TO LOCK TO A FREQUENCY RAMP MODULATED SIGNAL

A-100-Z-0048

from this figure that when the initial phase error is $-\frac{\pi}{2}$ radians, the maximum frequency error (for locking to occur) decreases as the normalized damping coefficient, ϵ_1 , increases. This is due to the fact that when the phase error, ϕ , becomes more negative than $-\frac{\pi}{2}$ radians, the damping force becomes negative. This negative damping force makes locking more difficult. However, locking is still possible when the phase error exceeds $-\frac{\pi}{2}$ radians.

The result obtained using a phase plane analysis is similar to the result obtained using the piecewise-linear technique. The approximation of a constant coefficient of damping in the piecewise-linear analysis results in the differences between the two curves. These results should be contrasted to the result obtained from a simple linear analysis. Using the simple linear analysis, it can be shown that locking will always occur; a result which is obviously incorrect when $a \neq 0$. (It is noted however, that the simple linear analysis is only valid for small phase errors. It should not be used to discuss locking phenomenon, which requires a knowledge of the systems' response when the phase error is large).

2.4.3 The Response to an FM Signal

The piecewise-linear solution can also be used to obtain the response of the APC System to an arbitrary frequency modulated signal. To illustrate this, consider a sinusoidally phase modulated signal,

$$e_c(t) = \sin (\omega_1 t - A \sin \omega_m t) . \qquad (2.4.10)$$

Then

$$\frac{d^2\phi}{dt^2} + \omega_n \zeta \cos \phi \frac{d\phi}{dt} + \omega_a \omega_n \sin \phi = -A \omega_m^2 \sin \omega_m t \qquad (2.4.11)$$

and

$$\frac{d^2\phi}{d\tau^2} + \epsilon \cos \phi \frac{d\phi}{d\tau} + \sin \phi = -A\left(\frac{\omega_m^2}{\omega_a\omega_n}\right)\sin\left(\frac{\omega_m}{\sqrt{\omega_a\omega_n}}\right)\tau \quad . \quad (2.4.12)$$

The piecewise-linear equations become:

$$\frac{d^2\phi}{dv^2} + \epsilon_1 \frac{d\phi}{dv} + \phi = -\frac{\pi}{2} A\left(\frac{\omega_m^2}{\omega_a\omega_n}\right)\sin\sqrt{\frac{\pi}{2}}\left(\frac{\omega_m}{\sqrt{\omega_a\omega_n}}\right)v \quad , \quad -\frac{\pi}{2} \le \phi \le \frac{\pi}{2}$$

$$(2.4.13)$$

and

$$\frac{d^2\phi}{dv^2} - \epsilon_1 \frac{d\phi}{dv} - \phi = \pi - \frac{\pi}{2} A\left(\frac{\omega_m^2}{\omega_a\omega_n}\right)\sin\sqrt{\frac{\pi}{2}}\left(\frac{\omega_m}{\sqrt{\omega_a\omega_n}}\right)v \quad , \quad -\frac{3\pi}{2} \le \phi \le -\frac{\pi}{2} \quad .$$

$$(2.4.14)$$

Equations (2.4.13) and Eq. (2.4.14) are linear and can easily be solved. If the modulation was not sinusoidal, but was some periodic function, the phase error, $\phi(t)$, could be determined using superposition. If $\phi(t)$ is to represent the result of a demodulation, then $|\phi| \le \frac{\pi}{2}$, and the amplitude of $\phi(t)$ must be independent of ω_m. Solving Eq. (2.4.13), the steady state phase error becomes:

$$\phi(t)_{\text{(steady state)}} = \frac{A\delta^2(\delta^2 - 1)}{(\delta^2 - 1)^2 + \epsilon_1^2\delta^2}\left[\sin \omega_m t + \frac{\epsilon_1\delta}{\delta^2 - 1}\cos \omega_m t\right]$$

$$(2.4.15)$$

where

$$\delta^2 = \frac{\pi}{2}\left(\frac{\omega_m^2}{\omega_a\omega_n}\right) \qquad\qquad (2.4.16)$$

-35-

and

$$\epsilon_1 = \sqrt{\frac{2}{\pi} \left(\frac{\omega_n}{\omega_a}\right)} \zeta \quad . \tag{2.4.17}$$

It is seen that if

$$\delta^2 >> 1 \tag{2.4.18}$$

and

$$\delta^2 >> \epsilon_1 \tag{2.4.19}$$

the steady state phase error, $\phi(t)$, will faithfully reproduce the input phase modulation. In this case

$$\phi(t)_{\text{steady state}} = A \sin \omega_m t \quad . \tag{2.4.20}$$

Using a simple linear analysis the steady state response of the APC System to a phase modulated signal

$$e_c(t) = \sin (\omega_1 t - A \sin \omega_m t) \tag{2.4.21}$$

is

$$\phi(t)_{\text{steady state}} = \frac{A \Delta^2 (\Delta^2 - 1)}{(\Delta^2 - 1)^2 + \epsilon \Delta^2} \left[\sin \omega_m t + \frac{\epsilon \Delta}{\Delta^2 - 1} \cos \omega_m t \right] \tag{2.4.22}$$

where

$$\Delta^2 = \left(\frac{\omega_m^2}{\omega_a \omega_n}\right) = \frac{2}{\pi} \delta^2 \tag{2.4.23}$$

and

$$\epsilon = \sqrt{\frac{\pi}{2}} \epsilon_1 = \sqrt{\frac{\omega_n}{\omega_a}} \zeta \quad . \tag{2.4.24}$$

Thus, it is seen that similar results are obtained using the simple linear technique.

In order that the APC System perform as a phase demodulator Eq. (2.4.18) and Eq. (2.4.19) must be satisfied. Equation (2.4.18) requires that the modulation frequency

$$\omega_m > > \sqrt{\omega_a \omega_n} \qquad (2.4.25)$$

where $\sqrt{\omega_a \omega_n}$ is the effective coefficient of integration of the phase lag filter. Equation (2.4.19) requires that

$$\omega_m > > \omega_n \zeta \qquad (2.4.26)$$

where $\omega_n \zeta$ represents the effective coefficient of damping of the filter

If in steady state operation, $\phi(t)$ exceeds $\frac{\pi}{2}$ (this occurs if $A > \frac{\pi}{2}$, the phase error $\phi(t)$ becomes distorted and no longer faithfully reproduces the input modulation. Although Eq. (2.4.20) shows that it is possible for $\phi(t)$ to be proportional to the modulation, the voltage, $e_d(t)$, is proportional to the $\sin \phi$ not ϕ. Then

$$e_d(t) \simeq G_1 \sin \left(A \sin \omega_m t \right) \qquad (2.4.27)$$

Expanding in a Fourier series, Eq. (2.4.27) becomes:

$$e_d(t) \simeq 2G_1 J_1(A) \sin \omega_m t + 2G_1 J_3(A) \sin 3 \omega_m t + \dots \qquad (2.4.28)$$

If $A \geq 1$, the error in making the approximation

$$e_d(t) \simeq 2G_1 J_1(A) \sin \omega_m t \qquad (2.4.29)$$

is greater than 10 per cent.

It is seen from the above results that the APC System studied can be used as an FM receiver if the modulation index is small (narrow-band FM). An advantage of this type of receiver is that it can be used to communicate with an accelerating satellite.

THE RESPONSE OF AN APC SYSTEM TO NARROW-BAND GAUSSIAN NOISE[*]

3.1 Summary

In this chapter the response of an APC System to narrow-band Gaussian noise, is determined. It is shown that the input noise and the phase jitter present in the voltage controlled oscillator are uncorrelated. It is also shown that the statistics describing the output of the active phase lag filter, $e_o(t)$, are nonstationary. To determine the statistics of the difference frequency voltage, $e_d(t)$, the output voltage, $e_o(t)$, and the phase jitter, $\theta_2(t)$, an iteration technique is employed.

3.2 The Iteration Technique[3.1]

The iteration technique used in this analysis can be explained using Fig. 3.1. In order to obtain a first approximation of the solution, the phase jitter present in the output of the VCO is neglected. Then

$$e_{v_{o_o}}(t) = \cos \omega_2 t \ . \tag{3.2.1}$$

The first approximation of the statistics of the difference frequency voltage, $e_d(t)$ can be determined once the statistics of the noise are specified. Having determined $e_{d_1}(t)$, the statistics of $e_{o_1}(t)$ can be calculated, since $e_{o_1}(t)$ and $e_{d_1}(t)$ are related by the transfer function of the active phase lag fil-

---

[*] Appendix B.

-39-

PHASE DETECTOR

MULTIPLIER

FILTER

BW = ω_0

VCO

$e_c(t) = N(t)$

$e_{v_0}(t) = \cos(\omega_2 t)$

e_{m_1}

e_{d_1}

e_{o_1}

ω_2

$e_{v_1}(t) = \cos(\omega_2 t + \theta_{2_1}(t)) = \cos(\omega_2 t + \int_0^t G_2 e_{o_1}(\lambda) d\lambda)$
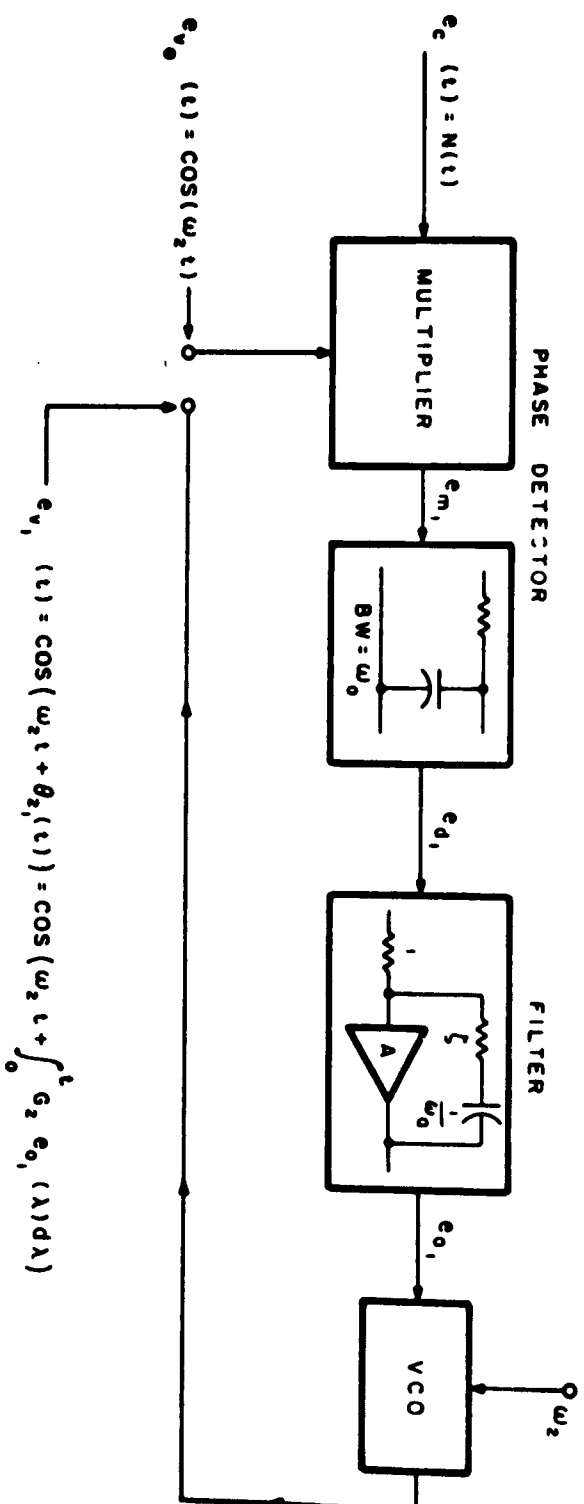
FIG. 3.1   THE INITIAL ITERATION

A-100-Z-0050

ter. Since the phase lag filter involves an integration, the statistics of $e_0(t)$ will be nonstationary. The first approximation of the output phase jitter, $\theta_{2_1}(t)$ is then

$$\theta_{2_1}(t) = G_2 \int_0^t e_{0_1}(\lambda)d\lambda \quad . \tag{3.2.2}$$

Using successive iterations, as illustrated in Fig. 3.2, the statistics of $e_{d_i}(t)$, $e_{0_i}(t)$ and $\theta_{2_i}(t)$ can be determined.

3.3   Characterization of the Input Noise

The results obtained below refer to an input consisting of narrow-band Gaussian noise. The noise is derived by passing white Gaussian noise through a single tuned IF filter, having a center frequency, ω_2 , and a bandwidth, α . The noise emanating from this filter has an autocorrelation function given by:

$$R_n(\tau) = \sigma_n^2 \, e^{-\alpha|\tau|} \cos \omega_2 \tau \tag{3.3.1}$$

and an expected value

$$E(N(t)) = 0 \quad . \tag{3.3.2}$$

The noise, $N(t)$, can be represented by[3.2]

$$N(t) = x(t)\cos \omega_2 t - z(t)\sin \omega_2 t \tag{3.3.3}$$

where

$$E(x(t)) = E(z(t)) = 0 \quad . \tag{3.3.4}$$

-41-

$$e_c(t) = N(t)$$

PHASE DETECTOR

MULTIPLIER

$e_{m_{(i+1)}}$

FILTER

$BW = \omega_0$

$e_{d_{(i+1)}}$

$\frac{\omega_0}{A}$

$e_{o_{(i+1)}}$

VCO

ω_2

$e_{v_i}(t) = \cos(\omega_2 t + \theta_{2_{i}}(t))$

$e_{v_{(i+1)}}(t) = \cos(\omega_2 t + \theta_{2_{(i+1)}}(t)) = \cos(\omega_2 t + \int_0^t G_2 e_{o_{(i+1)}}(\lambda) d\lambda)$
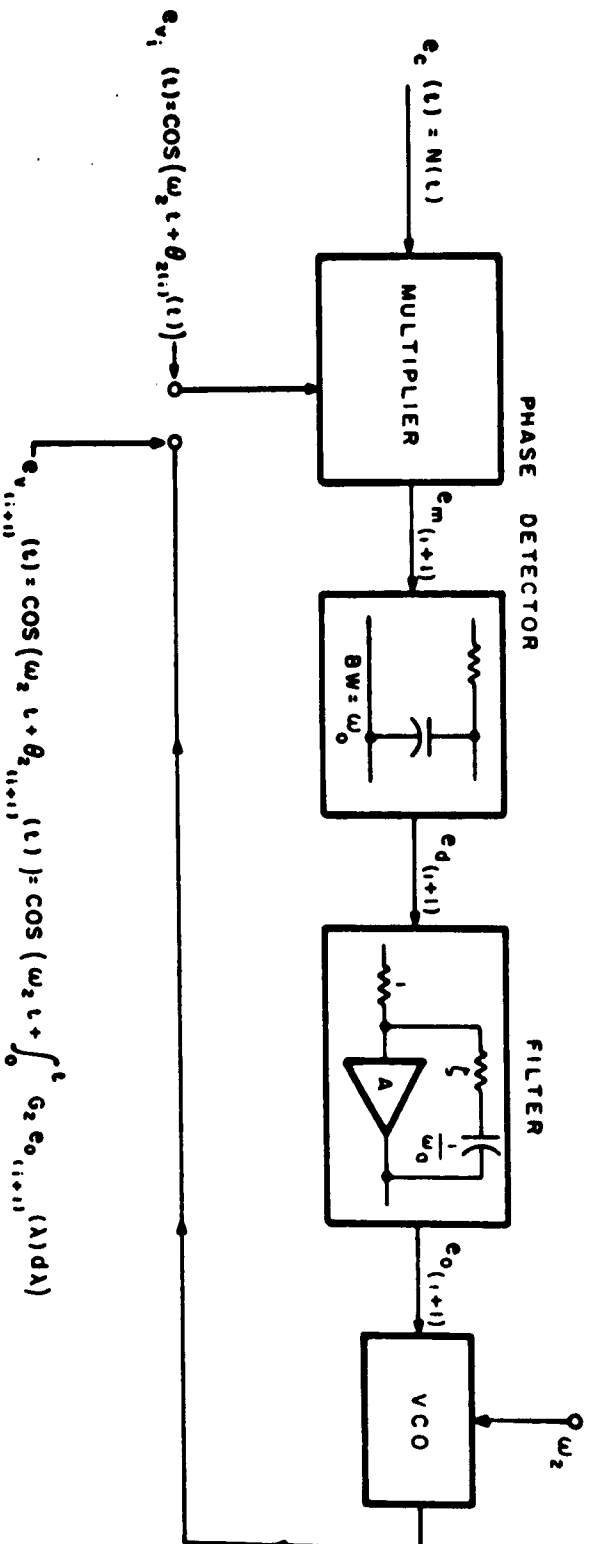
FIG. 3.2   THE (i+1) ITERATION

A-100-2-0051

The random variables $x(t)$ and $z(t)$ are uncorrelated, and,

$$R_x(\tau) = R_z(\tau) = \sigma_n^2 \, e^{-\alpha |\tau|} \quad . \tag{3.3.5}$$

The spectral density of x and z are then:

$$S_x(\omega) = S_z(\omega) = \frac{\sigma_n^2 \, \alpha}{\omega^2 + \alpha^2} \quad . \tag{3.3.6}$$

3.4 The First Iteration

To obtain the first iteration, we assume that there is no phase jitter present in the VCO (i.e., $\theta_{2_0} = 0$). The output voltage of the VCO (Fig. 3.1) is then

$$e_{v_0}(t) = \cos \omega_2 t \quad . \tag{3.4.1}$$

The output voltage of the multiplier, $e_{m_1}(t)$, is

$$e_{m_1}(t) = G_1 x(t) + G_1(x(t)\cos 2 \omega_2 t - z(t)\sin 2 \omega_2 t). \tag{3.4.2}$$

The voltage, $e_{m_1}(t)$, is then passed through an RC low-pass filter. The bandwidth, ω_0, of this filter is much less than the second harmonic frequency, $2\omega_2$. Therefore, in the expression obtained for the difference frequency voltage, $e_{d_1}(t)$, the components of $e_{m_1}(t)$ due to the second harmonic, $2\omega_2^1$, can be neglected. (In the experimental model a filter trap is inserted to further reduce the components due to the second harmonic.) Hence, to a first approximation, the difference frequency voltage, $E_{d_1}(\omega)$, is

$$E_{d_1}(\omega) = \frac{G_1}{1 + j\left(\frac{\omega}{\omega_0}\right)} X(\omega) \quad . \tag{3.4.3}$$

-43-

Equation (3.4.3) could also have been obtained if we had as-
sumed that the "multiplier" consisted of a multiplier, and an
ideal low-pass filter which has a gain of unity at frequen-
cies below $2\omega_2$, and provides infinite attenuation to all
frequencies at and above the second harmonic. Then the mul-
tiplier output is simply

$$e_{m_1}(t) = G_1 x(t) \quad . \tag{3.4.4}$$

Equation (3.4.3) immediately follows. Thus, the same result
for the difference frequency voltage (Eq. (3.4.3)) is obtain-
ed whether the second harmonic components are neglected at
the output of the multiplier (yielding Eq. (3.4.4)) or at the
output of the RC low-pass filter (in which case the output of
the multiplier is given by Eq. (3.4.2)). To simplify the al-
gebraic manipulation required, it is found useful to assume
the presence of the ideal low-pass filter, and use Eq. (3.4.4)
as the output of the multiplier rather than Eq. (3.4.2).

Using Eq (3.4.4) it is seen that the first approxima-
tion of the output of the multiplier is Gaussian with mean
zero, has an autocorrelation function

$$R_{e_{m_1}}(\tau) = G_1^2 \, \sigma_n^2 \, e^{-\alpha |\tau|} \quad , \tag{3.4.5}$$

and a spectral density

$$S_{e_{m_1}}(\omega) = \frac{G_1^2 \, \sigma_n^2 \, \alpha}{\omega^2 + \alpha^2} \quad . \tag{3.4.6}$$

A first approximation of the spectral density of the difference frequency voltage is then

$$S_{e_{d_1}}(\omega) = \frac{G_1^2 \, \sigma_n^2 \, \alpha}{\omega^2 + \alpha^2} \cdot \frac{1}{1 + \left(\frac{\omega}{\omega_o}\right)^2} \quad . \tag{3.4.7}$$

Since the bandwidth of the RC filter, ω_o , is much less than the bandwidth of the IF filter, α , Eq. (3.4.7) can be simplified:

$$S_{e_{d_1}}(\omega) \approx \frac{G_1^2 \, \sigma_n^2 \, \frac{\omega_o^2}{\alpha}}{\omega^2 + \omega_o^2} \quad . \tag{3.4.8}$$

The autocorrelation function of $e_{d_1}(t)$, is then:

$$R_{e_{d_1}}(\tau) \simeq \frac{\omega_o}{\alpha} \, G_1^2 \, \sigma_n^2 \, e^{-\omega_o |\tau|} \quad . \tag{3.4.9}$$

To a first approximation, $e_d(t)$ is stationary. The probability density of $e_d(t)$ is Gaussian with mean zero.

The statistics of $e_{o_1}(t)$ can be found using the relation,

$$e_{o_1}(t) = -\zeta \, e_{d_1}(t) - \omega_a \int_o^t e^{-\frac{\omega_a}{A}(t - \lambda)} e_{d_1}(\lambda) d\lambda \quad . \tag{3.4.10}$$

The autocorrelation function of $e_{o_1}(t)$ is derived in Appendix B, and is shown to be:

$$R_{e_{o_1}}(t,\tau) \simeq \frac{\omega_o \, \sigma_n^2 \, G_1^2}{\alpha}\left[\zeta^2 e^{-\omega_o |\tau|} + 2\zeta\left(\frac{\omega_a}{\omega_o}\right)e^{-\frac{\omega_a |\tau|}{A}}\right.$$

$$\left. + \left(\frac{\omega_a}{\omega_o}\right)\left(\frac{A}{2}\right)\left(1 - e^{-\frac{2\omega_a t}{A}}\right)\left(1 + e^{-\frac{\omega_a |\tau|}{A}}\right)\right] \quad (3.4.11)$$

This equation clearly illustrates the nonstationary character of $e_o(t)$. If the time of operation is such that

$$t << A/\omega_a \ ,$$

Eq. (3.4.11) can be simplified:

$$R_{e_{o_1}}(t,\tau) \simeq \frac{\omega_o \, \sigma_n^2 \, G_1^2}{\alpha}\left[\zeta^2 e^{-\omega_o |\tau|} + 2\zeta\left(\frac{\omega_a}{\omega_o}\right) + 2\frac{\omega_a^2}{\omega_o}t\right]. \quad (3.4.12)$$

Since $e_{d_1}(t)$ is Gaussian, $e_{o_1}(t)$ is also Gaussian with mean zero. The variance of $e_{o_1}(t)$, is however, an increasing function of time. (The significance of this result will be shown in Chapter 4 where the response of an APC System to a frequency ramp modulated signal embedded in noise is discussed.)

The autocorrelation function of the output phase jitter, $\theta_{2_1}(t)$, has also been derived in Appendix B. The autocorrelation function is

$$R_{\theta_{2_1}}(t,\tau) \simeq \frac{2 G_1^2 G_2^2 \sigma_n^2}{\alpha} \, t\left[\zeta^2 + \zeta(\omega_a t + |\omega_a \tau|) + \omega_a t\left(\frac{\omega_a t}{3} + \frac{|\omega_a \tau|}{2}\right)\right] \quad (3.4.13)$$

where

$$t << A/\omega_a \quad .$$

Equation (3.4.13) is seen to be nonstationary. Since the phase jitter, $\theta_2(t)$, is the integral of $e_{0_1}(t)$, it too is Gaussian with mean zero.

3.5   The Second Iteration

To obtain a second approximation of the output of the multiplier, $e_{m_2}(t)$, the input voltage, $e_c(t)$, and output voltage, $e_{v_1}(t)$, must be multiplied and passed through the ideal low-pass filter (i.e., second harmonic components are neglected). Then,

$$e_{m_2}(t) = G_1 x(t)\cos\theta_{2_1}(t) - G_1 z(t)\sin\theta_{2_1}(t) \qquad (3.5.1)$$

where

$$\theta_{2_1}(t) = -G_2\,\zeta \int_0^t e_{d_1}(\lambda)d\lambda - G_2\omega_a \int_0^t d\eta \int_0^\eta e_{d_1}(\lambda)d\lambda \qquad (3.5.2)$$

and

$$t \ll \lambda/\omega_a \quad . \qquad (3.5.3)$$

Since the difference frequency voltage, $e_{d_1}(t)$, is the response of an RC low-pass filter to noise, $x(t)$,

$$e_{d_1}(t) = \omega_0 G_1 \int_0^t e^{-\omega_0(t-\lambda)} x(\lambda)d\lambda \quad . \qquad (3.5.4)$$

To determine the statistics of $e_{m_2}(t)$, the expected value of $x\theta_{2_1}$ and $z\theta_{2_1}$ must be evaluated. Referring to Eq. (3.5.2) and Eq. (3.5.4), and noting that $x(t)$ and $z(t)$ are uncorrelated, it is seen that

-47-

$$E(z\theta_{2_1}) = 0 \; . \tag{3.5.5}$$

The expected value of $x\theta_{2_1}$ is

$$E(x\theta_{2_1}) = - \zeta \, G_2 \int_0^t E(x(t)e_{d_1}(\lambda))d\lambda$$

$$- \omega_a G_2 \int_0^t d\eta \int_0^\eta d\lambda \, E(x(t)e_{d_1}(\lambda)) \, , \tag{3.5.6}$$

and the expected value of $x(t)e_{d_1}(\lambda)$ is

$$E(x(t)e_{d_1}(\lambda)) = \omega_o G_1 \int_0^\lambda e^{-\omega_o(\lambda - \nu)} E(x(t)x(\nu))d\nu \, . \tag{3.5.7}$$

But,

$$E(x(t)x(\nu)) = R_x(|t - \nu|) = \sigma_n^2 \, e^{-\alpha|t - \nu|} \, . \tag{3.5.8}$$

Utilizing Eq. (3.5.8), Eq. (3.5.7) is easily integrated, and

$$E(x(t)e_{d_1}(\lambda)) = \frac{\omega_o G_1 \sigma_n^2}{\alpha} e^{-\alpha t} e^{-\omega_o \lambda}(e^{\alpha\lambda} - 1) \, . \tag{3.5.9}$$

Substituting Eq. (3.5.9) into Eq. (3.5.6) and integrating
yields:

$$\tag{3.5.10}$$

$$E(x(t)\theta_{2_1}(t)) = \frac{G_1 G_2 \omega_o \sigma_n^2}{\alpha} e^{-\alpha t} \left[\zeta \left(\frac{\left[e^{(\alpha - \omega_o)t} - 1\right]}{\alpha} - \frac{1}{\omega_o}\left(1 - e^{-\omega_o t}\right) \right) \right.$$

$$\left. + \left(\frac{\omega_a}{\alpha}\right)\left(\frac{\left[e^{(\alpha - \omega_o)t} - 1\right]}{\alpha} - t\right) - \left(\frac{\omega_a}{\omega_o}\right)\left(t - \frac{\left[1 - e^{-\omega_o t}\right]}{\omega_o}\right) \right]$$

-48-

where

$$\alpha \gg \omega_0 \; .$$

This result is only of interest when the RC low-pass filter is in steady state operation. Therefore, letting

$$t \gg 1/\omega_0 \; ,$$

we find that

$$E(x(t)\theta_{2_1}(t))\Big|_{t \gg \frac{1}{\omega_0}} = 0 \; . \qquad (3.5.11)$$

Thus, the input noise and the output phase jitter are uncorrelated, and

$$E(e_{m_2}(t)) = 0 \; . \qquad (3.5.12)$$

With the aid of Eq. (3.5.1), Eq. (3.5.5) and Eq. (3.5.11), the autocorrelation function of $e_{m_2}(t)$ becomes:

$$R_{e_{m_2}}(t,\tau) = G_1^2 \, E(x(t)x(t+\tau))E(\cos \theta_{2_1}(t)\cos \theta_{2_1}(t+\tau))$$

$$+ G_1^2 \, E(z(t)z(t+\tau))E(\sin \theta_{2_1}(t)\sin \theta_{2_1}(t+\tau)) \; .$$

$$(3.5.13)$$

This expression can be simplified, yielding:

$$R_{e_{m_2}}(t,\tau) = G_1^2\, \sigma_n^2\, e^{-\alpha|\tau|}\; E(\cos(\theta_{2_1}(t+\tau) - \theta_{2_1}(t)))\ .$$

$$(3.5.14)$$

It is shown in Appendix B that given a function $f(t)$,

$$E(\cos f(t)) = e^{-\frac{1}{2} E(f(t))^2} \tag{3.5.15}$$

where $f(t)$ is Gaussian with mean zero. Thus, Eq. (3.5.14) becomes:

$$R_{e_{m_2}}(t,\tau) = G_1^2\sigma_n^2 e^{-\alpha|\tau|}\; e^{-\frac{1}{2}\left[\sigma_{\theta_{2_1}}^2(t) + \sigma_{\theta_{2_1}}^2(t+\tau) - 2R_{\theta_{2_1}}(t,\tau)\right]}.$$

$$(3.5.16)$$

Using the results given in Eq. (3.4.13) for $R_{\theta_{2_1}}(t,\tau)$, the autocorrelation function of $e_{m_2}(t)$ is:

$$R_{e_{m_2}}(\tau) \simeq G_1^2\, \sigma_n^2\, e^{-\alpha|\tau|}\ . \tag{3.5.17}$$

(This result is derived in Appendix B.)

3.6   Conclusion

The second approximation of the autocorrelation function of the output of the multiplier (Eq. (3.5.17)) yields the same result as the first approximation (Eq. (3.4.5)). Thus, the statistics obtained for the ith iteration are the same as the statistics obtained for the first iteration.

Hence,

$$R_{e_{d_1}}(\tau) = R_{e_{d_1}}(\tau) = \frac{\omega_o}{\alpha} G_1^2 \sigma_n^2 e^{-\omega_o |\tau|} . \qquad (3.6.1)$$

$$R_{e_{o_1}}(t,\tau) = R_{e_{o_1}}(t,\tau)$$

$$\simeq \frac{\omega_o \sigma_n^2 G_1^2}{\alpha}\left[\zeta^2 e^{-\omega_o |\tau|} + 2\zeta\left(\frac{\omega_a}{\omega_o}\right) + 2\frac{\omega_a^2}{\omega_o}\, t\right] \qquad (3.6.2)$$

and

$$R_{\theta_{2_1}}(t,\tau) = R_{\theta_{2_1}}(t,\tau) \qquad (3.6.3)$$

$$\simeq \frac{2G_1^2 G_2^2 \sigma_n^2}{\alpha}\, t\left[\zeta^2 + \zeta(\omega_a t + |\omega_a \tau|) + \omega_a t\left(\frac{\omega_a t}{3} + \frac{|\omega_a \tau|}{2}\right)\right]$$

where

$$\frac{1}{\omega_o} \ll t \ll \frac{A}{\omega_a} . \qquad (3.6.4)$$

In addition, it has been shown that the input and output noise are uncorrelated. Consequently, the APC System responds to noise as an open loop system (Fig. 3.1), rather than as a closed loop system.

THE RESPONSE OF AN APC SYSTEM TO AN FM SIGNAL AND NOISE

4 1   Introduction

An extremely important feature of the APC System is its
ability to synchronize to a signal which is deeply embedded
in noise, even when the signal is frequency modulated. To
clearly demonstrate the operation of this device, the response
of the APC System to a signal and noise is obtained using the
linearization procedure employed by previous investigators.[4.1]
This technique is valid only when the S/N ratio is much
greater than unity and the noise peaks are limited.

It is then attempted to extend these results theoreti-
cally using an iteration technique, as in Chapter 3. Due to
the complexity of the problem, the iterative procedure is not
carried beyond the second iteration and no convergence is
demonstrated. The first iteration, however, is useful in pro-
viding qualitative results illustrating the effect of the sys-
tem parameters on the locking of the APC System to a signal,
even when the S/N ratio is much less than unity.

In the following discussion, it is assumed that the in-
put voltage

$$e_c(t) = S \sin \phi_1(t) + N(t) \ . \qquad\qquad (4.1.1)$$

The input voltage was generated by passing the incoming RF
signal (and noise) through a narrow-band IF filter. The fil-
ter had a center frequency, ω_2 rad/sec , which is the initial

frequency of the VCO, and a bandwidth, α rad sec. The input noise is then,

$$N(t) = x(t)\cos \omega_2 t - z(t)\sin \omega_2 t \quad . \qquad (4.1.2)$$

The input signal is assumed to be unaffected by the IF filter. Hence,

$$|\dot{\phi}_1(t) - \omega_2| < < \alpha \quad . \qquad (4.1.3)$$

4.2 The Response of a Linearized APC System to an FM Signal and Noise[4.2]

Let us assume the input voltage to be:

$$e_c(t) = S \sin(\omega_2 t + \theta_1(t)) + \left(x(t)\cos \omega_2 t - z(t)\sin \omega_2 t\right)$$

$$(4.2.1)$$

where $\theta_1(t)$ represents the phase modulation. If the input noise is limited and the S/N ratio is much greater than unity, Eq. (4.2.1) can be simplified:[*]

$$e_c(t) = S \sin(\omega_2 t + \theta_1(t) + \tfrac{1}{S}[x(t)\cos \theta_1(t) + z(t)\sin \theta_1(t)])$$

$$= S \sin(\phi_1(t) + \tfrac{1}{S} u(t)) \, , \qquad (4.2.2)$$

where

$$\phi_1(t) = \omega_2 t + \theta_1(t) \, ,$$

$$u(t) = x(t)\cos \theta_1(t) + z(t)\sin \theta_1(t) \, ,$$

and

$$|u(t)| < < S \qquad (4.2.3)$$

_____

[*] See Appendix C.

-53-

The output of the multiplier, $e_m(t)$, is then,

$$e_m(t) = G_1 \ S \ \sin(\phi_2(t) - \phi_1(t) - \frac{1}{S} u(t)) \quad . \qquad (4.2.4)$$

It is implicitly assumed, in Eq. (4.2.4), that the multiplier consists of a multiplier and an ideal filter, as discussed in Chapter 3.

Equation (4.2.4) can be linearized if

$$| \phi_2(t) - \phi_1(t) - \frac{1}{S} u(t)| < < 1 \text{ radian} \qquad (4.2.5)$$

This requirement implies that the system is almost synchronized to the incoming signal, and $\phi_2(t)$ is perturbed slightly from $\phi_1(t)$, due to the noise, $u(t)$. Noting that

$$\phi_2(t) = \omega_2 t + \theta_2(t) \ ,$$

and

$$\phi_1(t) = \omega_2 t + \theta_1(t) \quad ,$$

Eq. (4.2.4) becomes,

$$e_m(t) \simeq G_1 \ S(\theta_2(t) - \theta_1(t)) - G_1 \ u(t) \quad . \qquad (4.2.6)$$

Using this result, the APC System can be linearized, as shown in Fig. 4.1. The response of this linearized system to a signal and noise is then the response to the signal plus the response to the noise. Therefore,
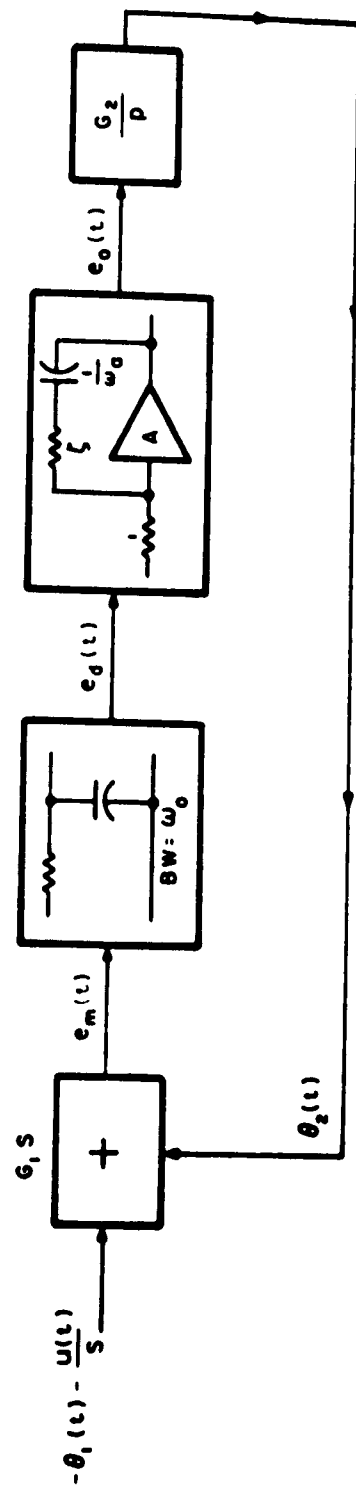
$$u(t) = x(t) \cos \theta_1(t) + z(t) \sin \theta_1(t)$$

FIG. 4.1   THE LINEARIZED MODEL OF THE APC SYSTEM

A-100-Z-0052

$$\theta_2(t) = \theta_{2_s}(t) + \theta_{2_n}(t) \qquad (4.2.7)$$

where $\theta_{2_s}(t)$ is the phase variation of the VCO, due to the signal's phase modulation, $\theta_1(t)$ $\theta_{2_n}(t)$ is the phase variation due to the noise, $u(t)/S$.

The response of a linearized system to an FM signal has been discussed in Chapter 2 and Appendix A. The steady state phase jitter present in the VCO is easily determined using Fig. 4.1.

$$\theta_{2_n}(\omega) = - \frac{\dfrac{\omega_n}{\omega^2}\left(\dfrac{\omega_a + j\omega\zeta}{1 + j\,\omega/\omega_o}\right)}{1 + \dfrac{\omega_n}{\omega^2}\left(\dfrac{\omega_a + j\omega\zeta}{1 + j\,\omega/\omega_o}\right)} \cdot \frac{U(\omega)}{S} \qquad . \qquad (4.2.8)$$

This equation shows that the linearized system responds as a closed loop system to the noise. This is a direct result of the initial assumption that the noise was limited.

Utilizing Eq. (4.2.8), the spectral density of the phase jitter at the output of the VCO can be obtained if the spectral density of the input noise is known. Let us assume that the spectral density of the input phase noise, $u(t)$, is:

$$S_u(\omega) = \frac{\sigma_u^2/\alpha}{1 + \dfrac{\omega^2}{\alpha^2}} \qquad . \qquad (4.2.9)$$

The spectral density of the phase jitter due to noise is then

$$S_{\theta_{2_n}}(\Omega^2) = \left(\frac{\sigma_u^2}{\alpha S^2}\right) \frac{1 + \epsilon^2\,\Omega^2}{\left(1 + \dfrac{\Omega^2}{\Omega_\alpha^2}\right)\left((1 + \Omega^2) + \Omega^2\left(\dfrac{\Omega^2}{\Omega_o} + \epsilon'\right)^2\right)} \qquad (4.2.10)$$

where α is the bandwidth of the IF filter,

$$\Omega^2 = \omega^2/\omega_a \omega_n \;,$$

$$\Omega_o^2 = \omega_o^2/\omega_a \omega_n$$

and

$$\Omega_\alpha^2 = \alpha^2/\omega_a \omega_n \qquad .$$

Equation (4.2.10) is plotted in Fig. 4.2 using the typical values

$\epsilon = 1$

$\omega_a = 1$ rad/sec

$\omega_o = 2000\pi$ rad/sec

$\alpha = 12000\pi$ rad/sec

and

$\omega_n = 400\pi$ rad/sec , and 2000π rad/sec .

These results are compared with the spectral density of the input phase noise. The phase jitter in the output of the VCO is much less than the phase jitter in the input. In addition, it is seen from Fig. 4.2 that as $\sqrt{\omega_a \omega_n}$ increases, the phase jitter increases. However, if the input signal is ramp modulated, the slope of the frequency ramp must be less than $\frac{1}{2} (\omega_a \omega_n)$ for locking to occur. If the slope of the ramp increases, $(\omega_a \omega_n)$ must be increased. Thus, the amount of noise reduction that can be obtained by adjusting $\omega_a \omega_n$, depends directly on the slope of the frequency ramp to be tracked.

The noise can also be reduced by reducing the normalized coefficient of damping, ϵ . Equation (4.2.10) shows that as ϵ is decreased, the spectral density of the phase
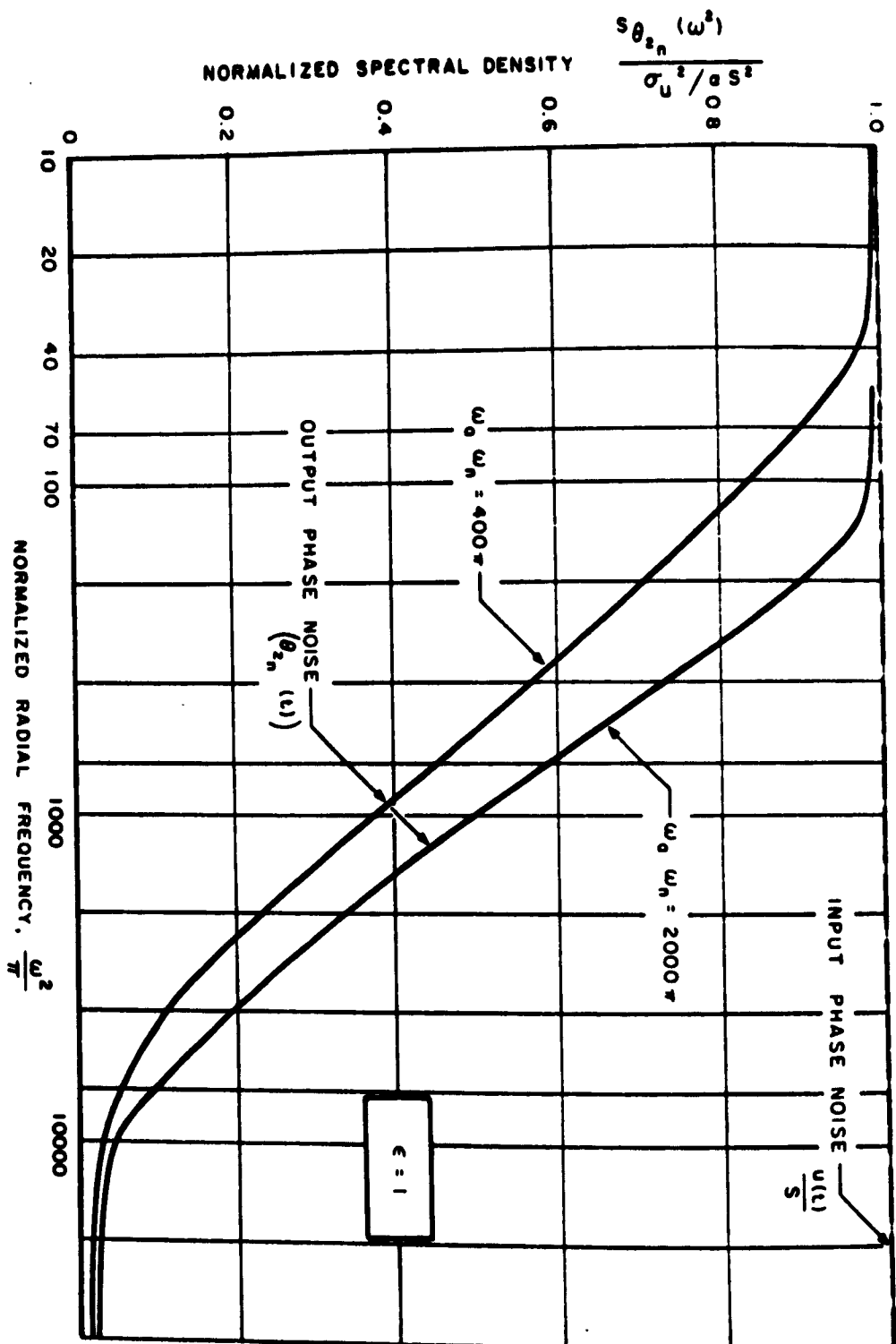
FIG. 4.2 COMPARISON OF INPUT AND OUTPUT PHASE JITTER

A-100-2-0053

jitter also decreases. During locking, ϵ should be critically damped to assure locking in the shortest possible time. However, after locking (steady state), ϵ could be reduced in order to reduce the noise.

4.3 The Iteration Technique*

The iterative procedure employed is similar to the technique used in Chapter 3. The input voltage is

$$e_c(t) = S \sin \phi_1(t) + (x(t)\cos \omega_2 t - z(t)\sin \omega_2 t) \quad . \quad (4.3.1)$$

The output of the VCO is initially assumed to be noise free. Thus,

$$e_{v_o}(t) = \cos \phi_{2_o}(t) = \cos(\omega_2 t + \theta_{2_{o_s}}(t)) \quad . \quad (4.3.2)$$

The first approximation of the output voltage of the multiplier, $e_{m_1}(t)$, is then

$$e_{m_1}(t) = G_1 S \sin \phi(t) + G_1 u_o(t) \quad (4.3.3)$$

where

$$\phi(t) = \phi_{2_o}(t) - \phi_1(t)$$

and

$$u_o(t) = x(t)\cos \theta_{2_{o_s}}(t) + z(t)\sin \theta_{2_{o_s}}(t) \quad . \quad (4.3.4)$$

---

* See Appendix D.

-59-

The statistics of the noise are derived in Appendix D. It is shown that $u_o(t)$ is Gaussian distributed with a zero mean. The autocorrelation function of $u_o(t)$ is

$$R_{u_o}(\tau) \simeq \sigma_n^2 \; e^{-\alpha |\tau|} \; , \qquad (4.3.5)$$

a result identical to Eq. (3.4.5).

The multiplier voltage, $e_{m_1}(t)$, can be written as:

$$e_{m_1}(t) = e_{m_{1_s}}(t) + e_{m_{1_n}}(t) \; , \qquad (4.3.6)$$

where

$e_{m_{1_s}}(t) = G_1 S \sin \phi(t)$, is the response to an FM signal (Chapter 2),

and

$e_{m_{1_n}}(t) = G_1 u_o(t)$, is the response to narrow-band noise.

The first approximation of the output phase of the VCO is then,

$$\phi_{2_1}(t) = \omega_2 t + \theta_{2_{1_s}}(t) + \theta_{2_{1_n}}(t) \qquad (4.3.7)$$

where

$\theta_{2_{1_s}}(t) = \theta_{2_{0_s}}(t)$, is the output phase due to an input signal,

and

$\theta_{2_{1_n}}(t)$ is the phase jitter due to noise, (Chapter 3).

-60-

If the output phase of the VCO due to the signal, $\theta_{2_{O_s}}(t)$, is much greater than the phase jitter, $\theta_{2_{1_n}}(t)$, Eq. (4.3.7) can be written as,

$$\phi_{2_1}(t) = \omega_2 t + \theta_{2_{1_s}}(t) + \theta_{2_{1_n}}(t) \approx \omega_2 t + \theta_{2_{O_s}}(t) = \phi_{2_O}(t) .$$

$$(4.3.8)$$

When Eq. (4.3.8) is valid, the iteration technique appears to converge. However, in order to rigorously demonstrate convergence, Eq. (4.3.7) should be used and a second iteration taken. This was not attempted.

Using Eq. (4.3.7), a S/N ratio of the output phase can be defined as:

$$\left(\frac{S}{N}\right)_{\text{(output phase)}} = \frac{\left| \theta_{2_{O_s}}(t) \right|}{\sigma_{\theta_{2_{1_n}}}(t)} .$$

$$(4.3.9)$$

When the output S/N ratio given in Eq. (4.3.9) is much greater than unity, the approximation made in Eq. (4.3.8) is valid. We would then expect the system to have a high probability of locking, since the phase jitter will only act as a slight perturbation of the output phase. The output phase $\theta_{2_{O_s}}(t)$ can be expressed in terms of the input phase modulation, since,

$$\phi(t) = \phi_{2_O}(t) - \phi_1(t) = (\omega_2 t + \theta_{2_{O_s}}(t)) - (\omega_1 t + \theta_1(t)) .$$

$$(4.3.10)$$

Therefore,

$$\theta_{2_{O_s}}(t) = \phi(t) + \theta_1(t) - \Omega t \qquad (4.3.11)$$

where

$$\Omega = \omega_2 - \omega_1 .$$

The normalized standard deviation of the phase jitter is derived in Appendix D:

$$\sigma_{\theta_{2_{1_n}}}(\tau) \doteq \left[\frac{\sqrt{\omega_a \omega_n}}{\alpha} \left(\frac{\sigma_n^2}{S^2/2} \right) \tau \left(\epsilon^2 + \epsilon \tau + \frac{\tau^2}{3} \right) \right]^{\frac{1}{2}} , \qquad (4.3.12)$$

where

$$\tau = \sqrt{\omega_a \omega_n} \ t .$$

The effect of the input S/N ratio and the system parameters on the output S/N ratio, can be demonstrated using the following example: Consider a frequency ramp modulated input signal with an amplitude of 10 volts embedded in noise. The rate of change of the frequency modulation is 400 rad/sec/sec. The APC loop is closed when the initial phase error is zero, and the initial frequency error is 22 rad/sec. The system parameters are chosen so that the APC system is critically damped. Then,

$$S = 10^V$$

$$\zeta = 53 \times 10^{-3}$$

$$\omega_a = 1 \text{ rad/sec}$$

$$\omega_n = 425\pi \text{ rad/sec}$$

and

$$\alpha = 12000\pi \text{ rad/sec} .$$

Using Eq. (2.1.12),

$$\epsilon = 2 \, ,$$

$$a = 0.3 \, ,$$

$$\phi(o) = 0$$

and

$$\left. \frac{d\phi}{d\tau} \right|_{\tau=0} = 0.6 \quad .$$

The normalized response, $\phi(\tau)$, to the frequency ramp modulated signal is then:

$$\phi(\tau) \approx 0.3(e^{-\tau} - 1) + 0.9\tau \, e^{-\tau} \quad . \qquad (4.3.13)$$

Equation (4.3.13) is obtained using the simple linear technique (Appendix A), which is valid since,

$$|\phi(\tau)| \leq 0.3 \text{ radians} \quad .$$

The normalized output phase, $\theta_{2_{O_s}}(\tau)$, and the standard deviation of the phase jitter, $\sigma_{\theta_{2_{1_n}}}(\tau)$, are shown in Fig. 4.3. It is seen from this figure, and from Eq. (4.3.11) that the standard deviation of the phase jitter will exceed $\theta_{2_{O_s}}(\tau)$ during some period of time, since $\theta_{2_{O_s}}(t)$ becomes zero when,

$$\theta_{2}(\tau) = \Omega_n \tau - \phi(\tau) \quad . \qquad (4.3.14)$$

If the standard deviation of the phase jitter is much less than $\frac{\pi}{2}$ radians when it exceeds $\theta_{2_{O_s}}(t)$, the system will prob-

FIG. 4.3 COMPARISON OF OUTPUT PHASE $\theta_{2_{O_s}}$ (τ) WITH THE OUTPUT PHASE JITTER $\sigma_{\theta_{2_{i_n}}}$ (τ)

A-100-Z-0054
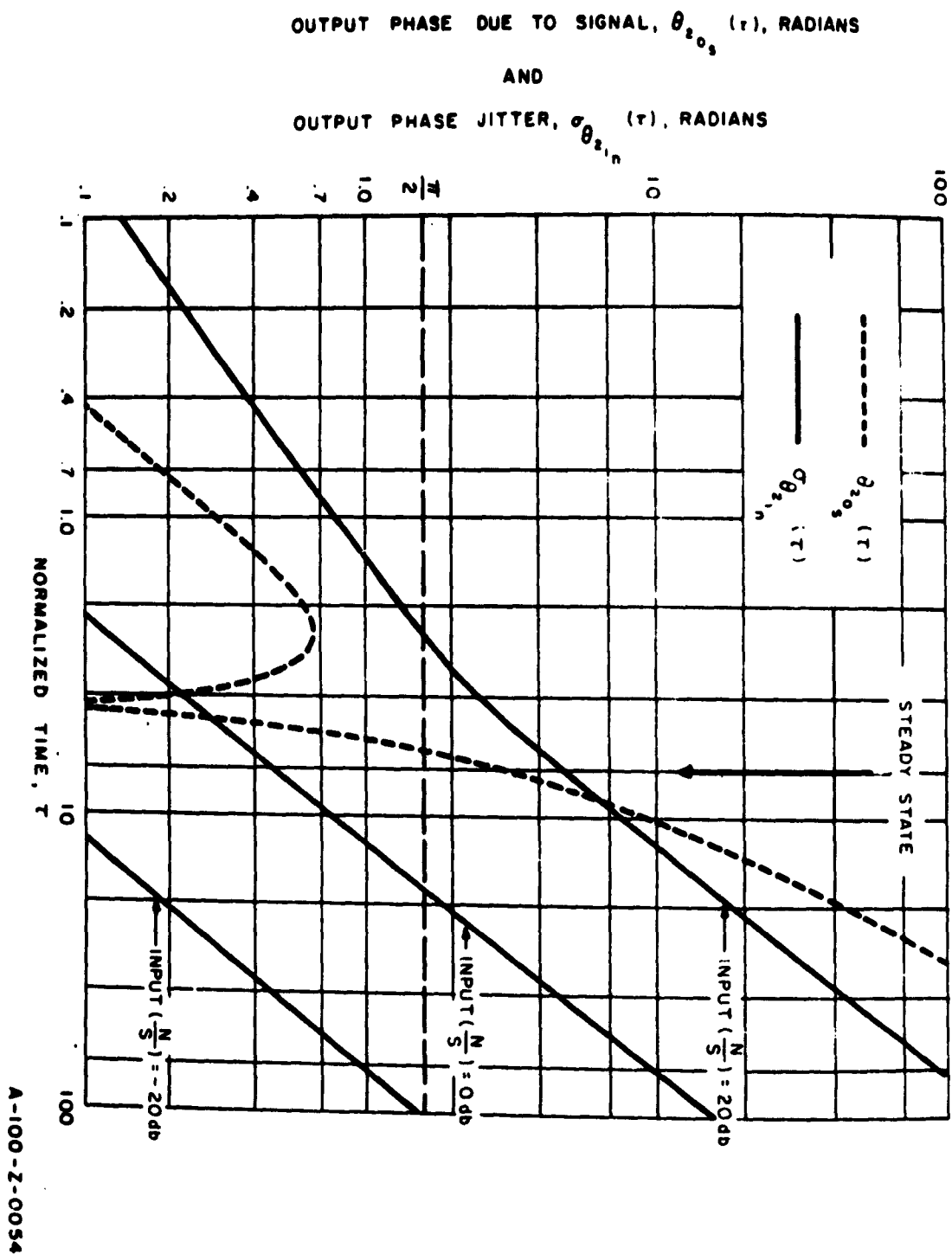
ably synchronize and remain synchronized to the input signal, If, however, the standard deviation is much greater than $\frac{\pi}{2}$ radians when it exceeds $\theta_{2_{O_g}}(t)$, the system will probably not lock to the signal. Referring to Fig. 4.3, it is seen that when the input N/S ratio ($\sigma_n^2/S^2/2$) is -20 db, the phase jitter is always much less than $\theta_{2_{O_g}}(\tau)$, except for a very short period of time. The standard deviation of the phase jitter during this time is much less than $\frac{\pi}{2}$ radians. The probability of the system locking to the input signal seems to be quite high. This should be compared to the curve showing an input N/S ratio of +20 db. The standard deviation of the phase jitter is larger than $\theta_{2_{O_g}}(\tau)$, until $\tau = 9$. The standard deviation is then 7 radians. The probability of the system locking to the input signal now appears to be small.

The maximum value of the input N/S ratio possible, to still achieve locking, is greatly affected by the choice of $\sqrt{\omega_a \omega_n}$ and the normalized damping factor, ϵ . It is seen from Eq. (4.3 12) that when $\sqrt{\omega_a \omega_n}$ is decreased, the phase jitter is decreased. However, a lower limit on the value of $\omega_a \omega_n$ is set by the slope of the frequency ramp.

The normalized damping factor, ϵ , effects not only the standard deviation of the phase jitter (Eq. (4.3.12)), but the time required for the APC System to reach steady state with respect to the signal ($\phi = -\sin^{-1} a$). It is shown in the next chapter that when the system is critically damped, ($\epsilon = 2$), it can tolerate a larger N/S ratio than if it were underdamped or overdamped.

EXPERIMENTAL RESULTS

5.1 Discussion of the Experimental Model

An experimental model of the APC System is shown in Fig. 5.1.

5.1.1 The Phase Detector

The Phase Detector consists of a multiplier, employing collector modulation, and an RC low-pass filter used to obtain the difference frequency signal, $e_d(t)$. A single-tuned circuit is also used to eliminate the first harmonic distortion from the output of the phase detector. The remaining distortion had a peak-to-peak amplitude of less than 50 mv, and negligible effect on the results obtained. The amplitude of the difference frequency signal, $e_d(t)$, was measured, and found to be 0.025 S.

The input signal, $e_c(t)$, is given by

$$e_c(t) = S \sin \phi_1(t) . \tag{5.1.1}$$

The difference frequency signal, $e_d(t)$, can then be written as:

$$e_d(t) = +0.025 \ S \ \sin(\phi_2 - \phi_1) = 0.025 \ S \ \sin \phi(t) . \tag{5.1.2}$$

Thus,

$$G_1 = 0.025 . \tag{5.1.3}$$
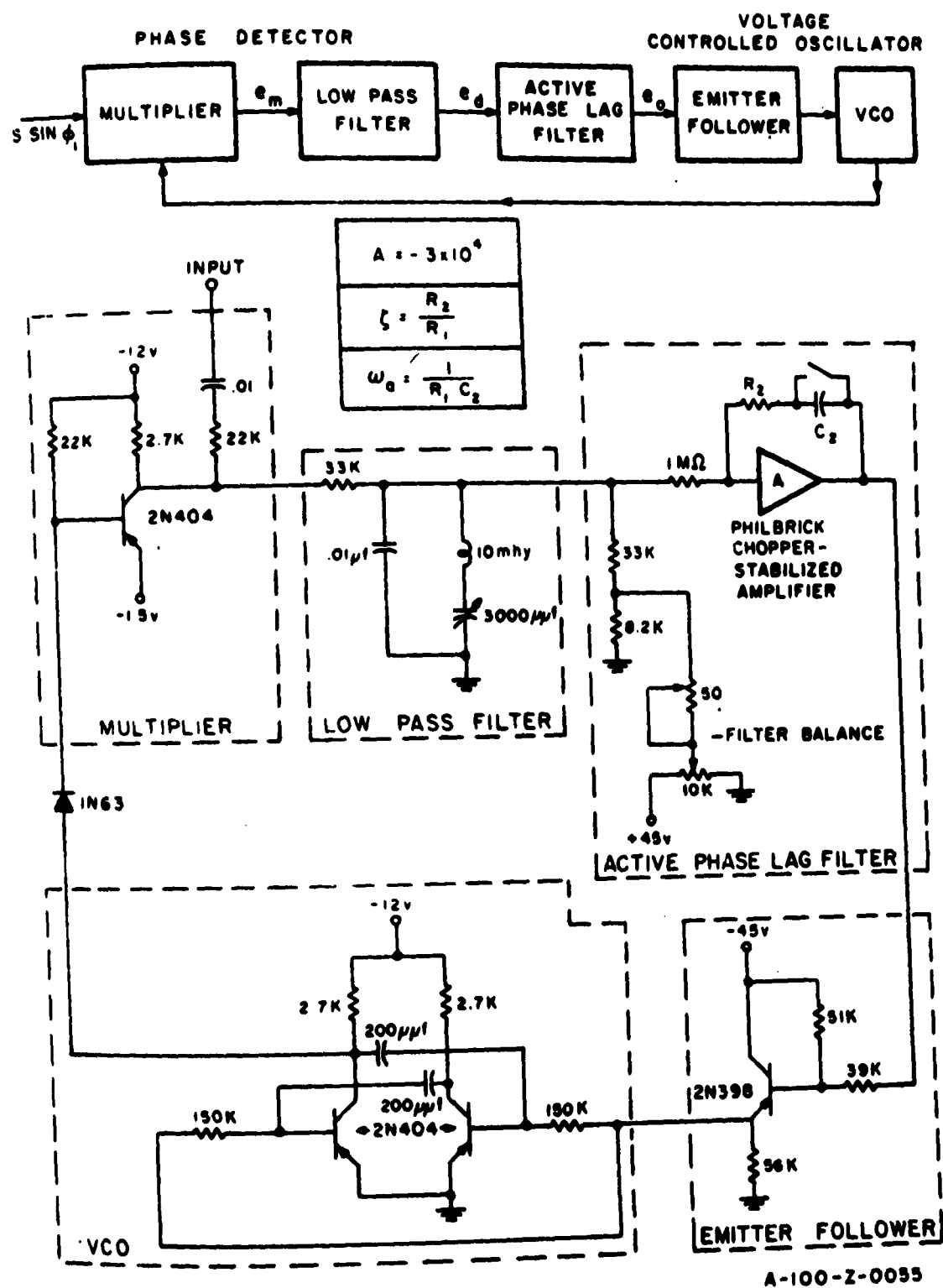
FIG. 5.1   EXPERIMENTAL MODEL OF APC SYSTEM

5.1.2 The Active Phase Lag Filter

The phase lag filter employs a Philbrick chopper stabilized amplifier with an open loop gain, A , of magnitude 30,000. The filter approximates the transfer function

$$\frac{E_o(p)}{E_d(p)} = H(p) = - \zeta - \frac{\omega_a}{p} \tag{5.1.4}$$

as long as

$$t << \frac{A}{\omega_a} \quad \text{seconds} . \tag{5.1.5}$$

Since ω_a was always chosen to be less or equal to unity, the filter is operational for periods of time exceeding one hour. In the time domain, the filter output, $e_o(t)$, becomes,

$$e_o(t) = - \zeta \, G_1 \, S \, \sin \, \phi - \omega_a \, G_1 \, S \int_0^t \sin(\lambda) d\lambda . \tag{5.1.6}$$

The minus sign is due to the inversion inherent in the operational amplifier.

5.1.3 The Voltage Controlled Oscillator (VCO)

An astable multivibrator was used as the VCO. The multivibrator was employed because of its great versatility. It was capable of being operated up to a carrier frequency of 200 kcps. The frequency of oscillation, f , of the VCO can be shown to be

$$f = \frac{1}{2RC \, \ln(1 + \frac{V}{E})} \tag{5.1.7}$$

where

V is the collector voltage,

E is the control voltage applied to each base,

and

RC is the time constant of the astable multivibrator.

Using a Taylor series expansion,

$$f \approx f_2 + \frac{df}{dE} \, dE \quad . \tag{5.1.8}$$

The sensitivity of the VCO, $\frac{df}{dE}$, can be obtained by differentiating Eq. (5.1.7)

$$\frac{df}{dE} = 2 \, f^2 \, RC \, \frac{\frac{V}{E^2}}{1 + \frac{V}{E}} \quad . \tag{5.1.9}$$

It should be noted that E represents the "DC" control voltage while dE represents the variation of the control voltage and is proportional to $e_o(t)$. In the experimental model, the VCO had a time constant,

RC $\approx$ 30 × 10^{-6} seconds,

a collector voltage, V = 12^V,

and a "DC" control voltage, E = 20^V,

so that the initial frequency of oscillation, f_2 = 35 kcps.

The measured sensitivity of the emitter follower-astable multivibrator combination was about 850 cps/volt.

-69-

Using Eq. (5.1.9) and noting that the emitter follower attenuates its input signal (e_o), by 4/9 (see Fig. 5.1) the calculated value obtained was 750 cps/volt. This verifies the measured value. The sensitivity of the VCO, G_2, is then

$$G_2 \approx 1700 \ \pi \ \text{rad/sec/volt} . \qquad (5.1.10)$$

The sensitivity (loop gain) of the system,

$$\omega_n = G_1 \ G_2 \ S = 42.5 \ \pi \ S \ \text{rad/sec} . \qquad (5.1.11)$$

5.2   The Response of an APC System to an FM Ramp

5.2.1 Introduction

A frequency ramp was obtained, using a H-P 200 CD oscillator. The frequency of the oscillator was controlled by coupling the tuning shaft of the oscillator to a small, constant speed DC motor. A gear reducing system was used to obtain frequency ramps from 3 cps/sec to 60 cps/sec. Although the frequency dial on the oscillator is nonlinear, a linear variation was obtained over a 2-kcps deviation at 35 kcps, which was the center frequency used in these experiments. (The total frequency range on the scale is 60 kcps.)

The linearity of the ramp obtained in this manner can be demonstrated using the APC System. When the system is locked,

$$e_d = 0.025 \ S \ \sin \phi_{(\text{steady state})} = 0.025 \ S \ a . \qquad (5.2.1)$$

The voltage, $e_o(t)$, is then

$$e_o(t)_{(\text{steady state})} \quad -\zeta \ \frac{S}{4} \ a - \omega_a \ \frac{S}{4} \ at + \text{constant} \qquad (5.2.2)$$

-70-

Therefore, if the signal is ramp modulated, $e_o(t)$, should resemble Eq. (5.2.2). This is demonstrated in Fig. 5.2, which is a Sanborn recording of $e_o(t)$ showing the "steady state" response of an APC System to an applied frequency ramp modulated signal.

To determine the transient response of the system to an input signal, the difference frequency voltage, $e_d(t)$, was monitored using the Sanborn recorder. It should be noted that $e_d(t)$ is proportional to sin ϕ, not to the phase error, ϕ . Figure 5.3 shows the response of a slightly underdamped·system to a frequency ramp. The slope of the applied frequency ramp was approximately 15 cps/sec. The signal amplitude, S, was 20 volts, $\zeta = 10^{-2}$, and $\omega_a = \frac{1}{11}$ rad/sec. When $t < 0$, the frequency error was too large for locking to occur and the system "slipped" in phase. As the frequency error decreased, it is seen that the time required for the phase to slip by 2π increased. When the time, t , became greater than zero, the system started to lock. The maximum phase error during the locking cycle exceeded $\frac{\pi}{2}$, causing the extended maximum shown in Fig. 5.3. This effect can be visualized by referring to the phase plane sketch shown in Fig. 5.4. When $\phi = \frac{\pi}{2}$, the sin $\phi = 1$; when ϕ exceeded $\frac{\pi}{2}$, the sin ϕ became less than unity; and when ϕ again became $\frac{\pi}{2}$, the sin ϕ again became equal to unity. As the system is slightly underdamped (i.e., $\frac{\zeta^2}{4} < \frac{\omega_a}{\omega_n}$), it locked with only a slight overshoot.

The steady state phase error is proportional to the slope of the frequency ramp, (sin $\phi_{(steady\ state)} = -a$). This is seen from Fig. 5.3 as the steady state phase error is not at zero, but at some negative value. A rough calculation yielded:

$$\sin \phi_{(steady\ state)} = -a \cong -\frac{3}{7} . \qquad (5.2.3)$$
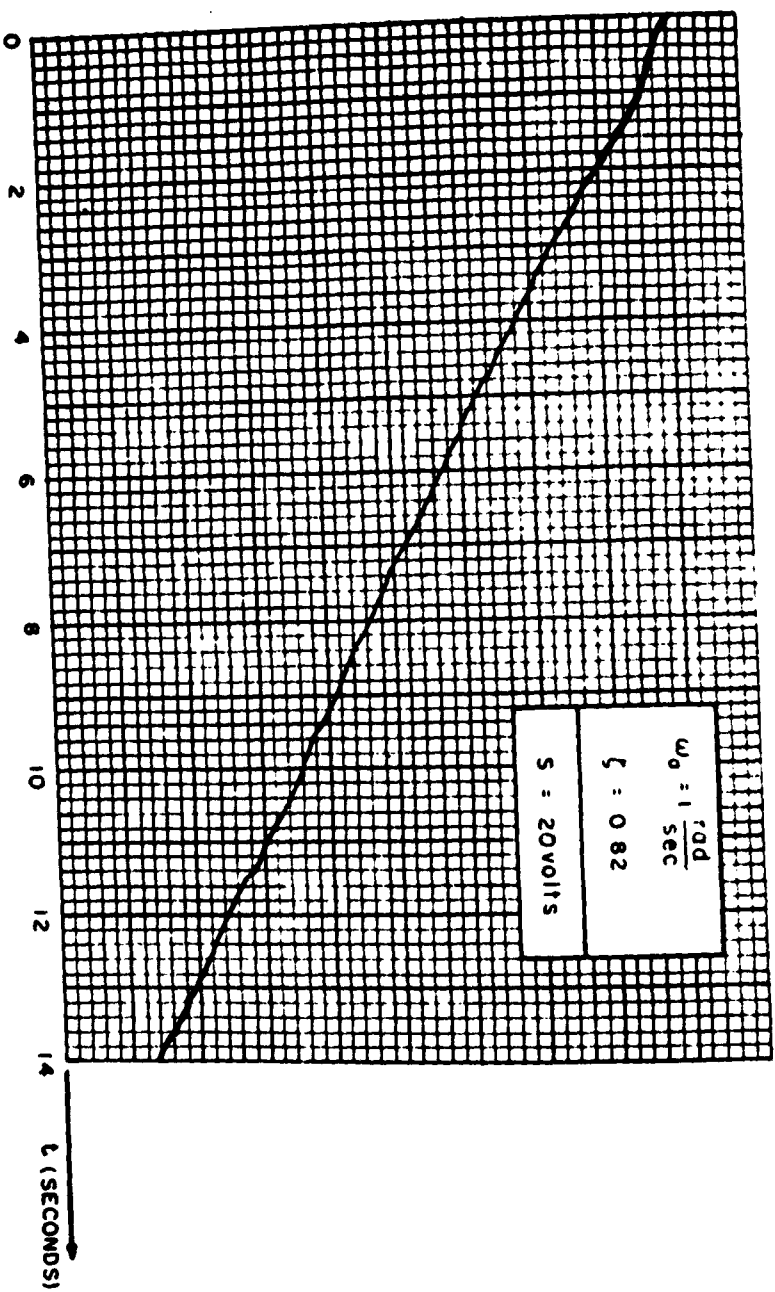
FIG. 5.2 A SANBORN RECORDING OF $e_o(t)$, AFTER THE SYSTEM IS SYNCHRONIZED TO A SIGNAL HAVING FREQUENCY MODULATION, SHOWING THE LINEARITY OF THE RAMP MODULATION

A-100-2-0056
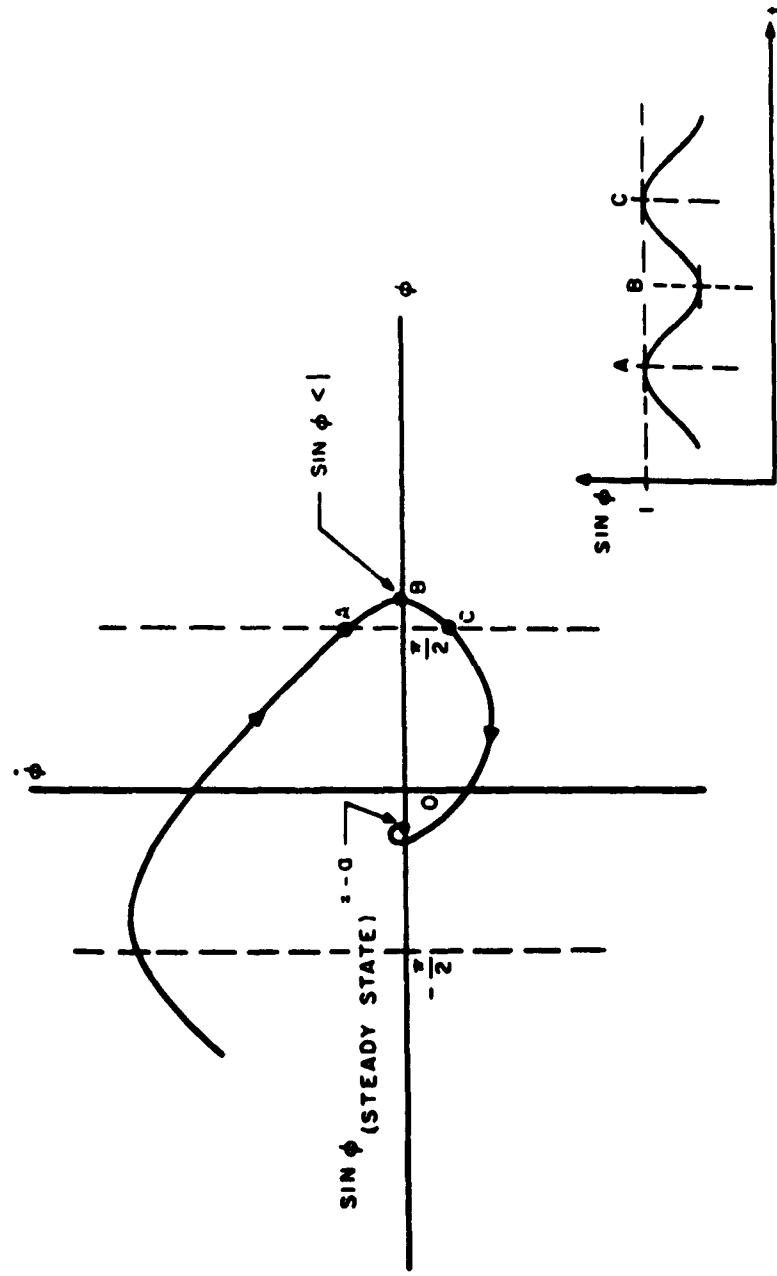
FIG. 5.4   A PHASE PLANE SKETCH, ILLUSTRATING THE LOCKING OF THE APC SYSTEM TO A FREQUENCY RAMP WHEN THE PHASE ERROR EXCEEDS $\frac{\pi}{2}$ RADIANS

A-100-Z-0058

$e_d(t)$

-10 -9 -8 -7 -6 -5 -4 -3 -2 -1 0 1 2 3 4 5

t (SECONDS)

| S = 20 VOLTS |
| $\zeta = 10^{-2}$ |
| $\omega_o = \frac{1}{11}$ RAD / SEC |
| $a \simeq 15$ CPS / SEC |
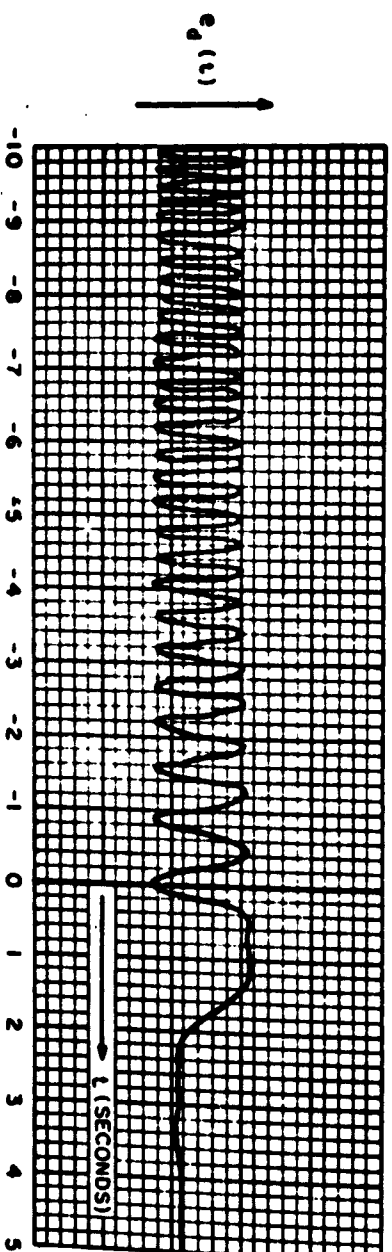
FIG. 5.3   THE DIFFERENCE FREQUENCY SIGNAL, e_d, SHOWING THE RESPONSE OF THE
APC SYSTEM TO A FREQUENCY RAMP

A-100-Z-0057

Thus,

$$\alpha = \omega_a \omega_n a = \left(\frac{1}{11}\right)(42.5 \pi \cdot 20)\left(\frac{3}{7}\right)$$

$$\approx 1000 \text{ rad/sec}^2 \approx 16 \text{ cps/sec} , \qquad (5.2.4)$$

verifying the directly measured value of the ramp (15 cps/sec).

5.2.2 Comparison of Experimental and Theoretical Results

To compare the experimental results with the theoretical results (obtained using the perturbation, piecewise-linear, and simple linear techniques shown in Fig. 2.5), the system coefficients were chosen to be

$$\epsilon = 0.25 \qquad (5.2.5)$$

and

$$a = 0.157 . \qquad (5.2.6)$$

Choosing a signal strength, $S = 10$ volts and $\omega_a = 1$ rad/sec, α and ζ were calculated:

$$\alpha = \omega_a \omega_n a \approx 33 \text{ cps/sec} \qquad (5.2.7)$$

and

$$\zeta = \sqrt{\frac{\omega_a}{\omega_n}} \epsilon \approx 6.94 \times 10^{-3} . \qquad (5.2.8)$$

Letting $R_1 = 1M\Omega$, C_2 and R_2 become

$$C_2 = 1 \mu f \qquad (5.2.9)$$

and

$$R_2 = 6.8 \text{ K}\Omega .$$

(5.2.10)

The difference frequency signal, e_d , was recorded for
two cases: that of a frequency ramp with $\alpha = 0$, and a fre-
quency ramp with $\alpha = 33$ cps/sec. The result obtained when
the input signal is unmodulated $(\alpha = 0)$ is shown in Fig. 5.5.
The response shown in the figure is underdamped as expected.
When the phase error exceeded $\frac{\pi}{2}$ radians, the time to com-
plete a period of the motion was greater than when the phase
error was much less than $\frac{\pi}{2}$ radians. The time per cycle was
approximately 0.3 sec, when the phase error exceeded $\frac{\pi}{2}$ ra-
dians and was approximately 0.2 sec when the phase error was
less than $\frac{\pi}{2}$ radians. When the phase error became small,
the system seemed to stop locking, and a continual phase jit-
ter was present. This phase jitter was inherent in the in-
put signal source. (As astable multivibrator, similar to the
multivibrator used as the VCO, was built and used as the in-
put signal The "phase jitter" was greatly reduced when the
transitorized multivibrator was used.)

When one observes the locking phenomenon, shown in Fig.
5.5, it becomes apparent that a simple linear solution is ex-
tremely restrictive. Locking begins when the phase error is
much greater than $\frac{\pi}{2}$ radians. (This is seen by the dip in
the peak of the curve. The dip indicates that $e_d (= \sin \phi)$
becomes less than unity, and therefore, the phase error, ϕ ,
becomes greater than $\frac{\pi}{2}$.) During the time that it takes the
maximum phase error to decrease from π radians to 1 radian,
the simple linear solution is of little value.

The response of the system to a frequency ramp modulat-
ed signal $(\alpha \approx 33$ cps/sec) is shown in Fig. 5.6. The wave-
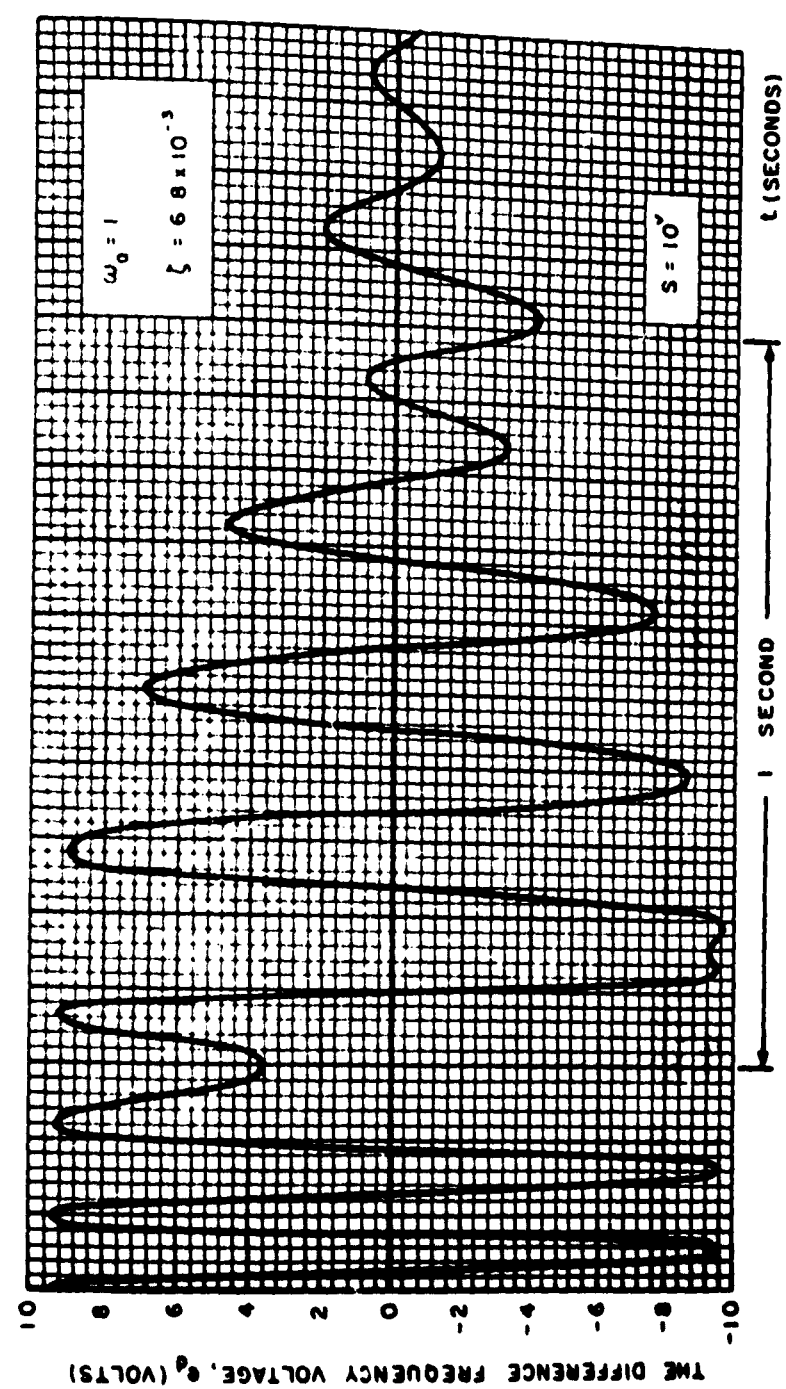
FIG. 5.6   THE RESPONSE OF AN APC SYSTEM TO A RAMP MODULATED INPUT SIGNAL

A-100-2-0060
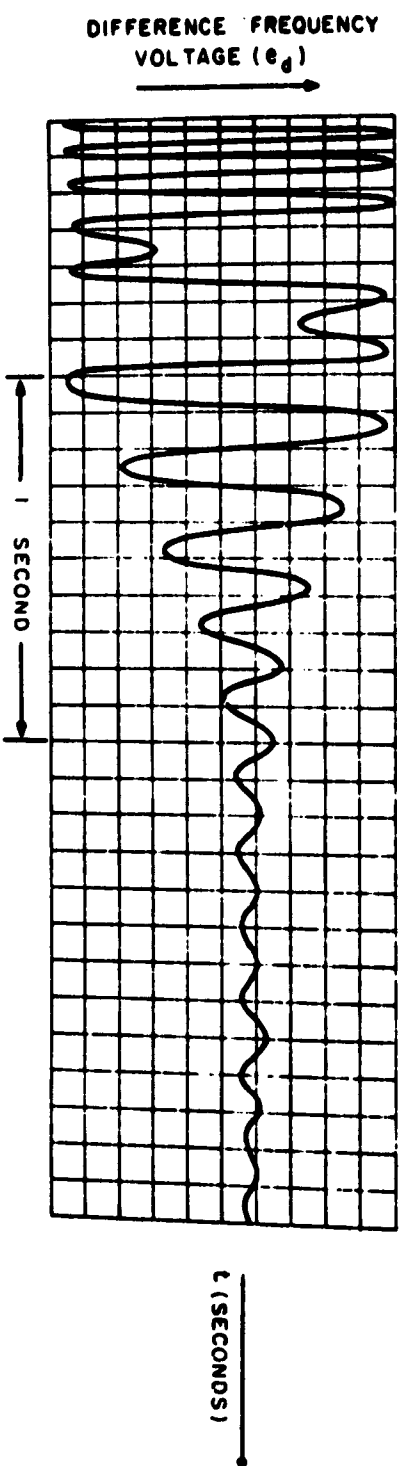
FIG. 5.5   THE RESPONSE OF THE APC SYSTEM TO AN UNMODULATED INPUT SIGNAL

A-100-2-0059

form is proportional to the sin ϕ, not to the phase error, ϕ. The phase error shown in Fig. 5.7 was calculated using Fig. 5.6. A comparison is made in Table I between the theoretical results, and the experimental results obtained from Fig. 5.7

TABLE I			
	Averaged Normalized Time (τ) Per Cycle		-m- Average Damping
	Phase Error $>$ 1 Rad	Phase Error $<$ 1 Rad	Factor
Experimental	10.1	7.9	0.051
Perturbation	7.8	7.4	0.053
Piecewise-Linear	7.85	7.85	0.08
Simple Linear	6.3	6.3	0.125

$$\phi(\tau) \sim e^{-m\tau} \cos \beta\tau$$

$$\tau = \sqrt{\omega_a \omega_n} \ t = 36 \ t \ \text{radians}$$

Table I compares the "average normalized time, τ, per cycle" and the "average damping factor" obtained experimentally, with the theoretically determined values. The "average damping factor" is calculated by considering the phase error, ϕ, to be approximated by a damped sinusoid of the form
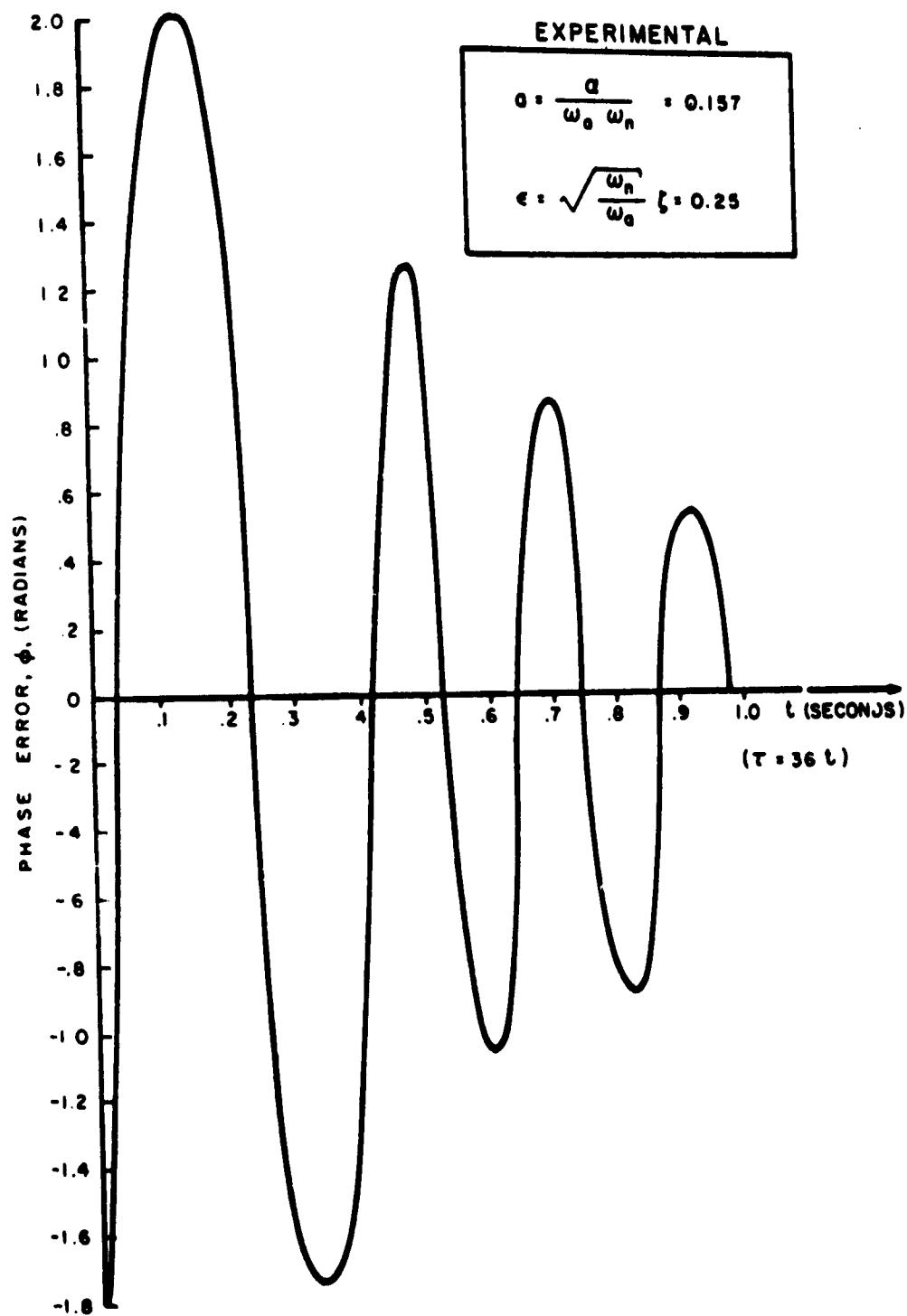
FIG 5 7 THE PHASE ERROR $\phi(t)$ VS. t, WHEN THE INPUT SIGNAL IS RAMP MODULATED

$$\phi \sim e^{-m\tau} \cos(\beta\tau + \psi) \ . \tag{5.2.11}$$

Using the simple linear solution, the response of the system to a frequency ramp, is

$$\phi(\tau) = \Phi_0 \ e^{-\frac{\epsilon}{2}\tau} \cos(\tau + \psi_0) - a \tag{5.2.12}$$

where

$$\epsilon = 0.25$$

$$a = 0.157 \ .$$

Therefore, the normalized time per cycle is

$$T = 2\pi \tag{5.2.13}$$

and the average damping factor is,

$$m = \frac{\epsilon}{2} = 0.125 \ . \tag{5.2.14}$$

Using the piecewise-linear solution, the phase error is

$$\phi(\tau) = \Phi_1 \ e^{-\frac{2}{\pi}\left(\frac{\epsilon}{2}\right)\tau} \cos\left(\sqrt{\frac{2}{\pi}} \ \tau + \psi_1\right) - \frac{\pi}{2} a \tag{5.2.15}$$

where

$$\epsilon = 0.25 \qquad .$$

and

$$a = 0.157 \ .$$

The normalized time per cycle is then

$$T = \sqrt{\frac{\pi}{2}} \; 2\pi \simeq 7.85 \qquad (5.2.16)$$

and the average damping factor is

$$m = \frac{2}{\pi}\left(\frac{\epsilon}{2}\right) \simeq 0.08 \; . \qquad (5.2.17)$$

The time per cycle was obtained correctly from Fig. 2.5 for the solution derived using the perturbation technique. The average damping factor was obtained by calculating the relative attenuation of the phase error between the positive peaks shown in this figure. At each peak $\phi(t)$ is simply

$$\phi(\tau) = \Phi_2 \; e^{-m\tau} \; . \qquad (5.2.18)$$

Rough calculations showed that

$$\phi(1.7) = \Phi_2 \; e^{-1.7m} = 1.5 \qquad (5.2.19)$$

and

$$\phi(9.2) = \Phi_2 \; e^{-9.2m} = 1 \; . \qquad (5.2.20)$$

Therefore,

$$e^{7.5m} = 1.5 \qquad (5.2.21)$$

and

$$m = 0.053 \qquad (5.2.22)$$

The experimental results were obtained in a similar manner from Fig. 5 7   The normalized time, τ, is

$$\tau = \sqrt{\omega_a \omega_n}\ t = 36\ t\ . \qquad (5.2.23)$$

The average damping factor is then calculated:

$$\phi(0.49) = \Phi_3\ e^{-36(0.49)m} = 1.28 \qquad (5.2.24)$$

and

$$\phi(0.7) = \Phi_3\ e^{-36(0.7)m} = 0.87\ . \qquad (5.2.25)$$

Therefore,

$$e^{7.56m} = 1.47 \qquad (5.2.26)$$

and

$$m = 0.051\ . \qquad (5.2.27)$$

The results given in Table I clearly indicate that the perturbation technique approximates the experimental results more closely than the piecewise-linear or the solution obtained using the simple linear approximation. The experimental and perturbation results would have checked even more precisely if the initial conditions of each would have been closer. The maximum phase error obtained with the perturbation technique was 1.6 radians, while the maximum phase error obtained experimentally was 2 radians. This caused the slight discrepancies which occurred in the "time per cycle" readings.

It should be noted, however, that an excellent comparison is obtained in determining the average damping factor m . This indicates that the time/cycle does not remain constant since it is a function of the maximum phase error. The damping factor, however, does remain fairly constant.

5.3 The APC System as a Phase Demodulator

As mentioned previously the APC System can be used as an FM demodulator, where the demodulated output is proportional to the input phase modulation. It was shown in Eq. (2.4 25) and Eq. (2 4.26) that in order to obtain a good reproduction of the input modulating signal, the modulating frequency, ω_m , had to be greater than $\zeta\omega_n$ and $\sqrt{\omega_a\omega_n}$. To verify these conditions, which determine the minimum fundamental modulation frequency that can be used, a frequency modulated input signal with an amplitude, S , equal to 30^V, was applied to the system, and steady state established. The resultant loop gain of the system was

$$\omega_n = 1275 \tau \text{ rad/sec} .$$

The modulation frequency was reduced until the demodulated output became noticeably distorted.

Table II compares the experimental and calculated values of the minimum frequencies for which an undistorted demodulation was possible. The minimum frequency possible is seen to be 8 cps and is determined by $\sqrt{\omega_a\omega_n}$. As the damping increases. $\zeta\omega_n$. increases and the minimum fundamental frequency also increases.

Photographs were taken to illustrate the operation of the APC System as a phase demodulator when a square wave frequency modulated input signal is applied. Sketches of these

-84-

photographs are shown in Fig. 5.8. The modulating frequency
used was 110 cps, and the carrier frequency was 35 kcps.

TABLE II			
ζ	$f_m(min)$ Calculated (cps)		$f_m(min)$ Measured (cps)
	$\dfrac{2}{\pi}\left(\dfrac{\omega_n}{2\pi}\right)\zeta$	$\dfrac{\sqrt{\dfrac{2}{\pi}\,\omega_a\omega_n}}{2\pi}$	
6.8×10^{-3}	2.8	8	15
47×10^{-3}	20	8	50
820×10^{-3}	333	8	700
$\omega_a = 1$ rad/sec			
$S = 30$ volts			
$\omega_n = 1275\ \pi$ rad/sec			

Figure 5.8a represents the input frequency modulating signal.
The demodulated waveform shown in Fig. 5.8b is the integral
of the square wave input modulation, as the demodulated out-
put is proportional to the phase modulation. The thickness
of the saw-tooth waveform is due to inadequate filtering of
the second, third and higher harmonics of the 35-kcps carrier
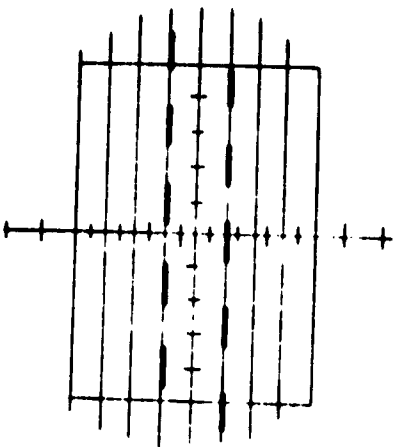
a) THE MODULATION SIGNAL

b) THE DIFFERENCE FREQUENCY SIGNAL, e_d

$f_M = 110$ CPS

$f_2 = 35$ KCPS

$\omega_0 = \dfrac{RAD}{SEC}$

$\zeta = 47 \times 10^{-3}$

$S = 30^v$

$\omega_N = 1275_w$
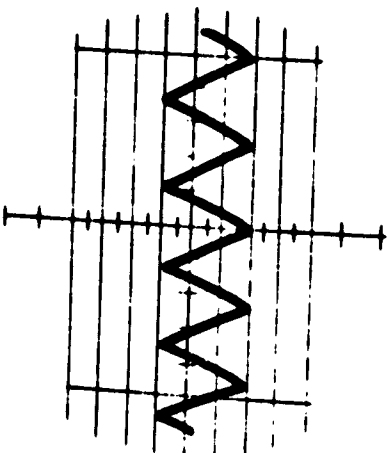
FIG. 5.8   THE APC SYSTEM AS A PHASE DEMODULATOR

A-100-2-0062

frequency It can be seen from this figure that the APC System is an excellent phase demodulator.

5.4 The Experimental Response of an APC System to Narrow-Band Gaussian Noise

To determine the response of the APC System to a signal embedded in noise, the response of the system to narrow-band Gaussian noise when no signal was present, was first investigated. The theoretical aspect of this investigation was discussed in Chapter 3. That discussion, and the discussion of the signal plus noise, relies on the fact that the response of the system to noise can be analyzed using the iteration technique. One of the more important results obtained using this technique was that the system acted as an open loop system to the noise. The following discussion describes the experiments performed and clearly shows that the theoretical model is correct.

5.4.1 The Input Noise

Figure 5.9 illustrates the manner in which the narrow-band Gaussian noise was obtained. (The APC System used is shown in Fig. 5.1.) The tuned circuit shown in Fig. 5.9 was adjusted for a resonant frequency of 35 kcps. The resultant bandwidth was measured and found to be approximately 6 kcps. The noise leaving the emitter-follower was tested for being Gaussian by comparing the rms noise measured using a Ballantine true rms meter, with that obtained using a peak detector.

The noise can be written as[5.1]

$$N(t) = y(t)\cos(\omega_2 t + \theta(t))$$ (5.4.1)

where $N(t)$ is Gaussian, with a zero mean and a variance σ^2.

GR NOISE GENERATOR

TEKTRONIC 10 MC PREAMPLIFIER

12 K

10 mhy

1000 - 3000 μμf

$$BW = \frac{Q}{2\pi} = 6 \text{ KCPS}$$

CENTER FREQUENCY = f_2 = 35 KCPS

AUTOMATIC PHASE CONTROL SYSTEM

INPUT

2N398

22 K

560 K

-45v
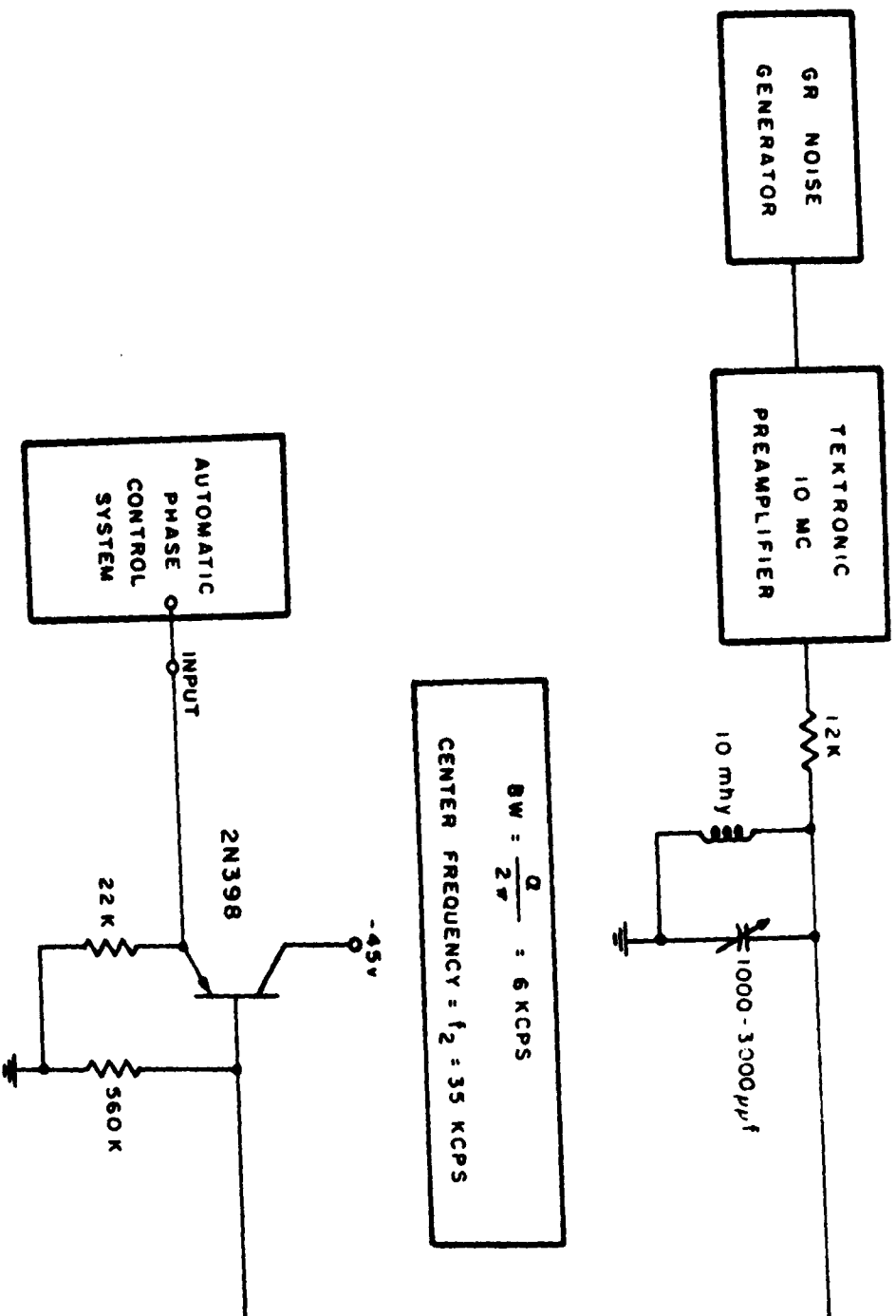
FIG 5 9   EXPERIMENTAL GENERATION OF COLORED GAUSSIAN NOISE

A-100-Z-0063

If the noise is narrowband, $y(t)$ is Rayleigh. A peak reading meter, such as the HPVTVM, reads

$$\langle y(t) \rangle = \lim_{T \to \infty} \frac{1}{T} \int_0^T y(t)dt \quad . \tag{5.4.2}$$

Since the probability of a Rayleigh distribution is,

$$p(y) = \frac{y}{\sigma^2} e^{-y^2/2\sigma^2} \tag{5.4.3}$$

and since $p(y)$ is stationary, the average value of the Rayleigh distribution is given by

$$\langle y \rangle = \bar{y} = \int_0^\infty \frac{y^2}{\sigma^2} e^{-y^2/2\sigma^2} dy = \sqrt{\frac{\pi}{2}} \sigma \tag{5.4.4}$$

which is a well known result.

A graph of the readings obtained using the peak detector $\sqrt{\frac{\pi}{2}}$, vs the true rms meter readings (σ) over the range of rms values that were intended for use throughout the experiments, is shown in Fig. 5.10. The slope of the curve differed by less than 3 per cent from the theoretical value, $\sqrt{\frac{\pi}{2}}$. It should be noted that even with this close agreement, one cannot say that the noise is definitely Gaussian. It is conceivable that some other distribution could yield the same result. However, it was expected that the noise was approximately Gaussian, and for all intensive purposes this prediction was verified.

$$\frac{\Delta\ e_p}{\Delta\ e_{rms}} = 1.28$$

PEAK DETECTOR READING, e_p

TRUE RMS VOLTAGE, e_{RMS}
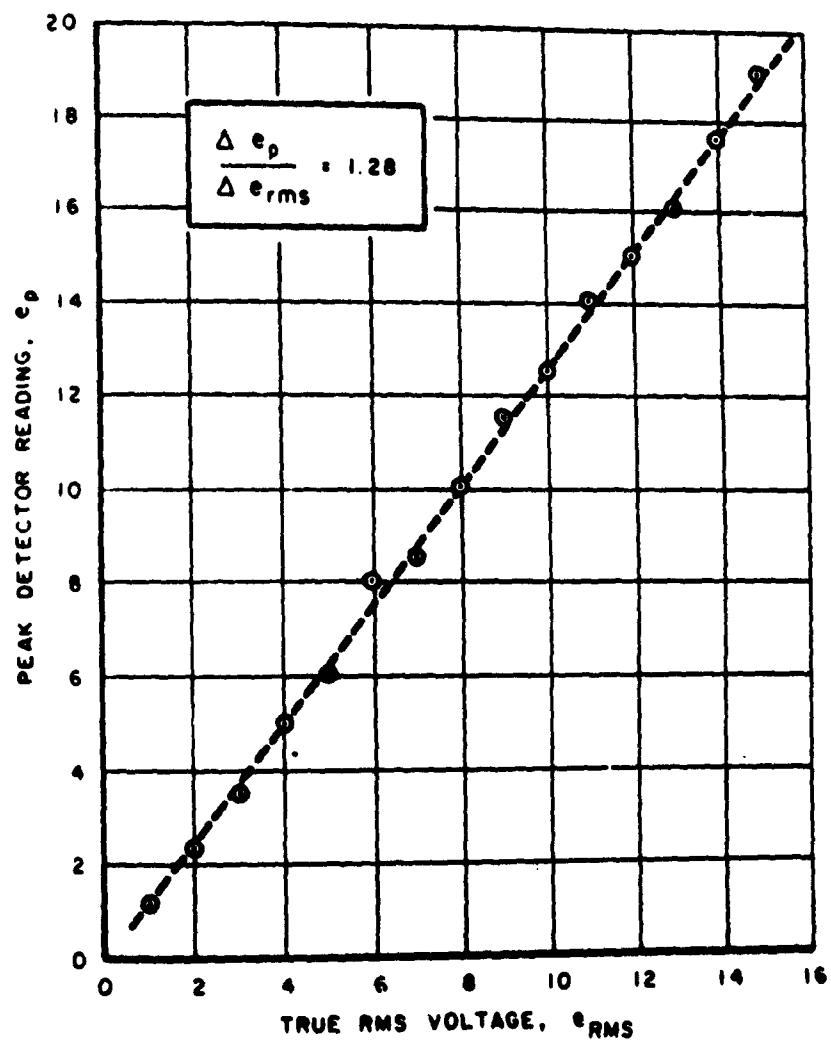
A-100-2-0064

FIG. 5.10   VERIFICATION OF GAUSSIAN CHARACTER OF THE INPUT NOISE

5.4.2 A Comparison of the Theoretically and Experimentally Determined Rms Noise at e_d and e_o

Using a true rms meter, the relation between the rms input noise, $e_{d_{rms}}$ and $e_{o_{rms}}$ was determined using different parameters of the phase lag filter. The results of this measurement are shown in Table III.

TABLE III					
ζ	σ_n	$e_{d(rms)}$	$e_{o(rms)}$	$e_{d(rms)}$	$e_{o(rms)}$
		measured		calculated	
	(volts)	(volts)		(volts)	
6.8×10^{-3}	35	.38	2.8×10^{-3}	.35	2.4×10^{-3}
47×10^{-3}	35	38	17.5×10^{-3}	.35	17.9×10^{-3}
100×10^{-3}	35	.38	40×10^{-3}	.35	38×10^{-3}
820×10^{-3}	35	.38	330×10^{-3}	.35	312×10^{-3}

$$e_{d_{rms}}(calc) = G_1 \sqrt{\frac{1000}{6000}} \; \sigma_n$$

$$e_{o_{rms}}(calc) = \zeta \; e_{d_{rms}}$$

Same values obtained for all ω_a between

$$\frac{1}{11} \leq \omega_a \leq 1$$

Since the statistics of the difference frequency volt-age, e_d , are stationary, the rms noise measured using a true rms meter is seen to yield the same result as the standard de-viation calculated using the equation:

$$e_{d_{rms}} = \sigma_{e_d} = G_1 \sqrt{\frac{\omega_o}{\alpha}} \, \sigma_n \qquad (5.4.5)$$

where

$$G_1 = 0.025$$

$$\omega_o = 2\pi(1000)\,rad/sec$$

and

$$\alpha = 2\pi(6000)\,rad/sec \quad .$$

Since the statistics of e_o are nonstationary, the rms value of e_o is not the same as its standard deviation. The measured rms values of e_o were found to be independent of ω_a.

The rms value of the output voltage was calculated using the relation

$$e_{o_{rms}} = \zeta \, e_{d_{rms}} \quad . \qquad (5.4.6)$$

This result can be justified by the following argument: The average value of e_d is zero. Since e_d is stationary, the time average of e_d is also zero. Thus,

$$\langle e_d \rangle = \lim_{t \to \infty} \frac{1}{T} \int_0^T e_d(\lambda)d\lambda \quad . \qquad (5.4.7)$$

If the time is fairly large,

$$\int_0^T e_d(\lambda)d\lambda \simeq T \langle e_d \rangle = 0 \quad . \qquad (5.4.8)$$

Then $e_o(T)$ is,

$$e_o(T) = - \zeta\, e_d(T) - \omega_a \int_o^T e_d(\lambda)d\lambda \approx -\zeta\, e_d(T) . \qquad (5.4.9)$$

This approximation is valid only when ω_a is small.

The measured values $e_{o_{rms}}$, and the values calculated using Eq. (5.4.6) are seen to correspond.

The measurements shown in Table III were made when the system operated (normally) in the closed loop position, and again, with the system operating as an open loop system, with e_o disconnected from the VCO. The same values were obtained in each case for $e_{d_{rms}}$ and $e_{o_{rms}}$. This clearly indicates that the noise "sees" an open loop system.

5.4.3 Verification of the Gaussian Character of e_d

To determine the probability distribution of e_d, the voltage was recorded using a Sanborn recorder and 1656 samples were obtained from the recording over 24 amplitude intervals. The estimated probability that the noise is below the mth interval is

$$P(e_d < E_d) = \sum_{i=1}^{m} \frac{n_i}{n} \qquad (5.4.10)$$

where

E_d is the difference frequency voltage in the mth interval,

n_i is the number of samples present in the ith interval,

and

n is the total number of samples recorded.

-93-

The probability that the difference frequency voltage, e_d, is less than a specified voltage, E_d, is plotted on probability paper in Fig. 5.11. The resulting curve approximates a straight line and therefore, approximates the Gaussian distribution found theoretically. Table IV shows the probability density per interval, I. A change in e_d of approximately one millivolt was required for a change of one interval.

A χ^2 "goodness of fit" test[5.2] was also performed. The χ^2 distribution can be approximated by

$$\chi^2 = n \left[\sum_{i=1}^{m} \frac{1}{P_i} \left(\frac{n_i^2}{n} \right) - 1 \right] \qquad (5.4.11)$$

where

n_i is the number of samples in the ith interval,

n is the total number of samples,

and

P_i is the actual Gaussian probability density,

as found from a table of Gaussian distributions.[5.3] From Table IV, it is seen that the expected value of the voltage, e_d, is in the twenty-fifth interval, or

$$E(I) = 25 \qquad (5.4.12)$$

where I is any amplitude interval. The estimated variance

$$\hat{\sigma}_I^2 = \sum_{i=1}^{m} \frac{n_i}{n} (I - 25)^2 \quad . \qquad (5.4.13)$$
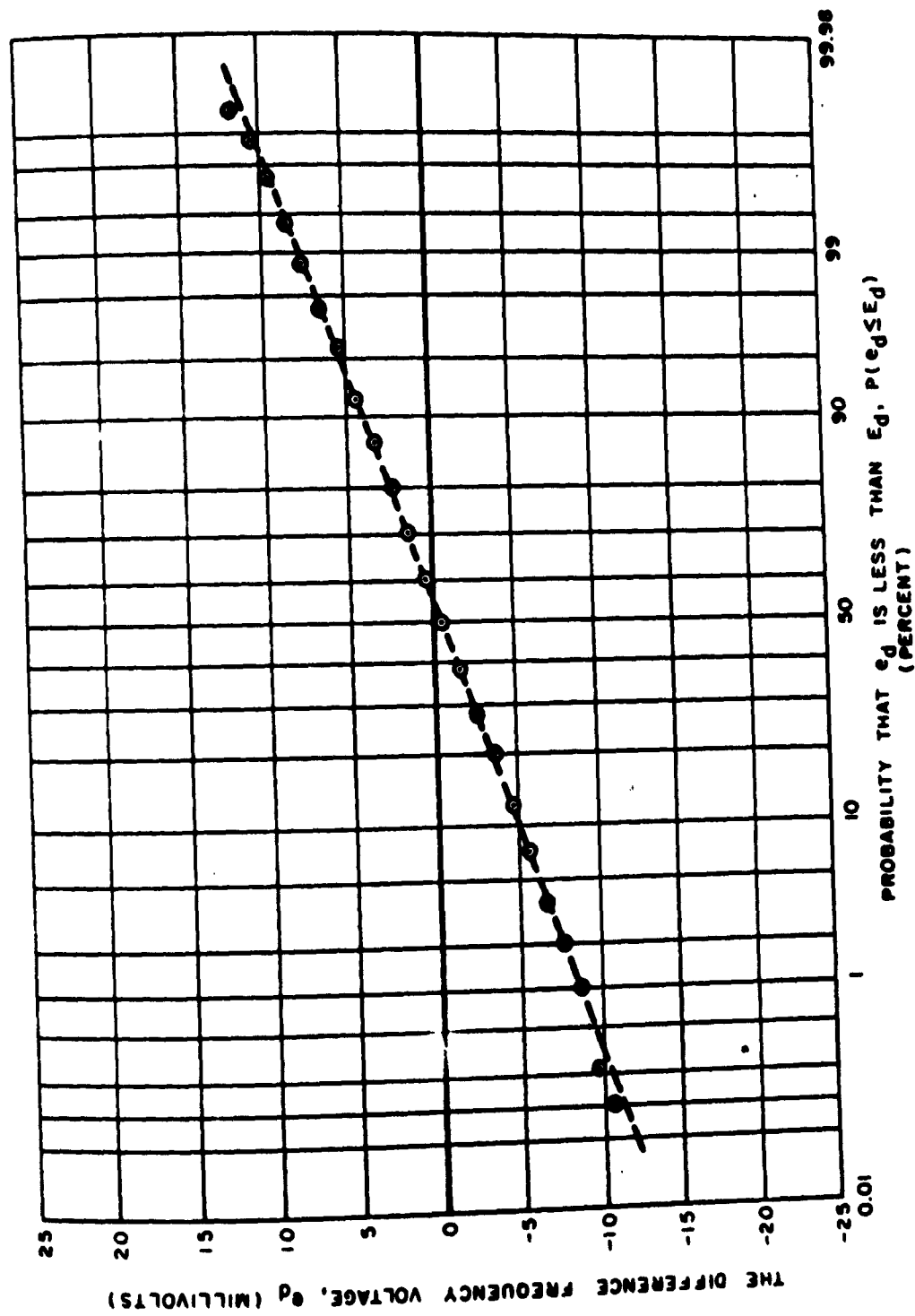
FIG. 5.11   EXPERIMENTAL VERIFICATION OF THE GAUSSIAN RESPONSE OF THE DIFFERENCE
FREQUENCY VOLTAGE, e_d, TO GAUSSIAN INPUT NOISE

A-100-2-0065

TABLE IV			
Interval (I)	e_d(millivolts)	Number of Samples per Interval	$n_i/n(\times 10^{-2})$
0-14		0	0
14-15	-10.5	2	.1207729468
15-16	- 9.5	2	.1207729468
16-17	- 8.5	13	.7850241542
17-18	- 7.5	19	1.1473429946
18-19	- 6.5	28	1.6908212552
19-20	- 5.5	61	3.6835748774
20-21	- 4.5	87	5.2536231
21-22	- 3.5	117	7.0652173878
22-23	- 2.5	145	8.756038643
23-24	- 1.5	163	9.8429951642
24-25	- 0.5	191	11.5338164194
25-26	+ 0.5	186	11.2318840524
26-27	+ 1.5	169	10.2318840524
27-28	+ 2.5	144	8.6956521696
28-29	+ 3.5	118	7.1256038612
29-30	+ 4.5	83	5.0120772922
30-31	+ 5.5	58	3.5024154572
31-32	+ 6.5	29	1.7512077286
32-33	+ 7.5	22	1.3285024148
33-34	+ 8.5	9	.5434782606
34-35	+ 9.5	6	.3623188404
35-36	+10.5	2	.1207729468
36-37	+11.5	1	.063864734
37-38	+12.5	1	.063864734
38-		0	0
		1656	0.9999999992

Equation (5.4.13) can be evaluated using Table IV. Then

$$\hat{\sigma}_I^2 = 12.274324 \qquad (5.4.14)$$

and the estimated standard deviation is

$$\hat{\sigma}_I = 3.50347 . \qquad (5.4.15)$$

Knowing the estimated standard deviation, the probability density, p_i , was found and χ^2 calculated.

$$\chi^2 = 10.214 . \qquad (5.4.16)$$

There are 24-amplitude intervals, and, since the variance was estimated, 23 degrees of freedom. These results indicate that by chance alone, if the probability distribution is Gaussian, then with a probability of 0.99, the χ^2 test would indicate a worse fit than the one actually observed.

It should be noted that the Sanborn recorder has a 3-db bandpass of about 45 cps. Thus, the recorder itself does a great deal of filtering of the voltage e_d .

5.5   The Experimental Response of an APC System to a Frequency Ramp Modulated Signal and Narrow-Band Gaussian Noise

5.5.1 Introduction

A frequency ramp modulated signal and narrow-band Gaussian noise were simultaneously applied to the APC System. The initial frequency error

$$\dot{\phi}(o) = \omega_2 - \omega_1 = \Omega \qquad (5.5.1)$$

was always chosen to be greater than zero, to insure locking if noise were not present (see Fig. 2.3). During the locking process it was observed that if the phase error between the input signal and the output of the voltage controlled oscillator exceeded $\frac{\pi}{2}$ radians a large percentage of the time, the system would not synchronize to the incoming signal. This condition was determined by observing the output voltage of the multiplier, e_m , on a high persistance oscilloscope screen.

5.5.2 The Effect of Limiting on the Response of the APC System

Two random noise generators were used in this experiment. The output of the first noise generator, when filtered, produced Gaussian noise. The second noise generator produced limited (clipped) Gaussian noise. It was observed that when the amplitude of the noise was limited, the rms value of the noise required to prevent the system from locking, increased considerably beyond the rms value of the noise required when the noise was not limited.[5.4]

5.5.3 The Effect of Varying the Parameters, ϵ and a, on the Response of the APC System

The effect of varying the filter parameters, ϵ and 'a', on the performance of an APC System is shown in Fig. 5.12. These curves were obtained by first adjusting the noise to obtain a particular N/S ratio and then seeing if the system locked. It the system locked, the noise was increased in 1-volt rms steps until the system locked only part of the time. The noise was then decreased by 1-volt rms and the reading taken. (A threshold level of approximately 2-volts rms seemed to exist.) The measurements, shown in Fig. 5.12, were made with a signal amplitude

$$S = 5 \text{ volts,} \tag{5.5.2}$$
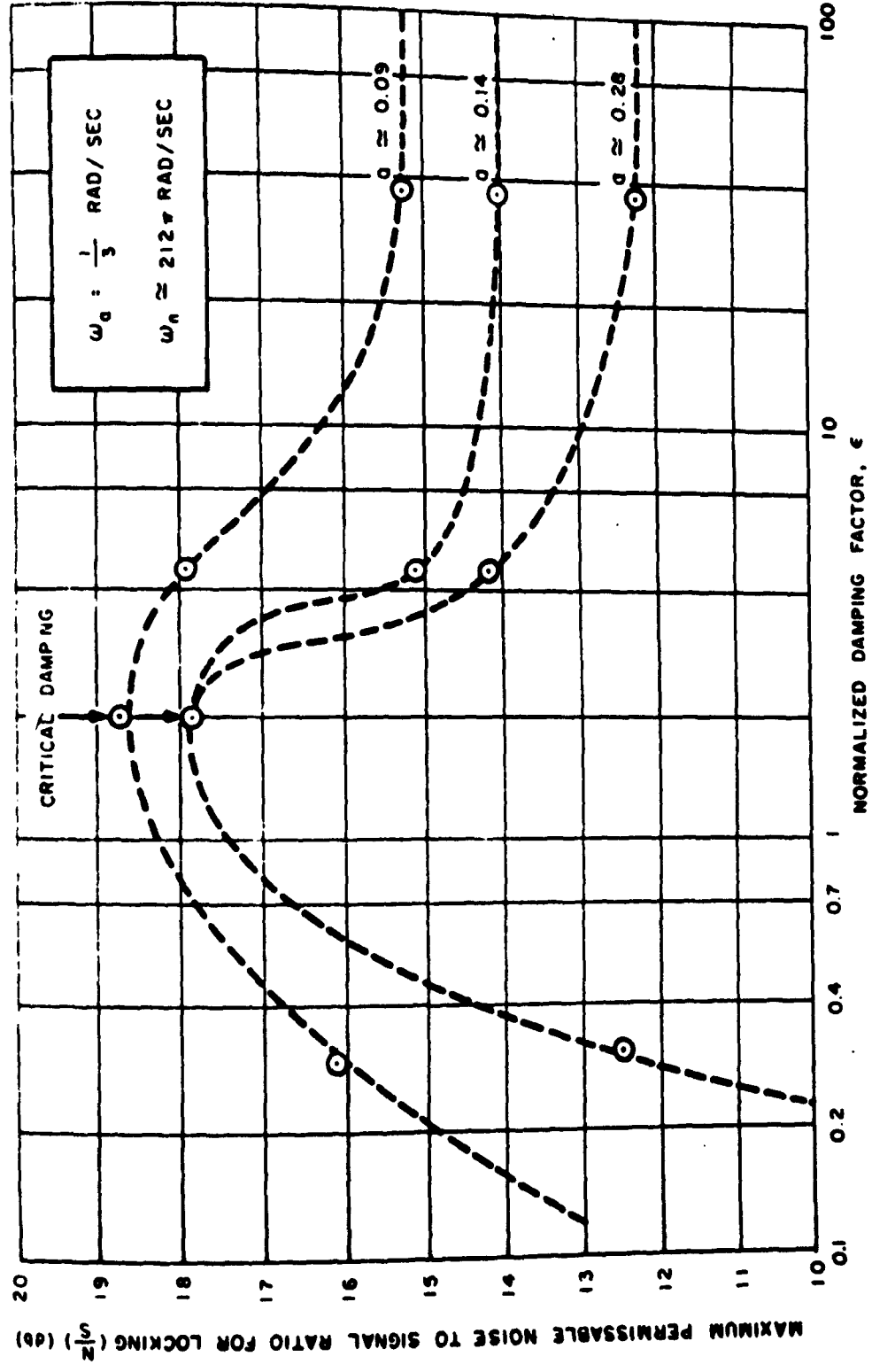
FIG. 5.12   EXPERIMENTALLY DETERMINED MAXIMUM PERMISSABLE N/S RATIO FOR LOCKING TO OCCUR

and

$$\omega_a = \frac{1}{3} \text{ rad/sec} .$$ (5.5.3)

Therefore,

$$\omega_n = 212\pi \text{ rad/sec} .$$ (5.5.4)

It is seen that as 'a' increased, the N/S ratio had to be decreased to still insure locking. When 'a' exceeded 1/2, the system was found to be unable to synchronize to the input signal unless the noise was reduced to zero. Even then, the system did not lock if the initial conditions were not adjusted properly (see Fig. 2.4). This result follows immediately from the experimentally observed that the requirement phase error must be less than $\frac{\pi}{2}$ most of the time. In steady state, the phase error due to the signal is,

$$\left| \phi_{(\text{steady state})} \right| = \sin^{-1} a .$$ (5.5.5)

Thus, as 'a' increases $\phi_{(\text{steady state})}$ approaches $\frac{\pi}{2}$ radians and the maximum value of the noise must be decreased to insure locking.

Optimum results were obtained when the normalized damping factor, ϵ , was adjusted so that the system was critically damped. When the system was underdamped or overdamped, large phase errors (due to the signal) resulted over a long period of time. This increased the probability that the noise would prevent the system from locking.

These results show that during the locking process the system should be critically damped. After locking, however, ϵ should be reduced to decrease the variance of the phase jitter, θ_{2_n} .

Chapter 6

CONCLUSIONS

6.1   Conclusions

The two analytical techniques presented permit the calculation of the response of an Automatic Phase Control System to FM signals. The comparison made between the theoretical and the experimental results indicate that the perturbation and piecewise-linear techniques yield excellent approximations of the second-order nonlinear differential equation studied. The perturbation technique yields extremely good analytical results. However, it can be used only to determine the response of an underdamped system. A piecewise-linear solution is easier to obtain than the perturbation solution. However, the linearization of the system results in a loss in accuracy.

The response of the APC System to noise was obtained without "linearizing" the system equation, through use of an iteration technique. It was shown that with an RC low-pass filter and an active phase lag filter present in the loop, the system responded to noise as an open loop system. The noise rejection of this device is greater than that predicted using a linear analysis. (The response of a linearized APC System to noise was shown to result in a closed loop system.)

The APC System can synchronize to a frequency ramp modulated signal, if the slope of the frequency ramp

$$\alpha < \frac{1}{2} \left(\omega_a \omega_n \right) \quad .$$

$$(6.1.1)$$

When the signal is embedded in noise, the maximum input N/S ratio, to permit locking, varied inversely to $\sqrt{\omega_a \omega_n}$. This expression acts as an effective "bandwidth" of the system. (The term "bandwidth" is actually a misnomer, since the system response found is a transient, not a steady state response.)

It was shown experimentally that the normalized damping factor, ϵ , affected the probability of locking to a frequency ramp modulated signal. The critically damped condition was found to yield optimum results. The underdamped and overdamped responses required a longer time to lock, thus decreasing the probability that the system would synchronize to the incoming signal.

6.2   Suggestions for Future Work

The response of an APC System to an FM signal in the presence of an interfering signal should be investigated. Preliminary observations indicated that the system would lock to the closer of the two signals. It will fall out of lock, however, if the amplitude of the interfering signal is too great. The amplitude required to pull the system out of synchronism was found to be proportional to the frequency difference between the two signals.

The analysis used to determine the response to a signal and noise, should be extended. The results presented in this dissertation should be experimentally verified, and an attempt made to demonstrate convergence of the iteration technique

The active phase lag filter was used in the analysis presented, as it is used in the majority of APC Systems in operation today. An attempt should be made to find an "optimum" filter. In the past the APC System was linearized, and the linearized system "optimized." This does not neces-

sarily imply "optimum" results with regard to the locking problem. The possibility of using a nonlinear filter instead of the phase lag filter should be investigated. The use of a limiter should also be considered.

It is suggested that any theoretical work performed be supplemented by a great deal of experimental research.

BIBLIOGRAPHY

Chapter 1

1.1   Enloe, "Decreasing the Threshold in FM by Frequency Feedback," Proc. IRE, January 1962.

Gilchriest, "Application of a Phase-Locked Loop to Telemetry as a Discriminator or Tracking Filter," IRE Trans. on Telemetry and Remote Control, June 1958.

Jakes, et al., Project Echo, BSTJ, Vol. 40. No. 4, July 1961.

1.2   Kreindler, E., The Theory of Phase Synchronization of Oscillators with Application to the Doppler Tracking Filter, Electronics Research Laboratories, School of Engineering and Applied Science, Columbia University, New York 27, New York, Technical Report, T-1/157, August 1959.

1.3   Viterbi, A. J., Acquisition and Tracking Behavior of Phase-Locked Loops, JPL, CIT, External Publication, No. 673, July 1959.

1.4   Leek, R., "Phase-Lock AFC Loop," Electronic and Radio Engineer, April-May 1957.

1.5   Kreindler, E., op. cit., pp. 38-45.

Chapter 2

2.1   Celinski, D., Jelonek, Z. and Syski, R., "Pulling Effect in Synchronized Systems," Proc. IEE, Part IV, Vol. 101, p. 108, 1954.

2.2   Jaffe, R. and Rechtin, E., "Design and Performance of Phase-Lock Circuits Capable of Near-Optimum Performance over a Wide Range of Input Signal and Noise Levels," IRE Trans. PGIT, p. 66, March 1955.

2.3   Viterbi, op. cit.

Rue and Lux, "Transient Analysis of a Phase-Locked Loop Discriminator," IRE Trans. in Space Electronics and Telemetry, December 1961.

2.4   Viterbi, op. cit.

2.5   Cunningham, W. J., Nonlinear Analysis, McGraw-Hill, p. 36, 1958.

2.6   Viterbi, op. cit.

2.7   Milne-Thomson, L. M., *Jacobian Elliptic Function Tables*, Dover Publ., p. 38, 1950.

2 8   Cunningham, W. J., op. cit., p. 189.

2.9   Leek, R., op. cit.

2.10 Cayley, A., *Elliptic Functions*, Dover Publ., p. 3, 1961.

2.11 Milne-Thomson, L. M., op. cit., p. 13.

2.12 Viterbi, A. J., op. cit.

Chapter 3

3.1   Cunningham, W. J., op. cit., p. 188.

3.2   Rice, S. O., "Mathematical Analysis of Random Noise," BSTJ, Vol. 23, pp. 283-332, 1944; Vol. 24, pp. 46-156, 1945.

Chapter 4

4.1   Jaffe, R. and Rechtin, E., op. cit.

4.2   Margolis, S. G., "The Response of a Phase-Locked Loop to a Sinusoid Plus Noise," IRE Trans. on PGIT, p. 137, June 1957.

Chapter 5

5.1   Davenport, Jr., W. B. and Root, W. L., *Random Signals and Noise*, McGraw-Hill, p. 158, 1958.

5.2   Cramer, H., *Mathematical Methods of Statistics*, Princeton Univ. Press, Princeton, N. J., p. 416, 1946.

5.3   Lowen, A., W.P.A., "Table of Probability Functions," Vol. II.

5.4   Jaffe, R. and Rechtin, E., op. cit.

Appendix B

B.1   Lampard, D. G., "The Response of Linear Networks to Suddenly Applied Stationary Random Noise," IRE Trans. PGCT, p. 49, March 1955.

APPENDIX A

THE SOLUTION TO THE LINEARIZED MODEL

The second-order nonlinear differential equation to be analyzed is

$$\frac{d^2\phi}{d\tau^2} + \epsilon \cos \phi \frac{d\phi}{d\tau} + \sin \phi = -a \frac{de_m(\tau)}{d\tau} \quad . \qquad (A.1)$$

If the phase error

$$|\phi(\tau)| << 1 \text{ radian}, \qquad (A.2)$$

Eq. (A 1) can be linearized:

$$\frac{d^2\phi}{d\tau^2} + \epsilon \frac{d\phi}{d\tau} + \phi = -a \frac{de_m(\tau)}{d\tau} \quad . \qquad (A.3)$$

The solution to this equation is well known. For example, if

$$\epsilon = 0.25 , \qquad (A.4)$$

$$a \frac{de_m(\tau)}{d\tau} = \frac{\pi}{20} \quad ,$$

$$\phi(\omega) = 0$$

and

$$\left. \frac{d\phi}{d\tau} \right|_{\tau = 0} = 1.6$$

the phase error is

$$\phi(\tau) \approx 1.63 \; e^{-\frac{\tau}{8}} \; \sin(\tau + 0.0965) - \frac{\pi}{20} \; .$$

In this particular example, the phase error exceeds one radian, causing the result obtained using this technique to be significantly different from the results obtained using the perturbation and piecewise-linear techniques (Section 2.4) shown in Fig. 2.5.

THE RESPONSE OF AN APC SYSTEM TO NARROW-BAND GAUSSIAN NOISE

B.1   The Statistics of the Output Voltage

The output voltage

$$e_{o_1}(t) = -\zeta \, e_{d_1}(t) - \omega_a \int_0^t e^{-\frac{\omega_a}{A}(t - \lambda)} e_{d_1}(\lambda)d\lambda \, . \qquad (B.1.1)$$

The expected value of $e_{o_1}(t)$ is

$$(B.1.2)$$

$$E(e_{o_1}(t)) = -\zeta \, E(e_{d_1}(t)) - \omega_a \int_0^t e^{-\frac{\omega_a}{A}(t - \lambda)} E(e_{d_1}(\lambda))d\lambda \, .$$

Since

$$E(e_{d_1}(t)) = 0 \, , \qquad (B.1.3)$$

the expected value of the output voltage is

$$E(e_{o_1}(t)) = 0 \, . \qquad (B.1.4)$$

The autocorrelation function of $e_{o_1}(t)$ is

$$R_{e_{o_1}}(t,\tau) = \zeta^2 \, R_{e_{d_1}}(\tau) + \omega_a \, \zeta \int_0^t e^{-\frac{\omega_a}{A}(t - \lambda)} R_{e_{d_1}}(t + \tau - \lambda)d\lambda +$$

$$+ \omega_a \zeta \int_0^{t+\tau} e^{-\frac{\omega_a}{A}(t + \tau - \lambda)} R_{e_{d_1}}(t - \lambda) d\lambda \qquad (B.1.5)$$

$$+ \omega_a^2 \int_0^t d\lambda \int_0^{t+\tau} d\eta \left[e^{-\frac{\omega_a}{A}(2t + \tau - \lambda - \eta)} R_{e_{d_1}}(\eta - \lambda) \right]$$

where

$$R_{e_{d_1}}(u) = \frac{\omega_o}{\alpha} G_1^2 \sigma_n^2 e^{-\omega_o |u|} . \qquad (B.1.6)$$

The substitution of Eq. (B.1.6) into Eq. (B.1.5) results in several straightforward integrations. The first integral becomes:

$$\int_0^t e^{-\frac{\omega_a}{A}(t - \lambda)} R_{e_{d_1}}(t + \tau - \lambda) d\lambda$$

$$= \frac{\omega_o}{\alpha} G_1^2 \sigma_n^2 e^{-\frac{\omega_a}{A} t} \left[\frac{e^{-\omega_o(t + |\tau|)} \left(e^{\left(\omega_o + \frac{\omega_a}{A}\right) t} - 1 \right)}{\omega_o + \frac{\omega_a}{A}} \right] . \qquad (B.1.7)$$

The second integral is:

$$\int_0^{t+\tau} e^{-\frac{\omega_a}{A}(t + \tau - \lambda)} R_{e_{d_1}}(t - \lambda) d\lambda$$

$$= \int_0^t e^{-\frac{\omega_a}{A}(t + \tau - \lambda)} R_{e_{d_1}}(t - \lambda) d\lambda$$

$$+ \int_t^{t+\tau} e^{-\frac{\omega_a}{A}(t + \tau - \lambda)} R_{e_{d_1}}(\lambda - t) d\lambda =$$

$$= \frac{\omega_o}{\alpha} G_1^2 \sigma_n^2 e^{-\frac{\omega_a}{A}(t + |\tau|)} \left[\frac{e^{\frac{\omega_a}{A}t} - e^{-\omega_o t}}{\omega_o + \frac{\omega_a}{A}} + \frac{e^{\frac{\omega_a}{A}t}\left(1 - e^{-(\omega_o - \frac{\omega_a}{A})|\tau|}\right)}{\omega_o - \frac{\omega_a}{A}} \right].$$

(B.1.8)

The third integral can be evaluated using.[B.1] The double integral can then be written as

$$\int_o^t d\lambda \int_o^{t+\tau} d\eta = \int_o^t dx \int_o^{t-x} d\eta + \int_{-\tau}^o dx \int_o^t d\lambda + \int_{-(t+\tau)}^{-\tau} dx \int_o^{t+\tau-x} d\lambda$$

(B.1.9)

where

$$x = \lambda - \eta \quad .$$

Therefore,

$$\int_o^t d\lambda \int_o^{t+\tau} d\eta \left[e^{-\frac{\omega_a}{A}(2t + \tau - \lambda - \eta)} R_{e_{d_1}}(\eta - \lambda) \right]$$

$$= \int_o^t dx \int_o^{t-x} d\eta \left[e^{-\frac{\omega_a}{A}(2t + \tau - x - 2\eta)} R_{e_{d_1}}(x) \right]$$

$$+ \int_{-\tau}^o dx \int_o^t d\lambda \left[e^{-\frac{\omega_a}{A}(2t + \tau + x - 2\lambda)} R_{e_{d_1}}(x) \right]$$

$$+ \int_{-(t+\tau)}^{\tau} dx \int_o^{t+\tau-x} d\lambda \left[e^{-\frac{\omega_a}{A}(2t + \tau + x - 2\lambda)} R_{e_{d_1}}(x) \right] \text{(B.1.10)}$$

$$= \frac{\omega_o}{\alpha} G_1^2 \sigma_n^2 \frac{1}{2\frac{\omega_a}{A}} \left[\frac{\left(1 - e^{-(\omega_o + \frac{\omega_a}{A})t}\right)\left(1 + e^{-\omega_o |\tau|}\right)}{\omega_o + \frac{\omega_a}{A}} + \right.$$

$$x = \lambda - \eta$$
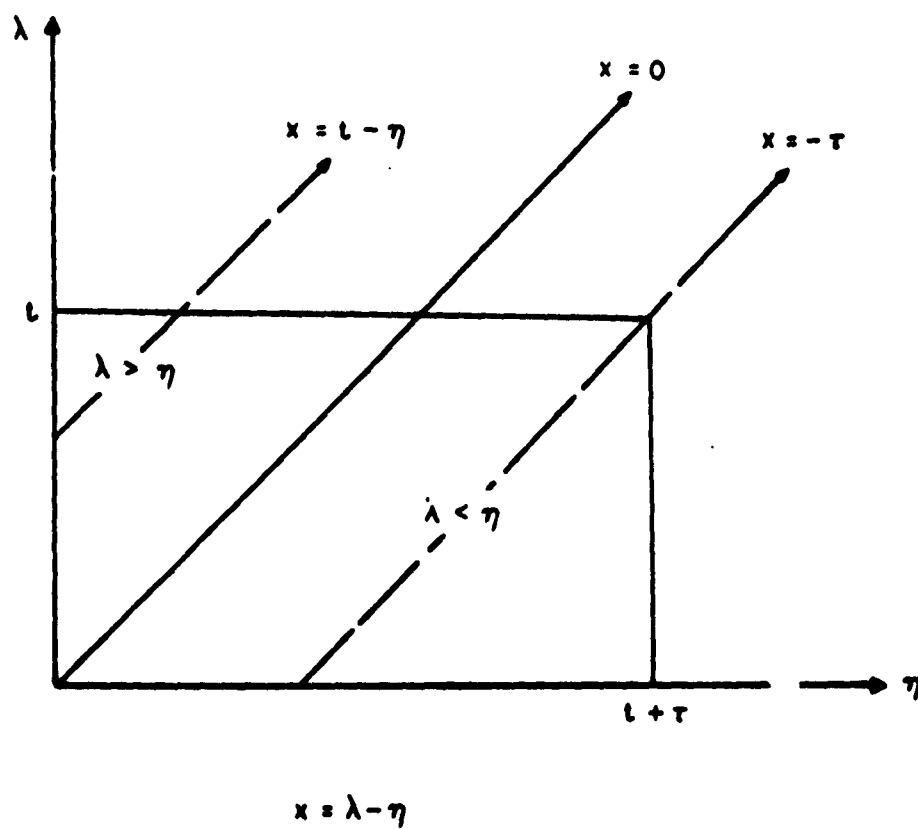
FIG. B.I   THE FORMULATION OF EQUATION (B.I.9)

$$-\frac{e^{-\frac{2\omega_a}{A}t}\left(1-e^{-\left(\omega_o-\frac{\omega_a}{A}\right)t}\right)\left(1+e^{-\omega_o|\tau|}\right)}{\omega_o-\frac{\omega_a}{A}} \qquad (B.1.11)$$

$$+\frac{\left(1-e^{-\frac{2\omega_a}{A}t}\right)\left(1-e^{-\left(\omega_o-\frac{\omega_a}{A}\right)|\tau|}\right)}{\omega_o-\frac{\omega_a}{A}}e^{-\frac{\omega_a}{A}|\tau|}\Biggr] \quad .$$

Since the RC low-pass filter is assumed to be operating in steady state,

$$e^{-\omega_o t} \ll 1 \quad . \qquad (B.1.12)$$

In addition,

$$\omega_o \gg \frac{\omega_a}{A} \qquad (B.1.13)$$

where

$$A \simeq 3 \times 10^4 ,$$

$$\omega_a \simeq 1 \text{ rad/sec}$$

and

$$\omega_o \approx 2000\,\pi \text{ rad/sec} \quad .$$

Using the above approximations (Eq. (B.1.12) and Eq. (B.1.13)) the autocorrelation function of the output voltage becomes:

$$R_{e_{o_1}}(t,\tau) \simeq \frac{\omega_o}{\alpha}\, G_1^2 \sigma_n^2 \Biggl[\zeta^2\, e^{-\omega_o|\tau|} + 2\zeta\,\frac{\omega_a}{\omega_o}\, e^{-\frac{\omega_a|\tau|}{A}} \qquad (B.1.14)$$

$$+ \left(\frac{\omega_a}{\omega_o}\right)\left(\frac{A}{2}\right)\left(1-e^{-2\frac{\omega_a}{A}t}\right)\left(1+e^{-\frac{\omega_a|\tau|}{A}}\right)\Biggr].$$

The third integral can be simplified in the following manner:

$$\int_0^{t+\tau} d\nu \int_0^t d\lambda \int_0^\nu d\eta \; R_{e_{d_1}}(\lambda - \eta) = \frac{\omega_0}{\alpha} G_1^2 \sigma_n^2 \int_0^{t+\tau} d\nu \; H(\nu,t) \quad (B.2.7)$$

where

$$H(\nu,t) = \begin{cases} H_1(\nu,t) = \int_0^t d\lambda \int_0^\nu d\eta \; e^{-\omega_0 \left| \lambda - \eta \right|} & \nu \leq t \\[2em] H_2(\nu,t) = \int_0^t d\lambda \int_0^\nu d\eta \; e^{-\omega_0 \left| \lambda - \eta \right|} & \nu \geq t \end{cases}$$

$H(\nu,t)$ can be evaluated (using Fig. B.2) in a similar manner to Eq. (B.1.9). Then

$$H_1(\nu,t) = \frac{2\nu}{\omega_0} - \frac{1}{\omega_0^2}\left(1 - e^{-\omega_0 \nu}\right) - \frac{1}{\omega_0^2}(e^{\omega_0 \nu} - 1)e^{-\omega_0 t} \quad (B.2.8)$$

and

$$H_2(\nu,t) = \frac{2t}{\omega_0} - \frac{1}{\omega_0^2}\left(1 - e^{-\omega_0 t}\right) - \frac{1}{\omega_0^2}(e^{\omega_0 t} - 1)e^{-\omega_0 \nu} . \quad (B.2.9)$$

Equation (B.2.7) can then be evaluated:

$$\int_0^{t+\tau} d\nu \int_0^t d\lambda \int_0^\nu d\eta \; R_{e_{d_1}}(\lambda - \eta)$$

$$= \frac{1}{\alpha} G_1^2 \sigma_n^2 \left[t^2 + 2t |\tau| - \frac{1}{\omega_0}\left((t + |\tau|)\left[1 - e^{-\omega_0 t}\right]\right)\right.$$

$$\left. - \frac{1}{\omega_0^2}\left(1 - e^{-\omega_0 t}\right)\left(1 - e^{-\omega_0 |\tau|}\right)\right]. \quad (B.2.10)$$
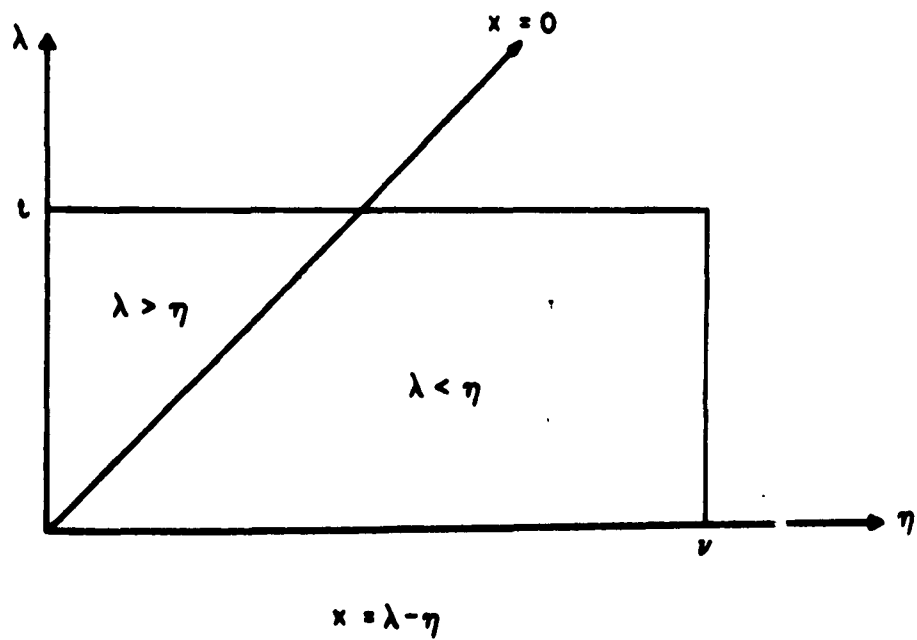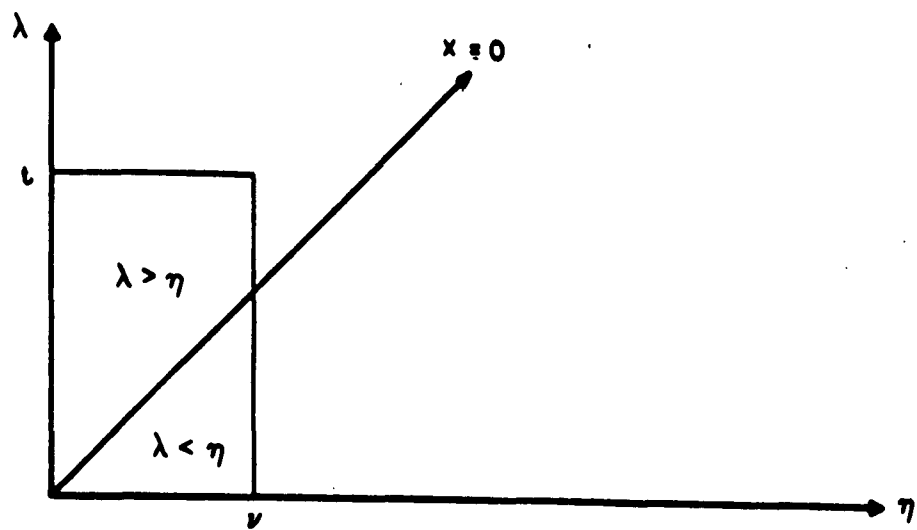
FIG. B.2 GRAPHICAL PROCEDURE USED TO EVALUATE EQUATIONS B.2.8 AND B.2.9

The third integral can be simplified in the following manner:

$$\int_0^{t+\tau} dv \int_0^t d\lambda \int_0^v d\eta \, R_{e_{d_1}}(\lambda - \eta) = \frac{\omega_o}{\alpha} G_1^2 \sigma_n^2 \int_0^{t+\tau} dv \, H(v,t) \quad \text{(B.2.7)}$$

where

$$H(v,t) = \begin{cases} H_1(v,t) = \int_0^t d\lambda \int_0^v d\eta \, e^{-\omega_o \left| \lambda - \eta \right|} & v \leq t \\[2ex] H_2(v,t) = \int_0^t d\lambda \int_0^v d\eta \, e^{-\omega_o \left| \lambda - \eta \right|} & v \geq t \end{cases}$$

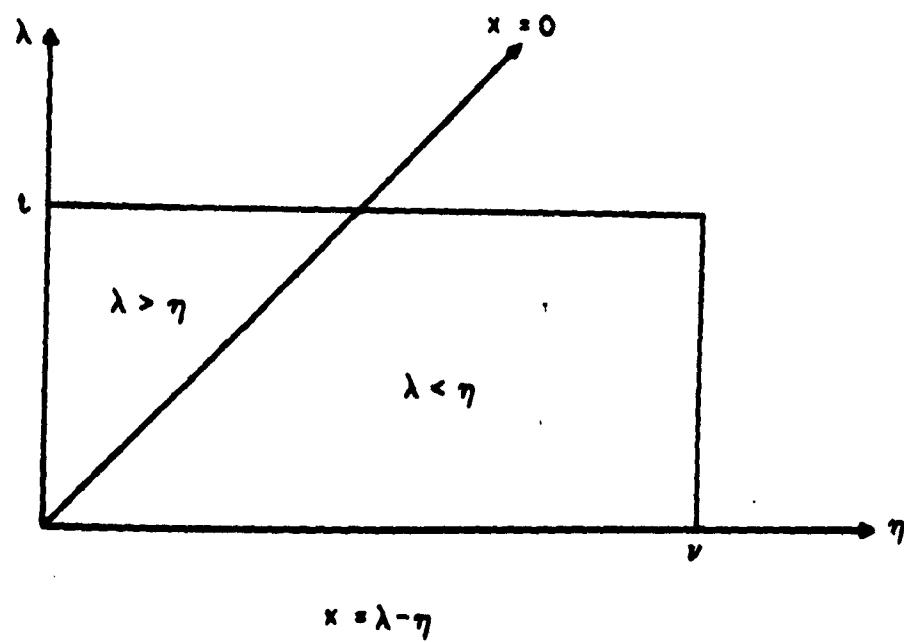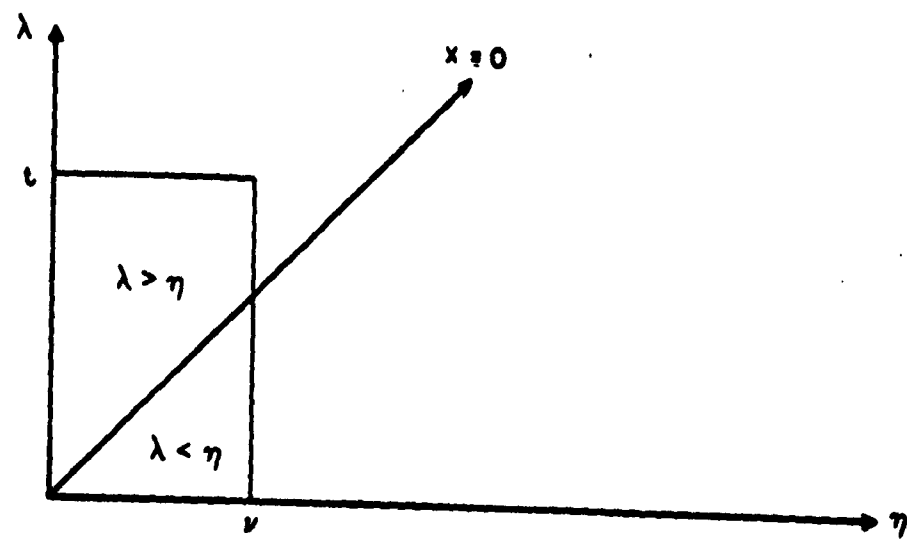$H(v,t)$ can be evaluated (using Fig. B.2) in a similar manner to Eq. (B.1.9). Then

$$H_1(v,t) = \frac{2v}{\omega_o} - \frac{1}{\omega_o^2}\left(1 - e^{-\omega_o v}\right) - \frac{1}{\omega_o^2}(e^{\omega_o v} - 1)e^{-\omega_o t} \quad \text{(B.2.8)}$$

and

$$H_2(v,t) = \frac{2t}{\omega_o} - \frac{1}{\omega_o^2}\left(1 - e^{-\omega_o t}\right) - \frac{1}{\omega_o^2}(e^{\omega_o t} - 1)e^{-\omega_o v} . \quad \text{(B.2.9)}$$

Equation (B.2.7) can then be evaluated:

$$\int_0^{t+\tau} dv \int_0^t d\lambda \int_0^v d\eta \, R_{e_{d_1}}(\lambda - \eta)$$

$$= \frac{1}{\alpha} G_1^2 \, \sigma_n^2 \left[t^2 + 2t \, |\tau| - \frac{1}{\omega_o}\left((t + |\tau|)\left[1 - e^{-\omega_o t}\right]\right) \right.$$

$$\left. - \frac{1}{\omega_o^2}\left(1 - e^{-\omega_o t}\right)\left(1 - e^{-\omega_o |\tau|}\right)\right]. \quad \text{(B.2.10)}$$

FIG. B.2 GRAPHICAL PROCEDURE USED TO EVALUATE EQUATIONS B.2.8 AND B.2.9

A-100-Z-0068

The last integral can be evaluated using the same simplifying procedures:

$$\int_0^t d\xi \int_0^\xi dv \int_0^{t+\tau} d\lambda \int_0^\lambda d\eta \, R_{e_{d_1}}(v-\eta) = \int_0^{t+\tau} d\lambda \int_0^t d\xi \, J(\xi,\lambda)$$

$$(B.2.11)$$

where

$$J = \begin{cases} J_1(\xi,\lambda) = \int_0^\xi dv \int_0^\lambda d\eta \, R_{e_{d_1}}(v-\eta) & \xi \leq \lambda \qquad (B.2.12) \\[2mm] J_2(\xi,\lambda) = \int_0^\xi dv \int_0^\lambda d\eta \, R_{e_{d_1}}(v-\eta) & \xi \geq \lambda \, . \qquad (B.2.13) \end{cases}$$

Equation (B.2.12) and Eq. (B.2.13) are similar to $H_1(v,t)$ and $H_2(v,t)$, given by Eq. (B.2.8) and Eq. (B.2.9). Therefore:

$$J_1(\zeta,\lambda) = \frac{1}{\alpha} G_1^2 \sigma_n^2 \left[2\xi - \frac{1}{\omega_0}\left(1 - e^{-\omega_0\xi}\right) - \frac{1}{\omega_0}\left(e^{\omega_0\xi} - 1\right) e^{-\omega_0\lambda} \right]$$

$$(B.2.14)$$

$$J_2(\zeta,\lambda) = \frac{1}{\alpha} G_1^2 \sigma_n^2 \left[\lambda \frac{1}{\omega_0} \left(1 - e^{-\omega_0\lambda}\right) - \frac{1}{\omega_0}\left(e^{\omega_0\lambda} - 1\right)e^{-\omega_0\xi} \right] .$$

$$(B.2.15)$$

The fourth-order integral has, therefore, been reduced to a second-order integral. This integral can be solved using the rules of Eq. (B.1.9). The final result is then:

$$\int_0^t d\xi \int_0^\xi dv \int_0^{t+\tau} \underline{d\lambda} \int_0^\lambda d\eta \, R_{e_{d_1}}(v-\eta) =$$

$$= \frac{1}{\alpha} G_1^2 \sigma_n^2 \left[\frac{2t^3}{3} - \frac{t^2}{\omega_o} + \left(\frac{1 - e^{-\omega_o t}}{\omega_o^3} - \frac{te^{-\omega_o t}}{\omega_o^2} \right) \left(1 - e^{-\omega_o |\tau|} \right) \right.$$

$$\left. + |\tau| \left(\frac{1 - e^{-\omega_o t}}{\omega_o^2} + t^2 - \frac{t}{\omega_o} \right) \right] . \qquad \text{(B.2.16)}$$

The RC filter is assumed to be operating in the steady state; therefore, we can assume as before that

$$e^{-\omega_o t} \ll 1 .$$

The autocorrelation function of the phase jitter is then:

$$R_{\theta_2^2_1}(t,\tau) = \frac{2 G_1^2 G_2^2 \sigma_n^2}{\alpha} t \left[\zeta^2 + \zeta(\omega_a t + |\omega_a \tau|) + \omega_a t \left(\frac{\omega_a t}{3} + \frac{\omega_a \tau}{2} \right) \right]$$

$$\text{(B.2.17)}$$

where

$$t \ll \frac{A}{\omega_a} .$$

The phase jitter results from the integration of a nonstationary Gaussian random process. Consequently, it too is a nonstationary random process and has a Gaussian distribution with a zero mean.

B.3   To Prove: $E(\cos f(t)) = e^{-\frac{1}{2} E[f(t)]^2} \equiv e^{-\frac{1}{2} \sigma_f^2(t)}$

If f is normal,

$$E(f^{2n}) = 1 \cdot 3 \cdot 5 \cdots (2n - 1)[E(f)^2]^n . \qquad \text{(B.3.1)}$$

Then

$$\cos f = 1 - \frac{f^2}{2!} + \cdots + (-1)^n \frac{f^{2n}}{(2n)!}$$

and

$$E(\cos f) = 1 - \frac{[E(f)^2]}{2!} + \frac{1 \cdot 3 [E(f^2)]^2}{4!} - \cdots$$

$$+ \frac{(-1)^n 1 \cdot 3 \cdot 5 \cdots (2n-1)[E(f)^2]^n}{(2n)!} \qquad (B.3.2)$$

$$= 1 - \frac{E(f)^2}{2} + \frac{[E(f)^2]^2}{2^2 \, 2!} - \cdots + (-1)^n \left[\frac{E(f)^2}{2}\right]^n \frac{1}{n!} \quad .$$

Therefore,

$$E(\cos[f(t)]) = e^{-\frac{1}{2} E[f(t)]^2} \equiv e^{-\frac{1}{2} \sigma_f^2(t)} \quad . \qquad (B.3.3)$$

B.4   **An Illustrative Example Demonstrating that**

$$R_{e_{m_2}}(t,\tau) \simeq R_{e_{m_1}}(t,\tau) = G_1^2 \, \sigma_n^2 \, e^{-\alpha |\tau|}$$

The second approximation to the autocorrelation function of the output of the multiplier is given by

$$R_{e_{m_2}}(t,\tau) = G_1^2 \sigma_n^2 e^{-\alpha |\tau|} e^{-\frac{1}{2}[\sigma_{\theta_1}^2(t) + \sigma_{\theta_1}^2(t+\tau) - 2R_{\theta_1}(t,\tau)]}$$

$$(B.4.1)$$

where

$$\frac{1}{\omega_o} \ll t \ll \frac{A}{\omega_a} \quad .$$

It is shown in this section that

$$\alpha \, |\tau| >> \frac{1}{2}\left(\sigma^2_{\theta_{2_1}}(t) + \sigma^2_{\theta_{2_1}}(t+\tau) - 2R_{\theta_{2_1}}(t,\tau)\right) \qquad \text{(B.4.2)}$$

and therefore,

$$R_{e_{m_2}}(t,\tau) \simeq G^2_1 \, \sigma^2_n \, e^{-\alpha\,|\tau|} \qquad . \qquad \text{(B.4.3)}$$

Equation (B.4.2) can be rewritten using Eq. (B.2.17):

$$\alpha \, |\tau| >> \frac{1}{\alpha} \, G^2_1 \, G^2_2 \, \sigma^2_n \Bigg[\zeta^2(2t + |\tau|) + \zeta\,\omega_a(t^2 + (t + |\tau|)^2)$$

$$+ \frac{\omega_a^2}{3}\left(t^3 + (t + |\tau|)^3\right) - 2\zeta^2 t - 2\zeta\,\omega_a(t^2 + t\,|\tau|)$$

$$- \omega_a^2\left(\frac{2}{3}\,t^3 + t^2\,|\tau|\right)\Bigg] . \qquad \text{(B.4.4)}$$

Equation (B.4.4) is easily simplified. The inequality then becomes

$$\alpha >> \frac{1}{\alpha} \, G^2_1 \, G^2_2 \, \sigma^2_n \left[(\zeta^2 + 2\zeta\,\omega_a t) + \omega_a(\zeta + \omega_a t)\,|\tau| + \frac{\omega_a^2}{3}\,\tau^2\right] . $$
$$\text{(B.4.5)}$$

The inequality expressed by Eq. (B.4.5) can be written as

$$f(t,\tau) = \tau^2 + \frac{3}{\omega_a}\,(\zeta + \omega_a t)\tau - \frac{3}{\omega_a}\left(\frac{\alpha^2}{G^2_1 G^2_2 \sigma^2_n} - 2\zeta\,\omega_a t - \zeta^2\right) << 0.$$
$$\text{(B.4.6)}$$

The inequality

$$f(t,\tau) \ll 0 \qquad (B.4.7)$$

need only be satisfied when

$$|\tau| \leq \frac{5}{\alpha}$$

and

$$t \ll \frac{A}{\omega_a} \quad .$$

If $|\tau| > \frac{5}{\alpha}$, Eq. (B.4.1) is approximately zero, as is $R_{e_{m_1}}(\tau)$. It is only of interest to show that

$$R_{e_{m_2}}(t,\tau) \simeq R_{e_{m_1}}(t,\tau) \qquad (B.4.8)$$

when these values are non-zero.

The following illustrative example clearly illustrates that the inequality presented in Eq. (B.4.7) is satisfied. Let

$$\alpha = 2\pi(6000)\text{rad/sec}$$

$$\omega_0 = 2\pi(1000)\text{rad/sec}$$

$$\omega_a = 1 \text{ rad/sec}$$

$$\zeta = 50 \times 10^{-3}$$

$$G_1 G_2 = 42.5 \, \pi\text{rad/sec/volt}$$

$$\sigma_n^2 = 100 \text{ (volt)}^2$$

and

$$A = 3 \times 10^4 \quad . \qquad (B.4.9)$$

The minimum value of $f(t,\tau)$ with respect to τ is found by differentiating with respect to τ.

$$\frac{\partial f(t,\tau)}{\partial \tau} = 2\tau + \frac{3}{\omega_a} (\zeta + \omega_a t) = 0 . \qquad (B.4.10)$$

Therefore,

$$|\tau| = \left| \frac{3}{2\omega_a} (\zeta + \omega_a t) \right| >> \frac{5}{\alpha} . \qquad (B.4.11)$$

Thus, in the range of interest, $f(t;\tau)$ is an increasing function of τ as shown in Fig. B.3. It is seen from this figure, that $f(t,\tau)$ is closest to zero in the interval.

$$-\frac{5}{\alpha} \leq \tau \leq \frac{5}{\alpha} , \qquad (B.4.12)$$

when

$$\tau = \frac{5}{\alpha} . \qquad (B.4.13)$$

Thus, letting $\tau = \frac{5}{\alpha}$, and using Eq. (B.4.9)

$$f(t,\frac{5}{\alpha}) = \left(\frac{15}{\alpha} + 6\zeta \right) t - \left(\frac{3\alpha^2}{\omega_a \ G_1^2 \ G_2^2 \ \sigma_n^2} - \frac{3\zeta^2}{\omega_a} - \frac{15\zeta}{\omega_a \alpha} - \frac{25}{\alpha^2} \right) .$$
$$(B.4.14)$$

After the APC System has been in operation for one-half hour (which is an extremely long time)

$$f\left(1800,\frac{5}{\alpha}\right) \approx -1860 << 0 . \qquad (B.4.15)$$

-122-

FIG. B.3 $f(\iota, \tau)$ VS. τ, TO SHOW THAT $f(\iota, \tau) << 0$, WHEN $|\tau| \le \dfrac{5}{a}$

$$f\left(\iota, \frac{5}{a}\right) \propto \left(6\zeta + \frac{15}{a}\right)\iota - \left(\frac{3a^2}{\omega_a G_1^2 G_2^2 \sigma_n^2} - \frac{3\zeta^2}{\omega_a} - \frac{15\zeta}{\omega_a a} - \frac{25}{a^2}\right)$$

$$f\left(\iota, -\frac{5}{a}\right) \propto \left(6\zeta - \frac{15}{a}\right)\iota - \left(\frac{3a^2}{\omega_a G_1^2 G_2^2 \sigma_n^2} - \frac{3\zeta^2}{\omega_a} + \frac{15\zeta}{\omega_a a} - \frac{25}{a^2}\right)$$

A-100-Z-0069
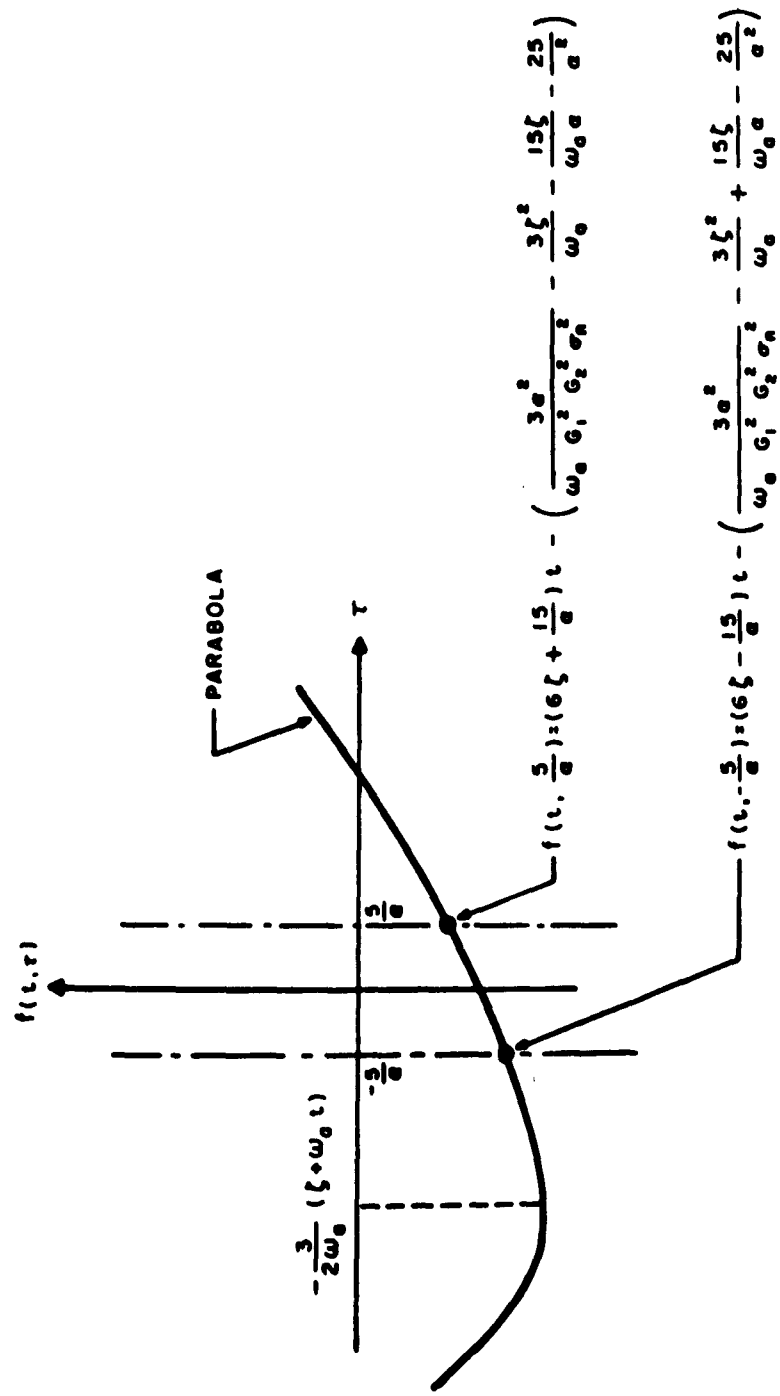
Therefore, to all intents and purposes, we have shown that

$$R_{e_{m_2}}(t,\tau) \simeq R_{e_{m_1}}(t,\tau) = G_1^2 \, \sigma_n^2 \, e^{-\alpha |\tau|} \qquad (B.4.16)$$

when

$$|\tau| \leq \frac{5}{\alpha}$$

and

$$t << \frac{A}{\omega_a} \quad .$$

THE RESPONSE OF A LINEARIZED APC SYSTEM
TO AN FM SIGNAL AND NOISE

The input voltage to the APC System is,

$$e_c(t) = S \sin \phi_1(t) + N(t) \tag{C.1}$$

where

$$\phi_1(t) = \omega_2 t + \theta_1(t)$$

and

$$\theta_1(t) \quad \text{is the phase modulation.}$$

The additive noise, $N(t)$, is narrow-band Gaussian noise, and can be written as:

$$N(t) = x(t) \cos \omega_2 t - z(t) \sin \omega_2 t = C(t) \sin(\omega_2 t + \psi_n(t)) \tag{C.2}$$

where, x and z are independent Gaussian random variables (see Chapter 3, Sec. 3), $C(t)$ is Rayleigh distributed, and $\psi_n(t)$ is a uniformly distributed phase angle having a probability density,

$$p(\psi) = \begin{cases} \dfrac{1}{2\pi} & 0 \leq \psi \leq 2\pi \\[2ex] 0 & \text{elsewhere} \end{cases}$$

The input voltage can then be written as:

$$e_c(t) = S \sin(\omega_2 t + \theta_1(t)) + C(t)\sin(\omega_2 t + \psi_n(t))$$

$$= E_c(t)\sin(\omega_2 t + \psi_c(t)) \quad .$$

(c.3)

$E_c(t)$ and $\psi_c(t)$ are easily determined using the phasor diagram shown in Fig. C.1. Then

$$E_c^2(t) = S^2 \left[1 + \frac{c^2(t)}{S^2} + 2 \frac{C(t)}{S} \cos(\psi_n(t) - \theta_1(t)) \right]$$

(c.4)

and

$$\psi_c(t) = \theta_1(t) + \tan^{-1}\left(\frac{C(t)\sin(\psi_n(t) - \theta_1(t))}{S + C(t)\cos(\psi_n(t) - \theta_1(t))} \right).$$

(c.5)

If the noise is limited so that

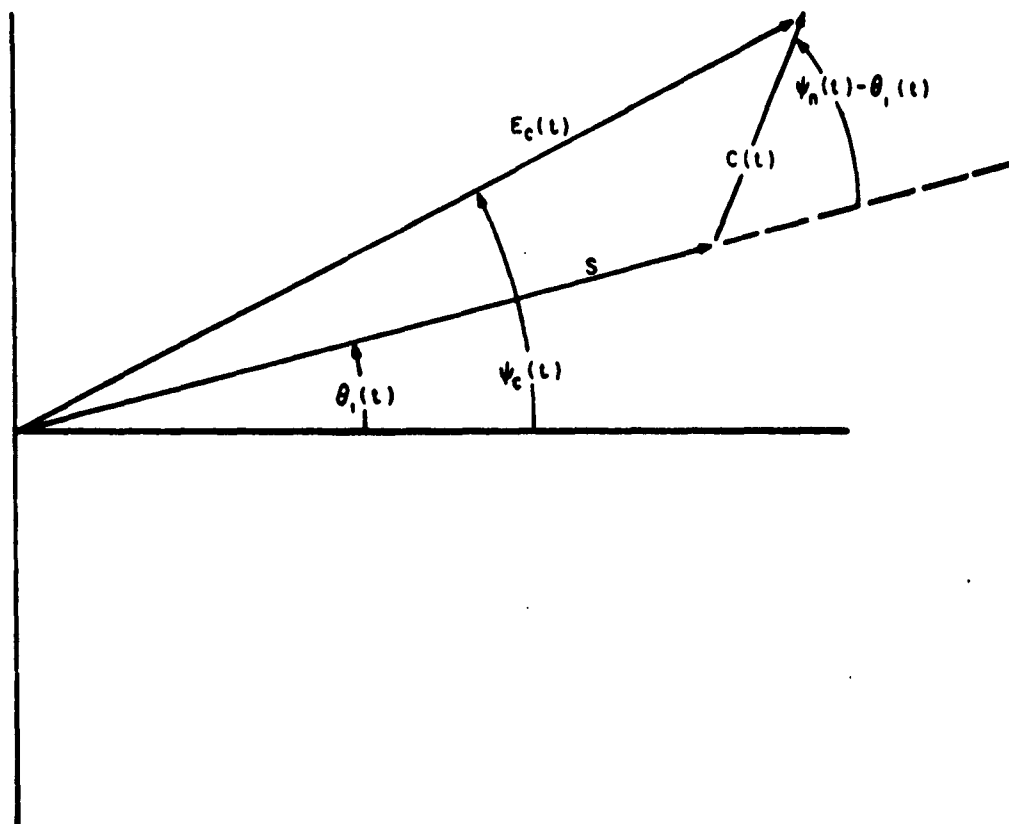$$|C(t)| \ll S \, ,$$

(which requires a large S/N ratio),

$$E_c(t) \simeq S$$

(c.6)

and

$$\psi_c(t) \simeq \theta_1(t) + \frac{C(t)}{S} \sin(\psi_n(t) - \theta_1(t)) \quad .$$

(c.7)

Utilizing Eq. (C.2), it is seen that

$$C(t)\sin(-\theta_1(t) + \psi_n(t)) = x(t)\cos\theta_1(t) + z(t)\sin\theta_1(t) \quad .$$

(c.8)

A-100-2-0070

FIG. C.1   PHASOR ADDITION OF SIGNAL AND NOISE

If $u(t) \equiv x(t)\cos \theta_1(t) + z(t)\sin \theta_1(t)$ $\qquad$ (C.9)

then Eq. (C.7) becomes

$$\psi_c(t) \simeq \theta_1(t) + \frac{1}{S} u(t) \quad . \qquad (C.10)$$

Therefore, the input voltage

$$e_c(t) \simeq S \sin(\omega_2 t + \theta_1(t) + \frac{1}{S} u(t)) = S \sin(\phi_1(t) + \frac{1}{S} u(t)).$$
$$\qquad (C.11)$$

The statistics of $u(t)$ are easily determined.

$$E(u(t)) = 0 ,$$

and

$$R_u(t,\tau) = R_x(\tau)\cos(\theta_1(t + \tau) - \theta_1(\tau))$$

$$\simeq \sigma_n^2 \, e^{-\alpha |\tau|} \cos \left[\left(\frac{d\theta_1}{dt}\right) \tau \right] . \qquad (C.12)$$

The input signal was originally passed through an IF filter having a center frequency, ω_2 , and a bandwidth, α. The maximum frequency of the modulating signal is assumed to be much less than α . Therefore,

$$\frac{d\theta_1}{dt} \ll \alpha \quad . \qquad (C.13)$$

Equation (C.10) is only of interest when

$$\tau \leq \frac{5}{\alpha} \quad . \qquad (C.14)$$

The autocorrelation function of $u(t)$ is then:

$$R_u(t,\tau) \simeq \sigma_n^2 \, e^{-\alpha |\tau|} \qquad (C.15)$$

THE RESPONSE OF AN APC SYSTEM TO AN FM SIGNAL AND NOISE

D.1   The Iteration Technique

The input voltage to the APC System is

$$e_c(t) = S \sin \phi_1(t) + N(t) \quad . \tag{D.1.1}$$

The noise is narrow-band Gaussian noise and can be written as,

$$N(t) = x(t)\cos \omega_2 t - z(t)\sin \omega_2 t \quad . \tag{D.1.2}$$

The output phase of the VCO is initially assumed to be noise free. Thus,

$$e_{v_{O_O}}(t) = \cos \phi_{2_{O_O}}(t) = \cos(\omega_2 t + \theta_{2_{O_S}}(t)) \quad . \tag{D.1.3}$$

The first approximation of the output voltage of the multiplier, $e_{m_1}(t)$, is then,

$$
\begin{aligned}
e_{m_1}(t) &= G_1 \, S \, \sin(\phi_{2_O}(t) - \phi_1(t)) \\
&\quad + G_1(x(t)\cos \theta_{2_{O_S}}(t) + z(t)\sin \theta_{2_{O_S}}(t)) .
\end{aligned}
\tag{D.1.4}
$$

Letting,

$$\phi = \phi_{2_O}(t) - \phi_1(t) \, , \tag{D.1.5}$$

and
$$u_O(t) = x(t)\cos\theta_{2_{O_s}}(t) + z(t)\sin\theta_{2_{O_s}}(t) \quad,$$

the multiplier voltage,

$$e_{m_1}(t) = G_1\ S\ \sin\phi + G_1\ u_O(t) \quad. \qquad (D.1.6)$$

D.1.1 The Statistics of $u_O(t)$

The expected value of $u_O(t)$ is:

$$E(u_O(t)) = E(x(t))\cos\theta_{2_{O_s}}(t) + E(z(t))\sin\theta_{2_{O_s}}(t) = 0. \quad (D.1.7)$$

The probability density of $u_O(t)$ is determined by evaluating its moments:

$$E(u_O^2(t)) = E(x^2)\cos^2\theta_{2_{O_s}}(t) + E(z^2)\sin^2\theta_{2_{O_s}}(t) \quad. \qquad (D.1.8)$$

However,

$$E(x^2) = E(z^2) = \sigma_x^2 \quad. \qquad (D.1.9)$$

Therefore,

$$\sigma_{u_O}^2 = \sigma_x^2 \quad. \qquad (D.1.10)$$

Similarly,

$$E(u_O^4) = 1\cdot 3\ \sigma_x^4 \quad, \qquad (D.1.11)$$

and

$$E(u_0^{2n}) = 1 \cdot 3 \cdots (2n - 1)\sigma_x^2 \quad . \tag{D.1.12}$$

Odd order moments are obviously zero. Thus, $u_0(t)$ is Gaussian distributed.

The autocorrelation function of $u_0(t)$ is

$$R_{u_0}(t,\tau) = E(u_0(t)u_0(t + \tau))$$

$$= E(x(t)x(t + \tau))\cos\theta_{2_{0_s}}(t)\cos\theta_{2_{0_s}}(t + \tau)$$

$$+ E(z(t)z(t + \tau))\sin\theta_{2_{0_s}}(t)\sin\theta_{2_{0_s}}(t + \tau), \tag{D.1.13}$$

since

$$E(xz) = 0 \quad . \tag{D.1.14}$$

Noting that

$$E(x(t)x(t + \tau)) = E(z(t)z(t + \tau)) = \sigma_n^2 e^{-\alpha|\tau|}, \tag{D.1.15}$$

Eq. (D.1.13) becomes,

$$R_{u_0}(t,\tau) = \sigma_n^2 e^{-\alpha|\tau|} \cos(\theta_{2_{0_s}}(t + \tau) - \theta_{2_{0_s}}(t)) \quad . \tag{D.1.16}$$

When $\tau > 5/\alpha$

$$R_{u_0}(t,\tau) \simeq 0 \quad . \tag{D.1.17}$$

-131-

When $\tau \leq 5/\alpha$

$$R_{u_o}(t,\tau) \approx \sigma_n^2 \, e^{-\alpha |\tau|} \cos \left[\left(\frac{d\theta_{2_{O_s}}}{dt} \right) \tau \right] . \qquad (D.1.18)$$

The instantaneous frequency of the response of the VCO to a signal is

$$\dot{\phi}_{2_O}(t) = \omega_2 + \dot{\theta}_{2_{O_s}}(t) . \qquad (D.1.19)$$

The frequency $\dot{\theta}_{2_{O_s}}(t)$, is always much less than the bandwidth of the RC low-pass filter. This requirement insures that the frequency of the input signal is not affected by the RC low-pass filter. Then,

$$| \dot{\theta}_{2_{O_s}}(t) | << \omega_o . \qquad (D.1.20)$$

However,

$$\omega_o < \alpha . \qquad (D.1.21)$$

(α is the bandwidth of the IF filter). Therefore,

$$(\dot{\theta}_{2_{O_s}}(t))\tau << 1 \text{ radian} . \qquad (D.1.22)$$

The autocorrelation function of $u_o(t)$ is,

$$R_{u_o}(t,\tau) \simeq \sigma_n^2 \, e^{-\alpha |\tau|} , \qquad (D.1.23)$$

which is the same as the result obtained from an analysis of noise alone.

D.1.2 The First Iteration

The output of the multiplier is composed of two terms: the first due to the response of the system to an FM signal (Chapter 2), and the second due to the response of the system to noise (Chapter 3). The first approximation of the output phase, $\theta_{2_1}(t)$, also consists of two terms:

$$\theta_{2_1}(t) = \theta_{2_{1_s}}(t) + \theta_{2_{1_n}}(t) \tag{D.1.24}$$

where $\theta_{2_{1_s}}(t) = \theta_{2_{0_s}}(t)$, is the output phase when a signal is applied to the system, and $\theta_{2_{1_n}}(t)$ is the result obtained from an analysis of noise alone (Chapter 3).

The second approximation of the output of the multiplier is then

$$e_{m_2}(t) = G_1 S \sin(\phi(t) + \theta_{2_{1_n}}(t)) + G_1 u_1(t) , \tag{D.1.25}$$

where

$$u_1(t) = x(t)\cos \theta_{2_1}(t) + z(t)\sin \theta_{2_1}(t) . \tag{D.1.26}$$

The first term in Eq. (D.1.25) shows that there is a phase jitter superimposed on the phase error, ϕ . The second term in the expression is due to noise.

D.1.3 The Statistics of $u_1(t)$

The expected value of $u_1(t)$ is

-133-

$$E(u_1(t)) = E\left[x(t)\cos(\theta_{2_{0_s}}(t) + \theta_{2_{1_n}}(t))\right]$$

$$+ E\left[z(t)\sin(\theta_{2_{0_s}}(t) + \theta_{2_{1_n}}(t))\right] \qquad (D.1.27)$$

However, from Eq. (3.5.5) and Eq. (3.5.6),

$$E\left(x\theta_{2_{1_n}}\right) = E\left(z\theta_{2_{1_n}}\right) = 0 \quad . \qquad (D.1.28)$$

Therefore,

$$E(u_1(t)) = 0 \quad . \qquad (D.1.29)$$

The autocorrelation function of $u_1(t)$ is

$$R_{u_1}(t,\tau) = \sigma_n^2\, e^{-\alpha|\tau|}\, E\left[\cos(\theta_{2_1}(t+\tau) - \theta_{2_1}(t))\right] \quad . \qquad (D.1.30)$$

But,

$$\cos(\theta_{2_1}(t+\tau) - \theta_{2_1}(t)) \qquad (D.1.31)$$

$$= \cos(\theta_{2_{1_s}}(t+\tau) - \theta_{2_{1_s}}(t) + \theta_{2_{1_n}}(t+\tau) - \theta_{2_{1_n}}(t)) \quad .$$

Therefore,

$$E\left[\cos(\theta_{2_1}(t+\tau) - \theta_{2_1}(t))\right] \qquad (D.1.32)$$

$$= E\left[\cos\left(\theta_{2_{1_n}}(t+\tau) - \theta_{2_{1_n}}(t)\right)\right]\cos\left(\theta_{2_{1_s}}(t+\tau) - \theta_{2_{1_s}}(t)\right) +$$

$$- E \left[\sin\left(\theta_{2_{1_n}}(t + \tau) - \theta_{2_{1_n}}(t) \right) \right] \sin\left(\theta_{2_{1_s}}(t + \tau) - \theta_{2_{1_s}}(t) \right)$$

$$= E \left[\cos\left(\theta_{2_{1_n}}(t + \tau) - \theta_{2_{1_n}}(t) \right) \right] \cos\left(\theta_{2_{1_s}}(t + \tau) - \theta_{2_{1_s}}(t) \right) .$$

Referring to Eq. (3.5.15), Eq. (3.5.16) and Eq. (3.5.17);
Eq. (D.1.30) becomes,

$$R_{u_1}(t, \tau) \simeq \sigma_n^2 \, e^{-\alpha |\tau|} \cos\left[\left(\dot{\theta}_{2_{0_s}} \right) \tau \right] . \qquad (D.1.33)$$

Thus, the statistics of $u_1(t)$ are the same as the statistics of $u_o(t)$

    The iterative procedure was not continued beyond this point.

D.2   The Standard Deviation of the Phase Jitter, $\sigma_{\theta_{2_{1_n}}}(t)$

    The standard deviation, $\sigma_{\theta_{2_{1_n}}}(t)$, is given by Eq. (3.4.13):

$$\sigma_{\theta_{2_{1_n}}}(t) \simeq \left(\frac{2G_1^2 \, G_2^2 \, \sigma_n^2}{\alpha} \, t \left[\zeta^2 + \zeta(\omega_a t) + \frac{\omega_a^2 t^2}{3} \right] \right)^{\frac{1}{2}} . \qquad (D.2.1)$$

When a signal and noise are present, this expression can be normalized using the relations:

$$\omega_n = G_1 \, G_2 \, S \text{ rad/sec} , \qquad (D.2.2)$$

$$\epsilon = \sqrt{\frac{\omega_n}{\omega_a}} \, \zeta \quad , \tag{D.2.3}$$

and

$$\tau = \sqrt{\omega_a \omega_n} \, t \quad . \tag{D.2.4}$$

Then,

$$\sigma_{\theta_{2_{1_n}}}(\tau) = \left(\frac{\omega_n^2}{\alpha} \left(\frac{\sigma_n^2}{s^2/2} \right) \frac{\tau}{\sqrt{\omega_a \omega_n}} \left[\frac{\omega_a}{\omega_n} \epsilon^2 + \left(\sqrt{\frac{\omega_a}{\omega_n}} \epsilon \right) \left(\omega_a \sqrt{\omega_a \omega_n} \right) \right. \right.$$

$$\left. \left. + \frac{\omega_a \tau^2}{3\omega_n} \right] \right)^{\frac{1}{2}} = \left(\frac{\sqrt{\omega_a \omega_n}}{\alpha} \left(\frac{\sigma_n^2}{s^2/2} \right) \tau \left[\epsilon^2 + \epsilon\tau + \frac{\tau^2}{3} \right] \right)^{\frac{1}{2}} \quad . \tag{D.2.5}$$

The variance of the phase jitter

$$\sigma_{\theta_{2_{1_n}}}^2 (\tau) = \frac{\sqrt{\omega_a \omega_n}}{\alpha} \left(\frac{\sigma_n^2}{s^2/2} \right) \left(\epsilon^2 + \epsilon\tau + \frac{\tau^2}{3} \right) \tau \tag{D.2.6}$$

is proportional to the "effective system bandwidth," $\sqrt{\omega_a \omega_n}$, the input N/S ratio, $\sigma_n^2/s^2/2$, the normalized damping factor, ϵ , and the normalized time, τ .

TECHNICAL AND FINAL REPORT DISTRIBUTION LIST

PHYSICAL SCIENCES DIRECTORATE

Commander 3
AF Office of Scientific Research
ATTN: SRY
Washington 25, D. C.

Commander 2
AF Office of Scientific Research
ATTN: SRGL
Washington 25, D.C.

Commander 4
Wright Air Development Division
ATTN: WWAD
Wright-Patterson Air Force Base
Ohio

Commander 1
AF Cambridge Research Laboratories
ATTN: CRREIA
L. G. Hanscom Field
Bedford, Massachusetts

Commander 2
European Office
Office of Aerospace Research
The Shell Building
Brussels, Belgium

P. O. Box AA 1
Wright-Patterson Air Force Base
Ohio

Aeronautical Research Laboratories 1
ATTN: Technical Library
Building 450
Wright-Patterson Air Force Base
Ohio

Armed Services Technical Information Agency
ATTN: TIPCR 10
Arlington Hall Station
Arlington 12, Virginia

Director of Research and Development
Headquarters, USAF 1
ATTN: AFDRD
Washington 25, D.C.

Office of Naval Research 1
Department of the Navy
ATTN: Code 420
Washington 25, D. C.

Director, Naval Research Lavoratory 1
ATTN: Technical Information Officer
Washington 25, D.C.

Chief of Research and Development 1
ATTN: Scientific Information Branch
Department of the Army
Washington 25, D. C.

Chief, Physics Branch 1
Division of Research
U. S. Atomic Energy Commission
Washington 25, D. C.

U. S. Atomic Energy Commission 1
Technical Information Extension
P.O. Box 62
Oak Ridge, Tennessee

National Bureau of Standards Library
Room 203, Northwest Building 1
Washington 25, D. O.

Physics Program 1
National Science Foundation
Washington 25, D. C

Director, Office of Ordnance Research
Box CM, Duke Station 1
Durham, NOrth Carolina

Director, Department of Commerce 1
Office of Technical Services
Washington 25, D. C.

AFDC (AFOIM) 1
Arnold Air Force Station
Tullahoma, Tennessee

Commander 1
AF Flight Test Center
ATTN: FTOTL
Edwards Air Force Base
California

Commander 1
AF Special Weapons Center
ATTN: SWOI
Kirtland Air Force Base
New Mexico

Commander 1
AF Missile Development Center
ATTN: HDOI
Holloman Air Force Base
New Mexico

Commander 1
Army Rocket and Guided Missile Agency
ATTN: ORDXR-OTL
Redstone Arsenal
Alabama

Commandant   1
Air Force Institute of Technology
(AU) Library
MCLI-LIB, Bldg. 125, Area B
Wright-Patterson Air Force Base
Ohio

Commander   6
Air Force Systems Command
ATTN: RDRS   2cy
Andrews Air Force Base
Washington 25, D.C.

Commanding General   1
U. S. Army Signal Corps Research
  and Development Laboratory
ATTN: SIGFM/EL-RPO
Ft. Monmouth, New Jersey

National Aeronautics and Space   6
 Administration
ATTN: Library
1520 H Street, N. W.
Washington 25, D. C.

Advanced Research Projects Agency   1
Washington 25, D. C.

Rand Corporation   1
1700 Main Street
Santa Monica, California

Chairman   (Unclass Reports) 1
Canadian Joint Staff
For DRD/DSIS
2450 Massachusetts Ave., N. W.
Washington 25, D. C.